REGULATION OF GENE EXPRESSION BY THE CIRCADIAN CLOCK COMPONENTS PRR7 AND PRR9 IN *ARABIDOPSIS THALIANA*

By

Tiffany L. Liu

A DISSERTATION

Submitted to
Michigan State University
in partial fulfillment of the requirements
for the degree of

Plant Biology – Doctor of Philosophy

2015

ABSTRACT

REGULATION OF GENE EXPRESSION BY THE CIRCADIAN CLOCK COMPONENTS PRR7 AND PRR9 IN *ARABIDOPSIS THALIANA*

By

Tiffany L. Liu

Almost every living organism exposed to the day/night cycle on earth has evolved time-keeping mechanisms that exhibit approximately 24-hour periods. Circadian clocks are present in life forms ranging from bacteria to humans, and enable organisms to keep track of time in a robust manner, as exemplified by the persistence of circadian rhythms under constant conditions. The ability to anticipate changes and respond accordingly is believed to confer an adaptive advantage. In *Arabidopsis thaliana*, the circadian clock is involved in nearly all aspects of growth and development and the PSEUDO-RESPONSE REGULATOR (PRR) family of circadian clock components are master regulators of diverse biological processes. Mutations in the PRRs result in delayed flowering times, elongated hypocotyl lengths, and an increased tolerance to drought and cold as observed in the *prr9prr7prr5* triple mutant. Up to 90% of expressed genes oscillate under diel conditions and approximately 30% of expressed genes are circadian regulated. However, not much is known regarding the exact processes that are regulated by specific clock components. To determine the outputs of the clock that are directly regulated by the PRRs, I identified the genome-wide targets of PRR9 and PRR7. I showed that PRR9 and PRR7 are directly involved in the repression of master regulators of plant growth, light signaling, and stress responses. A majority of PRR9 and PRR7 targets exhibited peak gene expression around dawn and were repressed by PRR9 and PRR7. These findings indicate that PRR9 and PRR7 are important for regulating cyclic gene expression by repressing the transcription of morning-expressed genes. I found an enrichment of PRR7 target genes involved

in abiotic stress responses and accordingly, we observed that PRR7 is involved in the oxidative stress response and the regulation of stomata conductance. PRR9 and PRR7 binding sites are located near transcriptional start sites showing low nucleosome occupancy and high DNase I hypersensitivity, indicating that PRR9 and PRR7 bind to regulatory regions of DNA. Furthermore, binding motif analyses revealed that PRR9 and PRR7 binding sites are located in noncoding regions conserved among at least nine Brassicaceae species and are enriched in G-box motifs, indicating that these sequences are functionally relevant. A comparison of binding site similarity among PRR9, PRR7, PRR5, and TOC1 provided insight on the overlapping and distinct roles of the PRRs.

This work is dedicated to my loving Grandparents.

ACKNOWLEDGEMENTS

I was blessed with many wonderful teachers throughout my academic career and I would like to first start by thanking my elementary school teachers for laying the solid foundation on which my education was built. Thank you Mrs. Guldner, Mrs. Lohman, Mrs. Cookie, Mrs. Freeman, Mrs. Hendricks, Mr. Tennis, and Mr. Olsen. I would also like to thank my high school teachers Mr. Zeddies (English), Mr. Robinson (A.P. European History), Mr. Goodhue (Ceramics), Mr. Dukes (A.P. Physics), my swim coach Jen, and Mrs. Barry (A.P. Biology) for loving the subjects that they taught and infecting me with their enthusiasm. I was fascinated by every subject in school, but it was Mrs. Barry who made me realize that science was the future. At Cal, my undergraduate research apprenticeship with Dr. Pablo Leivar in the Quail laboratory taught me skills in molecular biology and solidified my interest in conducting research. I am thankful to be a part of the Spartan family at MSU, especially in the Department of Plant Biology and the Plant Research Laboratory. It is here that I truly felt a sense of community and collaboration among scientists. The CompPLB group composed of the Buell, Farre, Jiang, and Shiu labs gave me the opportunity to practice giving presentations as well as hear many informative talks. One of my favorite classes was bioinformatics taught by Dr. Shinhan Shiu, which imparted me with the invaluable computational skills to analyze my large datasets. My committee members Dr. Robin Buell, Dr. Beronda Montgomery, and Dr. Steve van Nocker provided great discussions and advice, both academic and professional, which I appreciate greatly. The most important person in my graduate career has been Dr. Eva Farre. Thank you for this exciting project and for being the most wonderful P.I. that every graduate student wished they had. You nurtured me in the early years by critically discussing scientific papers together; taught me how to stand on my own by encouraging me to attend conferences, give talks, and study abroad; and finally pushed me out of

the nest because it was time to move onto the next stage in my academic career. I cannot thank you enough.

I would also like to acknowledge my friends and colleagues. I was lucky to have met my best friend Katrina in high school, with whom I shared many laughs in and out of class. Thank you, Huy, for encouraging me to pursue a higher degree and rooting for me every step of the way. I have made many long lasting friendships at MSU, which has enriched my experience in the beautiful state of Michigan. I am thankful towards Shichen and my cohort for our study sessions and scientific discussions. I want to thank my dissertation support group, composed of many impressive individuals, for sharing our experiences and helping each other get through this arduous process together. Without the Farré lab members, I would not have a story to tell. Special thanks to Dr. Jenny Carlsson, Linsey Newton, Tomomi Takeuchi, and Saundra Mason for the combined efforts.

Last, but not least, I am grateful for my family. I am fortunate for my Grandparents who raised me in a happy home and blessed me with the happiest childhood. My aunts and uncles played major roles, including Uncle Carl, Uncle Tim, Uncle Tyler, Uncle Kent, Aunt Suzie, and especially Aunt Nancy during my younger years. My Aunt Jan is a kindred spirit and I am thankful for our deep conversations and her sage advice. My Parents devoted themselves to provide me with financial stability and I thank them for that as well as for being patient, especially during my rebellious teenage years. I was given the freedom to pursue any career, and I thank my entire family for supporting me throughout this journey.

TABLE OF CONTENTS

LIST OF TABLES

LIST OF FIGURES

CHAPTER 1

LITERATURE REVIEW

Molecular mechanisms of circadian clocks

Part of the work presented in this chapter has been published:

The PRR family of transcriptional regulators reflects the complexity and evolution of plant circadian clocks

Eva M. Farré, Tiffany Liu (2013)

Current Opinion in Plant Biology 10.1016/j.pbi.2013.06.015

INTRODUCTION

Circadian clocks serve as time-keeping mechanisms, exhibiting approximately 24-hour periods, whereby external cues such as light and temperature entrain clocks to synchronize with the environment. The 24-hour periods are maintained under a broad range of physiologically relevant temperatures, known as temperature compensation. In addition, circadian clocks are defined as having persistent oscillations under constant conditions, thereby highlighting the endogenous nature of clocks. A classical view of how eukaryotic circadian clocks work includes transcription/translation feedback loops (TTFLs). In general, a positive regulator activates the transcription of a core clock component, which would in turn negatively regulate the expression of that positive regulator. However, recent discoveries indicate that circadian clocks are composed of complex signaling networks with multiple levels of regulation in order to fine-tune and maintain the robustness of the oscillator.

Studies in various organisms have shown that the clock confers a competitive advantage due to its synchronicity with the environment. Woelfle et al. (2004) showed that in cyanobacteria, clock mutants were able to compete with wild-type (WT) when grown under environmental conditions matching their altered periods, whereas the WT strain outcompeted the mutants under cycling 12 h light/12 h dark conditions (LD). Similarly in Arabidopsis, experiments with short or long period mutants compared to WT showed that each mutant excelled under the condition in which their endogenous period matched the environmental period (Dodd et al., 2005). Furthermore, competition experiments in Arabidopsis showed that a segregating population of clock mutants grown under short versus long periods resulted in a positive selection of plants with corresponding periods (Yerushalmi et al., 2011). Thus, the ability to anticipate environmental

changes and respond accordingly enhances the fitness of the organism (Yerushalmi and Green, 2009).

Circadian clocks in diverse organisms

Core clock components among bacteria, fungi, animals, and plants appear to be non-homologous, suggesting that circadian clocks in different organisms evolved independently. However, the presence of a transcription-less circadian oscillator driving peroxiredoxin oxidation-reduction rhythms found in all three domains of life suggests that some clocks share a common origin (O'Neill et al., 2011; Edgar et al., 2012). It has been hypothesized that the lack of conservation among core clock components may have resulted from natural selection acting on the clock controlled output pathways rather than the clock itself (McClung, 2013). For example, since clock components regulate many outputs directly, one can speculate that organisms with different morphologies, physiologies, and/or living in varying habitats may acquire non-homologous clock components to regulate distinct biological processes.

Cyanobacteria

More than 30% of expressed genes in the photosynthetic prokaryote *Synechococcus elongatus* oscillates under constant conditions, including those involved in various circadian regulated processes such as metabolism, photosynthesis, and cell division (Kondo and Ishiura, 2000; Ito et al., 2009). KaiA promotes KaiC phosphorylation during the day, which fosters KaiC binding to KaiB in the evening (Figure 1.1) (Golden and Canales, 2003). KaiB/KaiC then prevents KaiA from activating KaiC phosphorylation and by mid-morning, the complex dissociates, allowing the cycle to start anew (Figure 1.1) (Golden and Canales, 2003).

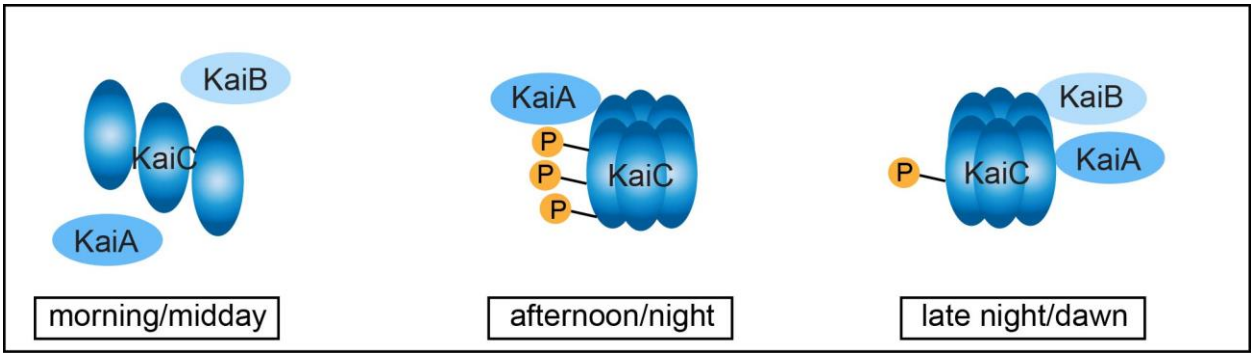

Figure 1.1. The cyanobacteria clock. Association of Kai proteins during a circadian cycle. "P" represents phosphorylation.

The cyanobacterial clock can maintain rhythmicity in the dark during which essentially no transcription occurs in this organism (Pattanayak et al., 2014). Indeed, an elegant study conducted by Nakajima et al. (2005) revealed that the reconstituted clock components KaiA, KaiB, and KaiC along with ATP were able to maintain oscillating KaiC phosphorylation *in vitro* . A mechanism by which clock outputs are regulated includes a two-component regulatory system whereby KaiC promotes SasA (Synechococcus adaptive sensor) autophosphorylation, resulting in the transfer of its phosphoryl group to RpaA (Regulator of phycobilisome associated) to activate gene expression (Mackey et al., 2011). At the same time, KaiC is implicated in negatively regulating outputs through LabA (Low-amplitude and bright), which has been shown to indirectly repress RpaA, kaiBC, and overall gene expression (Mackey et al., 2011).

Fungi

Approximately 25% of expressed genes oscillate under constant conditions in the model fungi *Neurospora crassa*, involving various clock controlled biological processes such as conidiation, cell cycle, and stress responses (Lakin-Thomas et al., 2011). In the *Neurospora*

transcription/translation feedback loop, FREQUENCY (FRQ) inhibits the White Collar Complex (WCC) composed of the PAS domain containing proteins WHITE COLLAR-1 (WC-1) and WC-2, whereas the WCC activates *frq* in return (Figure 1.2). Specifically, FRQ becomes more phosphorylated over the course of a day, which promotes the phosphorylation and inactivation of the WCC (Figure 1.2) (Baker et al., 2012). By late night, FRQ is targeted for ubiquitination and degradation, leading to WCC dephosphorylation by PROTEIN PHOSPHATASE 2A (PP2A) and WCC binding to the *frq* promoter to induce *frq* expression (Figure 1.2) (Brunner and Schafmeier, 2006).

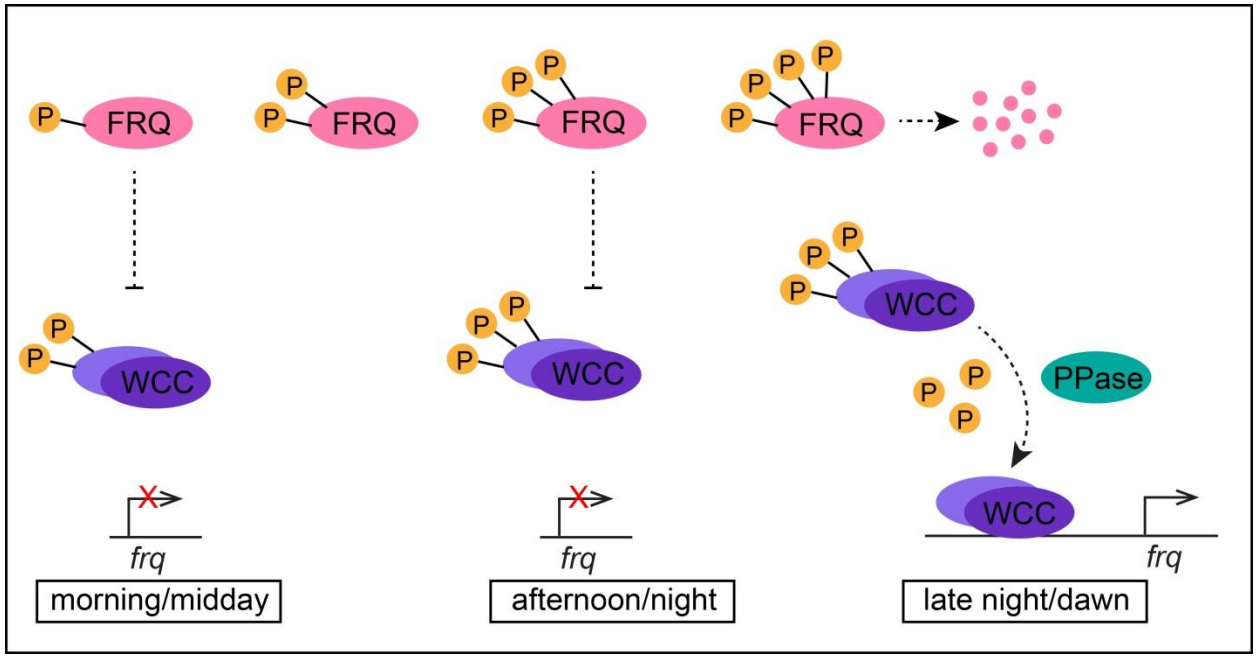

Figure 1.2. The *Neurospora crassa* clock. FRQ, FREQUENCY; WCC, White Collar Complex; PPase, phosphatase. "P" represents phosphorylation and small dots represent protein degradation.

Oscillating WCC regulates outputs by binding to LRE (Light-Response Elements) or WCC binding sites present in regulatory regions of various transcription factors that function to activate or repress clock-controlled genes (Lakin-Thomas et al., 2011).

Animals

Up to 10% of expressed genes cycle under constant conditions in the fruit fly *Drosophila melanogaster*, and examples of clock regulated behaviors include locomotion, courtship, and egg laying (Peschel and Helfrich-Forster, 2011; Tataroglu and Emery, 2014). One of the core transcription/translation feedback loops in *Drosophila* involves the bHLH and PAS domain-containing proteins Clock (Clk) and Cycle (Cyc) (Hardin, 2005). During the mid-day, Clk and Cyc form heterodimers to activate *Period* (*Per*) and *Timeless* (*Tim*) (Hardin, 2005). Per and Tim accumulate during the night and heterodimerizes as the kinase Doubletime (Dbt) progressively phosphorylates Per (Williams and Sehgal, 2001). Per, Tim, and Dbt form a complex that enters the nucleus and binds to Clk/Cyc to inhibit Clk/Cyc activity (Hardin, 2005). Thus, Per and Tim indirectly inhibit their own transcription. As Dbt itself becomes phosphorylated, Per/Tim/Dbt gets degraded and the cycle can begin once again (Hardin, 2005). *Per*, *Tim*, *Dbt*, *Clk*, and *Cyc* are all expressed in the photoreceptor cells of the compound eyes, as well as various parts of the fly brain (Helfrich-Forster, 2003). The fly brain houses circadian pacemaker neurons, in which the neuropeptide pigment dispersing factor (PDF) plays a major role in signaling to synchronize clusters of clock neurons and regulate downstream targets (Frenkel and Ceriani, 2011; Helfrich-Forster et al., 2011).

In mammals, depending on the tissues examined and the algorithms used for the data analysis, approximately 2-10% of expressed genes cycle under constant conditions, and clock-regulated

physiologies include thermoregulation, cardiovascular activity, and the sleep-wake cycle (Ko and Takahashi, 2006; Dibner et al., 2010). BHLH and PAS domain containing proteins BMAL1 (BMAL) and CLOCK (CLK) interact during the day to activate *PERIOD* (*PER*) and *CRYPTOCHROME* (*CRY*) transcription (Figure 1.3) (Takahashi et al., 2008). The phosphorylation of PER by CASEIN KINASE 1 (CK1) promotes PER interaction with CRY, resulting in their translocation into the nucleus (Robinson and Reddy, 2014). Here, PER/CRY inhibit BMAL/CLK resulting in the inhibition of *PER*/*CRY* expression (Figure 1.3) (Crane and Young, 2014). The hyperphosphorylation of PER/CRY leads to ubiquitination and degradation in the night, releasing BMAL/CLK to begin activation once again, thereby completing the loop (Figure 1.3) (Takahashi et al., 2008).

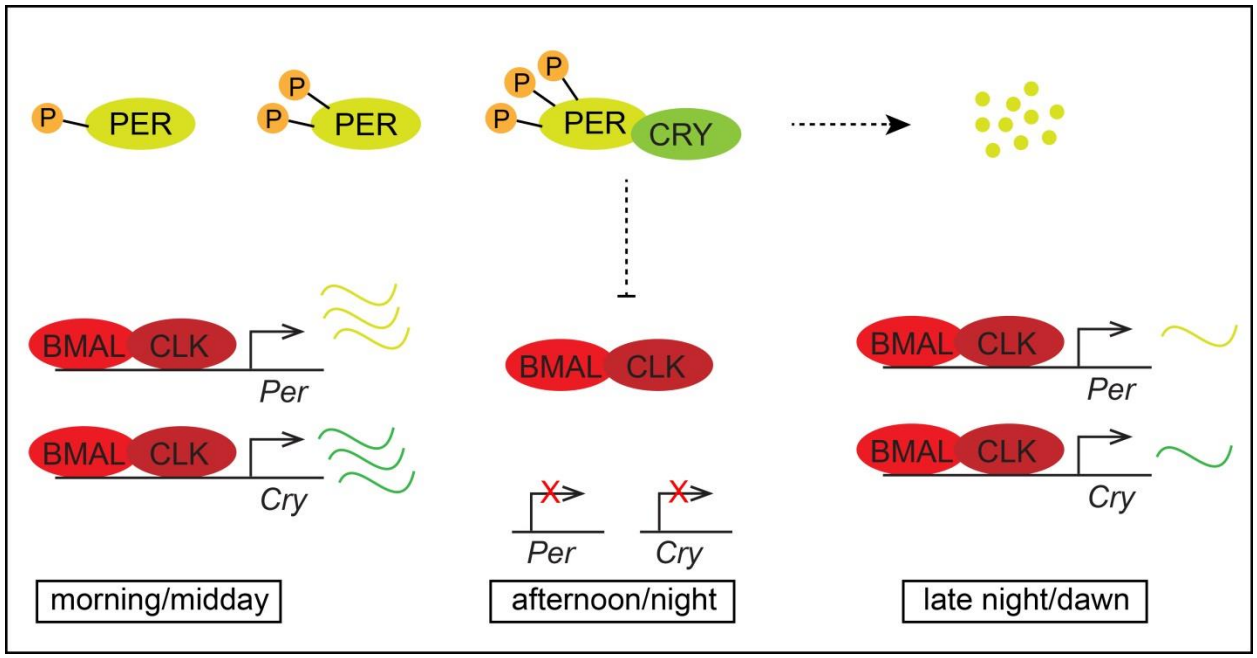

Figure 1.3. The animal clock. PER, PERIOD; CRY, CRYPTOCHROME; BMAL1, BRAIN AND MUSCLE ARNT-LIKE 1; CLK, CLOCK. "P" represents phosphorylation; small dots represent protein degradation; wavy lines represent gene expression.

Another BMAL/CLK target for activation is *Rev-erba,* in which REV-ERBA functions to repress *Bmal1* expression, thus forming another feedback loop in the mammalian clock (Takahashi et al., 2008). The central pacemaker is located in the suprachiasmatic nucleus (SCN) above the optic chiasma in the brain and receives light input from the retinas. Not only does the SCN regulate rhythmic hormonal and autonomic output, but the SCN also utilizes humoral or metabolic signals and glucocorticoid signaling to synchronize peripheral oscillators with the environment (Buijs et al., 2013). Additionally, the feed-fast cycle serves as a dominant entrainment signal and can directly entrain peripheral oscillators such as that of the liver (Dibner et al., 2010). Hepatic clock-regulated processes include fatty acid metabolism, glucose homeostasis, and cholesterol and bile acid synthesis (Dibner et al., 2010). Correspondingly, perturbations to the circadian clock have been linked to obesity, diabetes, and hypertension (Buijs et al., 2013).

Plants

One of the first observations made in circadian biology was the recurring opening and closing of plant leaves on a daily basis. Androsthenes is cited as the first documented observer of leaf movement back in 325 BC, Greece (Cumming and Wagner, 1968). In 1729, the French astronomer de Mairan observed that leaves continued to move even in darkness (Bunning, 1960). Similarly, in the mid-1700's Duhamel and Zinn independently confirmed that leaf movements were sustained under constant darkness in mimosa plants (Bunning, 1960). In regards to entrainment, the Swiss botanist de Candolle in 1832 reversed the normal light/dark exposure to dark/light and observed that leaf movements were altered accordingly (Bunning, 1960). In addition, the Swedish botanist Linnaeus wrote an essay on plants that "sleep" in 1755, and English naturalists Charles and Francis Darwin published "The Power of Movement in Plants"

depicting various plant movements including sleep movements of leaves in 1898 (Cumming and Wagner, 1968). Thus, the first key observations on circadian rhythms were made in plants and these findings contributed to the discovery of the circadian clock.

The plant circadian clock has been extensively studied and is best characterized in *Arabidopsis thaliana*. One of the first core clock components identified in Arabidopsis is TIMING OF CAB EXPRESSION 1 (TOC1) (Millar et al., 1995), a member of the PSEUDO RESPONSE REGULATOR (PRR) family of circadian clock components. The PRRs share a conserved Pseudo-Receiver (PR) domain similar to the Response Regulator (RR) domain of two-component response regulators, but Arabidopsis PRs contain a glutamate in place of the conserved phospho-accepting aspartate resulting in the loss of phospho-relay activity (Makino et al., 2000). Expression and protein accumulation of PRRs peak sequentially, starting with PRR9 during the day, PRR7 around dusk, PRR5 and PRR3 in the early night, and TOC1 thereafter (Figure 1.4) (Fujiwara et al., 2008). The PRRs share a conserved CCT (CONSTANS, CONSTANS-LIKE, and TOC1) motif, which is necessary for TOC1 and PRR5 binding to DNA (Gendron et al., 2012; Nakamichi et al., 2012). PRRs 9, 7, and 5 each contain an EAR (Ethylene-responsive element binding factor-associated Amphiphilic Repression) motif in the intervening region between the PR and CCT domains, which interacts with the Groucho/Tup1 corepressors TOPLESS/TOPLESS-RELATED (TPL/TPR) to confer transcriptional repression activity (Wang et al., 2013).

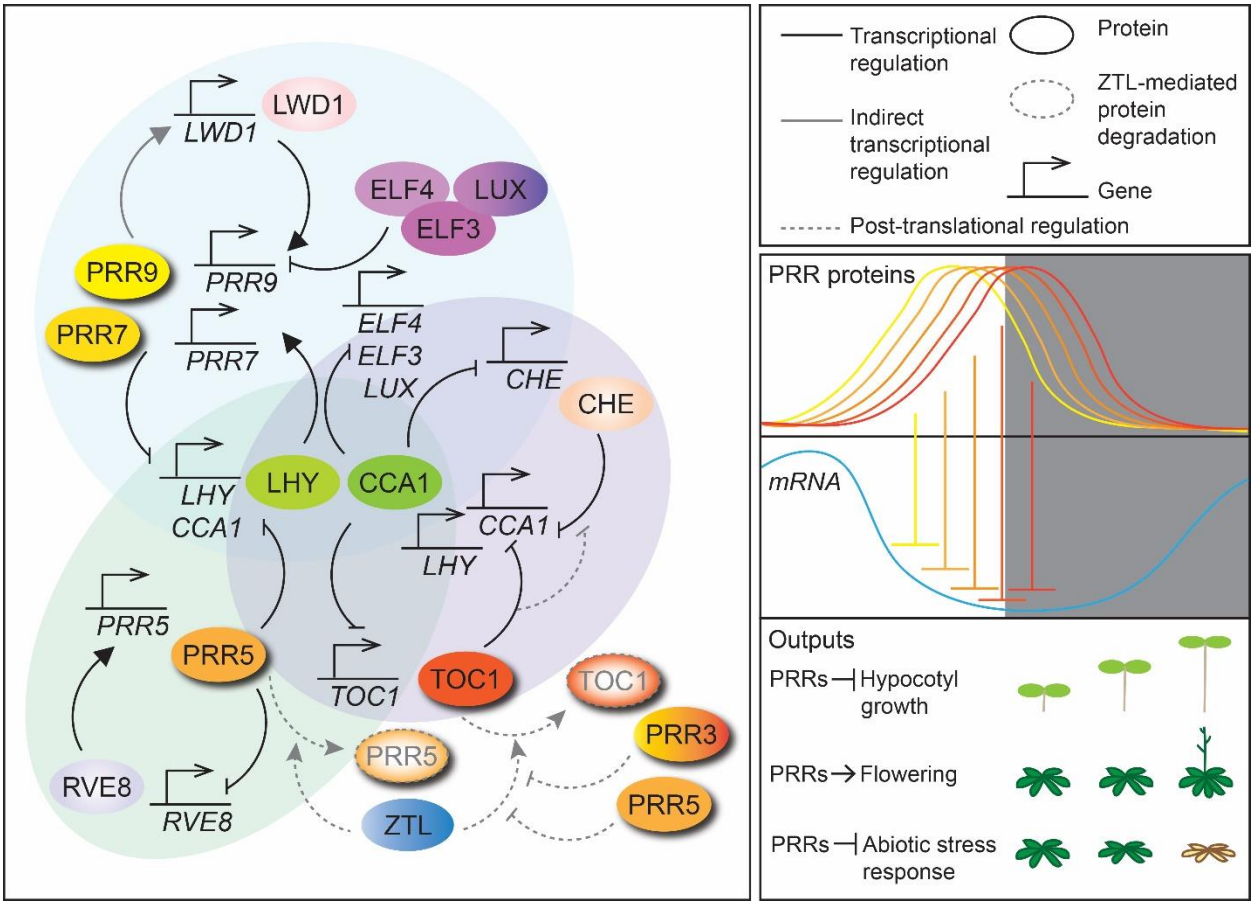

Figure 1.4. The Arabidopsis clock. Figure adapted from (Farre and Liu, 2013). Right panel: PRRs repress the expression of many morning-expressed genes influencing physiological processes. PRRs, PSEUDO RESPONSE REGULATORs; TOC1, TIMING OF CAB EXPRESSION 1; CCA1, CIRCADIAN CLOCK ASSOCIATED 1; LHY, LATE ELONGATED HYPOCOTYL; ELF4, EARLY FLOWERING 4; ELF3, EARLY FLOWERING 3; LUX, LUX ARRHYTHMO; CHE, CCA1 HIKING EXPEDITION; ZTL, ZEITLUPE; RVE8, REVEILLE 8; LWD1, LIGHT-REGULATED WD1.

TOC1 was thought to positively regulate the expression of two MYB transcription factors, *CCA1* and *LHY*, due to the low levels of their transcripts observed in the *toc1-2* mutant (Alabadi et al., 2001). This positive regulation was proposed to act through TOC1 sequestration of CCA1

HIKING EXPEDITION (CHE), a TCP (TEOSINTE BRANCHED, CYCLOIDEA, and PROLIFERATING CELL FACTOR) transcription factor that represses *CCA1* (Figure 1.4) (Pruneda-Paz et al., 2009). However, a TOC1 overexpressing line also showed dampened levels of *CCA1* and *LHY* expression (Makino et al., 2002). More recently, TOC1 was shown to directly bind the *CCA1* promoter to repress *CCA1* expression directly (Figure 1.4) (Gendron et al., 2012; Huang et al., 2012). In return, CCA1 and LHY negatively regulate *TOC1* by binding to its promoter (Figure 1.4) (Alabadi et al., 2001). CCA1 repression of *TOC1* also corresponds with histone deacetylation (Perales and Mas, 2007). Conversely, the MYB-containing transcription factor REVEILLE 8 (RVE8) is an activator of *TOC1* expression and RVE8 binding to the *TOC1* promoter correlates with histone acetylation (Farinas and Mas, 2011). Post-translational regulation of TOC1 involves ZEITLUPE (ZTL) -mediated protein degradation, which is hindered by TOC1 interacting with PRR3 (Figure 1.4) (Para et al., 2007). The interaction between TOC1 and PRR5 also promotes stability and accumulation in the nucleus (Wang et al., 2010). Among the PRRs, only TOC1 and PRR5 are targeted for proteolysis by F-box proteins ZTL, FKF1 (FLAVIN BINDING, KELCH REPEAT, F-BOX 1), and LKP2 (LOVE KELCH PROTEIN 2) (Figure 1.4) (Fujiwara et al., 2008; Baudry et al., 2010).

Similar to TOC1, PRRs 9, 7, and 5 bind to the promoters of *CCA1* and *LHY* to negatively regulate their expression (Figure 1.4) (Farre and Kay, 2007; Nakamichi et al., 2010). PRR9 forms a complex with TPL and histone deacetylase HDA6 to repress *CCA1* and *LHY* (Wang et al., 2013). In return, CCA1 and LHY positively regulate the expression of *PRR9* and *PRR7* (Figure 1.4) (Farre et al., 2005). LIGHT-REGULATED WD1 (LWD1) also directly activates *PRR9* expression, and likewise, PRR9 indirectly promotes the expression of *LWD1* (Figure 1.4) (Wang et al., 2011). The repression of *PRR9*, on the other hand, involves the direct binding of

the Myb-like GARP transcription factor LUX ARRYTHMO (LUX/PCL1), EARLY FLOWERING 3 (ELF3), and likely ELF4 to the *PRR9* promoter (Figure 1.4) (Helfer et al., 2011; Chow et al., 2012). *PRR9* levels are extremely repressed in a TOC1 overexpressing line (Makino et al., 2002), and TOC1 has been shown to directly bind to the *PRR9* promoter (Huang et al., 2012). Post-transcriptional regulation of *PRR9* involves PROTEIN ARGININE METHYL TRANSFERASE 5 (PRMT5) -mediated alternative splicing; *prmt5* mutants express *PRR9* transcripts with a higher retention of intron 3 (Sanchez et al., 2010). RVE8 plays a role in directly activating *PRR5*, whereas PRR5 represses *RVE8* in return (Figure 1.4) (Rawat et al., 2011). The PRRs play central roles within the circadian clock and mutations in the PRRs result in altered circadian rhythms, ultimately leading to elongated hypocotyl lengths, delayed flowering times, as well as increased tolerance to drought and cold as observed in the *prr9prr7prr5* (*prr975*) triple mutant (Figure 1.4) (Nakamichi et al., 2009).

Many clock components from the unicellular green alga *Chlamydomonas reinhardtii* share domains with Arabidopsis clock components (Matsuo and Ishiura, 2010). Approximately 3% of *Chlamydomonas* genes cycle under constant conditions, and clock-regulated outputs include phototaxis during the day and chemotaxis at night, cell division, and rhythmic starch content (Kucho et al., 2005; Matsuo and Ishiura, 2010). Likewise *Ostreococcus tauri*, the smallest free-living eukaryote located at the base of the green plant lineage, contains two putative TOC1 and CCA1 homologs (Corellou et al., 2009). TOC1 appears to activate *CCA1* whereas CCA1 likely represses *TOC1*, although this transcription/translation feedback loop may be an oversimplification since other factors are likely involved (Corellou et al., 2009; McClung, 2013). Phylogenetic analyses show conservation of PRR protein sequences in green algae, liverworts, mosses, and lycophytes (Farre and Liu, 2013). Thus, the presence of conserved clock

components within the green plant lineage suggests that plant clocks evolved early on and share a common ancestor.

Inputs to the plant clock

The circadian clock can be entrained by various cues to synchronize the internal oscillator with the external environment.

Light Input

Light is one of the most important external cues for entrainment and a prevailing question has been how external light cues get incorporated into the clock. Red/far-red light-absorbing photoreceptors, phytochromes (phy) phyA, phyB, phyD, and phyE as well as the blue light absorbing cryptochromes (cry) cry1 and cry2, mediate visible light input into the clock (Devlin and Kay, 2000). Yeom et al. (2014) recently showed that phyB may relay light quality information to the circadian clock by preferentially binding to CCA1 and TOC1 under far-red light, or to LUX under red light. In addition, phyB can bind to clock components LHY, GIGANTEA (GI), and ELF3 under both red and far-red light, but no interaction was observed between phyB and PRR9, PRR7, or ELF4 (Yeom et al., 2014). Further studies are necessary to investigate the relevance of these interactions. Blue light sensing F-box proteins ZTL, FKF1, and LKP2 also interact with GI; ZTL and GI were shown to form a stable complex under blue light conditions (Kim et al., 2007). The UV-B light photoreceptor UV RESISTANCE LOCUS 8 (UVR8) interacts with CONSTITUTIVELY PHOTOMORPHOGENIC 1 (COP1) under UV-B light, and these two components have been shown to be necessary for UV-B light entrainment of the circadian clock (Favory et al., 2009; Feher et al., 2011).

Temperature Input

C-REPEAT/DRE BINDING FACTOR 1 (CBF1) has been shown to mediate cold temperature input into the clock by directly binding to the *LUX* promoter and positively regulating its transcription (Chow et al., 2014). In addition, the evening complex (EC) composed of LUX, ELF3, and ELF4 has been implicated in temperature responsiveness since the upregulation and downregulation of *PRR7*, *GI*, and *LUX* is abolished in EC mutants during temperature upshifts and downshifts, respectively (Mizuno et al., 2014).

Metabolic Input

Although the exact mechanism is unknown, exogenous sucrose has an effect on the circadian clock, on both the amplitude as well as the period of different circadian reporters. Dalchau et al. (2011) conducted experiments in which sucrose was added at different times of the day, resulting in peak expression of circadian reporters approximately 24 hours after the time of sucrose addition. Haydon et al. (2013) observed that the inhibition of photosynthesis by DCMU (3-(3,4-dichlorophenyl)-1,1-dimethylurea) increased the amplitude and period length of the *PRR7* reporter, while the addition of sucrose resulted in a smaller amplitude and shortened period. No effect was observed in the *prr7* mutant upon sucrose addition. Therefore, the authors hypothesized that the output of photosynthesis in the form of sucrose serves as metabolic input in a feedback mechanism to entrain the clock through PRR7 (Haydon et al., 2013).

Outputs

Approximately 30% of the Arabidopsis transcriptome is circadian regulated, while around 90% of genes display oscillations in expression levels under cycling environmental conditions,

suggesting that many biological processes are circadian regulated (Covington et al., 2008; Michael et al., 2008). Of the clock-regulated outputs (Table 1.1), hypocotyl growth, photoperiodic control of flowering, and cold acclimation are the best described pathways, which will be further discussed below.

Table 1.1. Biological processes regulated by the circadian clock**.**

Circadian regulated biological processes	**Reference**
Rhythmic leaf movement	(Bunning, 1967; Millar et al., 1995)
Petal opening	(Bunning, 1967)
Elongation rate of stems, hypocotyls, and roots	(Lecharny et al., 1985; Dowson-Day and Millar, 1999; Nozue et al., 2007; Nusinow et al., 2011; Yazdanbakhsh et al., 2011)
Circumnutation of stems	(Niinuma et al., 2005)
Primary and secondary metabolite biosynthesis	(Warren and Wilkins, 1961; Kolosova et al., 2001; Blasing et al., 2005; Fukushima et al., 2009)
Hormone biosynthesis and responses	(Thain et al., 2004; Covington and Harmer, 2007; Covington et al., 2008; Michael et al., 2008; Mizuno and Yamashino, 2008)
Water stress responses	(Fowler et al., 2005; Bieniawska et al., 2008; Kidokoro et al., 2009; Legnaioli et al., 2009; Nakamichi et al., 2009)
Stomatal opening	(Holmes and Klein, 1986; Somers et al., 1998)
Ca2+ concentrations in certain cellular compartments	(Johnson et al., 1995; Xu et al., 2007)
Water uptake	(Takase et al., 2011)
Seed dormancy	(Penfield and Hall, 2009)
Defense against pathogens and herbivory	(Wang et al., 2011; Goodspeed et al., 2012)
UV-B signaling and stress response	(Feher et al., 2011; Takeuchi et al., 2014)
Starch turnover	(Graf et al., 2010)
Photoperiodic control of flowering	(Suarez-Lopez et al., 2001)
Iron homeostasis	(Duc et al., 2009)

Modified from (Nakamichi, 2011).

Hypocotyl Growth

The hypocotyledonous stem, or hypocotyl, is the stem of a germinating seedling. Hypocotyl growth in Arabidopsis is rhythmic, with elongation maximally occurring around dawn (Nozue et al., 2007). Regulators of hypocotyl growth include the PHYTOCHROME INTERACTING FACTOR (PIF) family of bHLH transcription factors, of which PIF4 and PIF5 are the best characterized in the context of the circadian clock. PIFs promote skotomorphogenesis in the dark. They accumulate to high levels during the late night and are degraded to low levels in the light (Nozue et al., 2007). Specifically, the EC binds to the promoters of *PIF4* and *PIF5* to repress hypocotyl growth during the early night (Nusinow et al., 2011). *PIF4* and *PIF5* are also targets for repression by PRR7, PRR5, and TOC1 (Huang et al., 2012; Nakamichi et al., 2012; Liu et al., 2013). This internal regulation by the circadian clock during the early night combined with light regulation of the PIF protein levels through phytochrome-mediated degradation during the day culminates in rhythmic hypocotyl growth (Nozue et al., 2007; Leivar and Quail, 2011).

Photoperiodic Flowering

The circadian clock is involved in the photoperiodic control of flowering in the long day plant Arabidopsis. The zinc-finger-containing protein CONSTANS (CO) promotes flowering by positively regulating *FLOWERING LOCUS T* (*FT*). During short days, *CO* mRNA peaks at night and CO proteins are quickly degraded in the dark (Yanovsky and Kay, 2003; Valverde et al., 2004). However, during long days CO transcription and translation coincides with daylight in the late afternoon, resulting in stable CO protein, which positively regulates *FT* to induce flowering (Yanovsky and Kay, 2003; Valverde et al., 2004). Circadian clock components PRR9, PRR7, and PRR5 promote flowering by negatively regulating *CYCLING DOF FACTOR 1* (*CDF1*),

which is a negative regulator of *CO* (Nakamichi et al., 2007). CDF1 is also post-translationally regulated through FKF1-mediated protein degradation, dependent on FKF1 interacting with circadian regulated GIGANTEA (GI) during long days (Imaizumi et al., 2005; Sawa et al., 2007). GI has also been shown to bind to the promoter of *FT* and induce *FT* expression independently of *CO* (Sawa and Kay, 2011). Altogether, the integration of light and the circadian clock provides day-length information to ensure flowering occurs at the appropriate time (Kinmonth-Schultz et al., 2013).

Cold Acclimation

Gating describes a feature of the circadian clock in which a particular stimulus can elicit a response (open gate) or little to no response (closed gate) depending on the time of exposure during a 24-hour cycle. CBF1, 2, and 3 are AP2/ERF domain-containing transcription factors that promote freezing tolerance in Arabidopsis, and cold induction of the *CBF*s is gated by the circadian clock (Fowler et al., 2005). CCA1 and LHY were shown to positively regulate the *CBF*s by binding to their promoters, and a *cca1lhy* double mutant showed reduced cold induction of the CBFs as well as impaired freezing tolerance (Dong et al., 2011). Constitutive expression of the CBFs confers freezing tolerance, but also results in impaired growth and development (Fowler et al., 2005). Thus, the circadian regulation of the cold acclimation pathway enables the organism to respond at appropriate times, resulting in optimized resource management.

AIMS OF THESIS RESEARCH

Upwards of 90% of expressed genes oscillate under cycling conditions, while approximately 30% of expressed genes continue to cycle under constant conditions, revealing that almost a third

of the Arabidopsis transcriptome is circadian regulated (Covington et al., 2008; Michael et al., 2008). Information regarding which core clock components are responsible for regulating these genes remains limited. Therefore, the main goal of my research was to define the regulatory network of two partially redundant circadian clock components, PRR9 and PRR7 (Farre et al., 2005). Out of the five PRR clock components, *PRR9* and *PRR7* have been shown to be positively regulated by CCA1 and LHY (Farre et al., 2005). In return, PRR9 and PRR7 directly bind to the promoters of *CCA1* and *LHY* to repress their gene expression, thereby completing a major transcriptional/translational feedback loop within the circadian clock (Farre and Kay, 2007; Nakamichi et al., 2010).

Mis-expression of PRR9 and PRR7 result in alterations to the clock and downstream processes. A PRR9 overexpressing line exhibits shorter periods and flowers early compared to WT (Matsushika et al., 2002). *prr9* single mutants, however, display very slight phenotypes, appearing similar to WT, except for a lengthened period under various fluences of red or blue light (Farre et al., 2005; Nakamichi et al., 2005). *prr7* mutants, on the other hand, display elongated hypocotyls and delayed flowering times under long days and these changes are exacerbated in the *prr9prr7* double mutant, indicating that PRR9 and PRR7 are partially redundant (Nakamichi et al., 2005). Additionally, the *prr9prr7prr5* triple mutant exhibits an increased tolerance to cold and drought compared to WT (Nakamichi et al., 2009). My first aim is to determine the genome-wide targets of PRR9 and PRR7, which would shed light on the mechanisms responsible for the observed mutant phenotypes as well as uncover new pathways regulated by PRR9 and PRR7. My experimental strategy involves conducting chromatin immunoprecipitation followed by high-throughput sequencing to identify PRR9 and PRR7 targets on a genome-wide scale. Without this knowledge, we would be unable to make specific

connections between the endogenous time-keeping mechanism and how it regulates overall plant physiology.

When I first started my research, there were no publications identifying the genome-wide targets of any circadian clock component. In addition, the mechanism by which the PRRs regulate target genes was poorly understood. Although the PRRs do not contain a known DNA binding domain, the CCT motif was shown to bind DNA *in vitro* and the PRR5 CCT motif associates with the *CCA1* promoter *in vivo* (Gendron et al., 2012; Nakamichi et al., 2012). These findings suggest that the PRRs can bind DNA directly, and I wanted to investigate whether this is the case for PRR9 and PRR7. I was also interested in determining whether PRR9 and PRR7 bind to a particular *cis*-regulatory element to regulate transcription. In addition, two separate research teams published articles detailing the genome-wide targets of PRR5 and TOC1 (Huang et al., 2012; Nakamichi et al., 2012). Using their data in combination with the ChIP-seq datasets that I generated for PRR9 and PRR7, I can explore how target genes compare among the four PRRs. Thus, my second aim is to investigate the mechanism by which PRRs regulate target genes. My experimental strategy is to uniformly analyze ChIP-seq data on PRR9, PRR7, PRR5, and TOC1 in order to conduct a comparative analysis and address open questions regarding PRR transcriptional regulation.

In Chapter 2, I determined the biological processes regulated by PRR7, showing that they can explain several *prr9prr7prr5* triple mutant phenotypes. In particular, PRR7 represses master regulators of plant growth, light signaling, and stress responses. Additionally, I found that G-box-containing elements are enriched at PRR7 binding sites. In Chapter 3, I determined the biological processes regulated by PRR9 and compared them to PRR7, PRR5, and TOC1 ChIP-

seq datasets. I showed that the PRRs bind to the same regions of DNA to regulate common target genes. In addition, I observed that PRR binding sites are located in functional regulatory regions, showing conservation among non-coding sequences of nine Brassicaceae species. Again, I found that G-box-containing elements are enriched at the binding sites for each of the four PRRs. Therefore, in Chapter 4 I explored whether PRR9 and PRR7 can directly bind G-boxes or if they interact with G-box binding transcription factors to regulate target genes. I did not observe direct binding of PRR9 and PRR7 to G-boxes in a heterologous system. I then hypothesized that PRR9 and PRR7 may be interacting with G-box binding transcription factors to mediate transcriptional regulation. I observed a high overlap between PRR9 and PRR7 targets with those of G-box binding transcription factors PIF1 and HY5, as well as FHY3. I have yet to identify a binding partner for PRR9 and PRR7 based on my initial studies, but I have explored potential candidates that can be further examined in future experiments.

Findings from my research have enabled me to comprehensively define the roles of PRR9 and PRR7 in transcriptionally regulating clock components and clock controlled genes, as well as develop and test new hypotheses regarding the mechanism of PRR transcriptional regulation. Thus, my large-scale study on PRR9 and PRR7 provides a rich resource, not only for circadian biologists, but also for researchers interested in identifying the master regulators of their genes of interest. Continued efforts in identifying the direct target genes of clock components would help elucidate the complex gene regulatory network of the circadian clock.

REFERENCES

REFERENCES

Alabadi D, Oyama T, Yanovsky MJ, Harmon FG, Mas P, Kay SA (2001) Reciprocal regulation between TOC1 and LHY/CCA1 within the Arabidopsis circadian clock. Science **293:** 880-883

Baker CL, Loros JJ, Dunlap JC (2012) The circadian clock of Neurospora crassa. Fems Microbiology Reviews **36:** 95-110

Baudry A, Ito S, Song YH, Strait AA, Kiba T, Lu S, Henriques R, Pruneda-Paz JL, Chua NH, Tobin EM, Kay SA, Imaizumi T (2010) F-box proteins FKF1 and LKP2 act in concert with ZEITLUPE to control Arabidopsis clock progression. Plant Cell **22:** 606-622

Bieniawska Z, Espinoza C, Schlereth A, Sulpice R, Hincha DK, Hannah MA (2008) Disruption of the Arabidopsis circadian clock is responsible for extensive variation in the cold-responsive transcriptome. Plant Physiology **147:** 263-279

Blasing OE, Gibon Y, Gunther M, Hohne M, Morcuende R, Osuna D, Thimm O, Usadel B, Scheible WR, Stitt M (2005) Sugars and circadian regulation make major contributions to the global regulation of diurnal gene expression in Arabidopsis. Plant Cell **17:** 3257-3281

Brunner M, Schafmeier T (2006) Transcriptional and post-transcriptional regulation of the circadian clock of cyanobacteria and Neurospora. Genes and Development **20:** 1061-1074

Buijs R, Salgado R, Sabath E, Escobar C (2013) Peripheral Circadian Oscillators: Time and Food. *In* MU Gillette, ed, Chronobiology: Biological Timing in Health and Diesease, Vol 119. Elsevier Academic Press Inc, San Diego, pp 83-103

Bunning E (1960) Opening address: Biological clocks. Cold Spring Harbor Symposia on Quantitative Biology **25:** 1-9

Bunning E (1967) The physiological clock. Springer-Verlag Inc., New York

Chow BY, Helfer A, Nusinow DA, Kay SA (2012) ELF3 recruitment to the PRR9 promoter requires other Evening Complex members in the Arabidopsis circadian clock. Plant Signaling and Behavior **7:** 170-173

Chow BY, Sanchez SE, Breton G, Pruneda-Paz JL, Krogan NT, Kay SA (2014) Transcriptional regulation of LUX by CBF1 mediates cold input to the circadian clock in Arabidopsis. Current Biology **24:** 1518-1524

Corellou F, Schwartz C, Motta JP, Djouani-Tahri E, Sanchez F, Bouget FY (2009) Clocks in the Green Lineage: Comparative Functional Analysis of the Circadian Architecture of the Picoeukaryote Ostreococcus. Plant Cell **21:** 3436-3449

Covington MF, Harmer SL (2007) The circadian clock regulates auxin signaling and responses in Arabidopsis. PLoS Biology **5:** 1773-1784

Covington MF, Maloof JN, Straume M, Kay SA, Harmer SL (2008) Global transcriptome analysis reveals circadian regulation of key pathways in plant growth and development. Genome Biology **9**

Crane BR, Young MW (2014) Interactive features of proteins composing eukaryotic circadian clocks. Annual Review of Biochemistry **83:** 191-219

Cumming BG, Wagner E (1968) Rhythmic Processes in Plants. Annual Review of Plant Physiology **19:** 381-416

Dalchau N, Baek SJ, Briggs HM, Robertson FC, Dodd AN, Gardner MJ, Stancombe MA, Haydon MJ, Stan G-B, Goncalves JM, Webb AAR (2011) The circadian oscillator gene GIGANTEA mediates a long-term response of the Arabidopsis thaliana circadian clock to sucrose. Proceedings of the National Academy of Sciences of the United States of America **108:** 5104-5109

Devlin PF, Kay SA (2000) Cryptochromes are required for phytochrome signaling to the circadian clock but not for rhythmicity. Plant Cell **12:** 2499-2509

Dibner C, Schibler U, Albrecht U (2010) The Mammalian Circadian Timing System: Organization and Coordination of Central and Peripheral Clocks. *In* Annual Review of Physiology, Vol 72. Annual Reviews, Palo Alto, pp 517-549

Dodd AN, Salathia N, Hall A, Kevei E, Toth R, Nagy F, Hibberd JM, Millar AJ, Webb AAR (2005) Plant circadian clocks increase photosynthesis, growth, survival, and competitive advantage. Science **309:** 630-633

Dong MA, Farre EM, Thomashow MF (2011) CIRCADIAN CLOCK-ASSOCIATED 1 and LATE ELONGATED HYPOCOTYL regulate expression of the C-REPEAT BINDING FACTOR (CBF) pathway in Arabidopsis. Proceedings of the National Academy of Sciences of the United States of America **108:** 7241-7246

Dowson-Day MJ, Millar AJ (1999) Circadian dysfunction causes aberrant hypocotyl elongation patterns in Arabidopsis. Plant Journal **17:** 63-71

Duc C, Cellier F, Lobreaux S, Briat JF, Gaymard F (2009) Regulation of Iron Homeostasis in Arabidopsis thaliana by the Clock Regulator Time for Coffee. Journal of Biological Chemistry **284:** 36271-36281

Edgar RS, Green EW, Zhao YW, van Ooijen G, Olmedo M, Qin XM, Xu Y, Pan M, Valekunja UK, Feeney KA, Maywood ES, Hastings MH, Baliga NS, Merrow M, Millar AJ, Johnson CH, Kyriacou CP, O'Neill JS, Reddy AB (2012) Peroxiredoxins are conserved markers of circadian rhythms. Nature **485:** 459-464

Farinas B, Mas P (2011) Functional implication of the MYB transcription factor RVE8/LCL5 in the circadian control of histone acetylation. Plant Journal **66:** 318-329

Farre EM, Harmer SL, Harmon FG, Yanovsky MJ, Kay SA (2005) Overlapping and distinct roles of PRR7 and PRR9 in the Arabidopsis circadian clock. Current Biology **15:** 47-54

Farre EM, Kay SA (2007) PRR7 protein levels are regulated by light and the circadian clock in Arabidopsis. Plant Journal **52:** 548-560

Farre EM, Liu T (2013) The PRR family of transcriptional regulators reflects the complexity and evolution of plant circadian clocks. Current Opinion in Plant Biology **16:** 621-629

Favory J-J, Stec A, Gruber H, Rizzini L, Oravecz A, Funk M, Albert A, Cloix C, Jenkins GI, Oakeley EJ, Seidlitz HK, Nagy F, Ulm R (2009) Interaction of COP1 and UVR8 regulates UV-B-induced photomorphogenesis and stress acclimation in Arabidopsis. EMBO Journal **28:** 591-601

Feher B, Kozma-Bognar L, Kevei E, Hajdu A, Binkert M, Davis SJ, Schafer E, Ulm R, Nagy F (2011) Functional interaction of the circadian clock and UV RESISTANCE LOCUS 8-controlled UV-B signaling pathways in Arabidopsis thaliana. Plant Journal **67:** 37-48

Fowler SG, Cook D, Thomashow ME (2005) Low temperature induction of Arabidopsis CBF1, 2, and 3 is gated by the circadian clock. Plant Physiology **137:** 961-968

Frenkel L, Ceriani MF (2011) Circadian plasticity: from structure to behavior. *In* N Atkinson, ed, Recent Advances in the Use of Drosophila in Neurobiology and Neurodegeneration, Vol 99. Elsevier Academic Press Inc, San Diego, pp 107-138

Fujiwara S, Wang L, Han L, Suh SS, Salome PA, McClung CR, Somers DE (2008) Post-translational regulation of the Arabidopsis circadian clock through selective proteolysis and phosphorylation of pseudo-response regulator proteins. Journal of Biological Chemistry **283:** 23073-23083

Fukushima A, Kusano M, Nakamichi N, Kobayashi M, Hayashi N, Sakakibara H, Mizuno T, Saito K (2009) Impact of clock-associated Arabidopsis pseudo-response regulators in metabolic coordination. Proceedings of the National Academy of Sciences of the United States of America **106:** 7251-7256

Gendron JM, Pruneda-Paz JL, Doherty CJ, Gross AM, Kang SE, Kay SA (2012) Arabidopsis circadian clock protein, TOC1, is a DNA-binding transcription factor.

Proceedings of the National Academy of Sciences of the United States of America **109:** 3167-3172

Golden SS, Canales SR (2003) Cyanobacterial circadian clocks - Timing is everything. Nature Reviews Microbiology **1:** 191-199

Goodspeed D, Chehab EW, Min-Venditti A, Braam J, Covington MF (2012) Arabidopsis synchronizes jasmonate-mediated defense with insect circadian behavior. Proceedings of the National Academy of Sciences of the United States of America **109:** 4674-4677

Graf A, Schlereth A, Stitt M, Smith AM (2010) Circadian control of carbohydrate availability for growth in Arabidopsis plants at night. Proceedings of the National Academy of Sciences of the United States of America **107:** 9458-9463

Hardin PE (2005) The circadian timekeeping system of Drosophila. Current Biology **15:** R714-R722

Haydon MJ, Mielczarek O, Robertson FC, Hubbard KE, Webb AAR (2013) Photosynthetic entrainment of the Arabidopsis thaliana circadian clock. Nature **502:** 689-692

Helfer A, Nusinow DA, Chow BY, Gehrke AR, Bulyk ML, Kay SA (2011) LUX ARRHYTHMO Encodes a Nighttime Repressor of Circadian Gene Expression in the Arabidopsis Core Clock. Current Biology **21:** 126-133

Helfrich-Forster C (2003) The neuroarchitecture of the circadian clock in the brain of Drosophila melanogaster. Microscopy Research and Technique **62:** 94-102

Helfrich-Forster C, Nitabach MN, Holmes TC (2011) Insect circadian clock outputs. *In* HD Piggins, C Guilding, eds, Essays in Biochemistry: Chronobiology, Vol 49. Portland Press Ltd, London, pp 87-101

Holmes MG, Klein WH (1986) Photocontrol of Dark Circadian Rhythms in Stomata of *Phaseolus vulgaris* L. Plant Physiology **82:** 28-33

Huang W, Pérez-García P, Pokhilko A, Millar AJ, Antoshechkin I, Riechmann JL, Mas P (2012) Mapping the Core of the Arabidopsis Circadian Clock Defines the Network Structure of the Oscillator. Science **336:** 75-79

Imaizumi T, Schultz TF, Harmon FG, Ho LA, Kay SA (2005) FKF1F-BOX protein mediates cyclic degradation of a repressor of CONSTANS in Arabidopsis. Science **309:** 293-297

Ito H, Mutsuda M, Murayama Y, Tomita J, Hosokawa N, Terauchi K, Sugita C, Sugita M, Kondo T, Iwasaki H (2009) Cyanobacterial daily life with Kai-based circadian and diurnal genome-wide transcriptional control in Synechococcus elongatus. Proceedings of the National Academy of Sciences of the United States of America **106:** 14168-14173

Johnson CH, Knight MR, Kondo T, Masson P, Sedbrook J, Haley A, Trewavas A (1995) Circadian oscillations of cytosolic and chloroplastic free calcium in plants. Science **269:** 1863-1865

Kidokoro S, Maruyama K, Nakashima K, Imura Y, Narusaka Y, Shinwari ZK, Osakabe Y, Fujita Y, Mizoi J, Shinozaki K, Yamaguchi-Shinozaki K (2009) The phytochrome-interacting factor PIF7 negatively regulates DREB1 expression under circadian control in Arabidopsis. Plant Physiology **151:** 2046-2057

Kim WY, Fujiwara S, Suh SS, Kim J, Kim Y, Han LQ, David K, Putterill J, Nam HG, Somers DE (2007) ZEITLUPE is a circadian photoreceptor stabilized by GIGANTEA in blue light. Nature **449:** 356-360

Kinmonth-Schultz HA, Golembeski GS, Imaizumi T (2013) Circadian clock-regulated physiological outputs: Dynamic responses in nature. Seminars in Cell and Developmental Biology **24:** 407-413

Ko CH, Takahashi JS (2006) Molecular components of the mammalian circadian clock. Human Molecular Genetics **15:** R271-R277

Kolosova N, Gorenstein N, Kish CM, Dudareva N (2001) Regulation of circadian methyl benzoate emission in diurnally and nocturnally emitting plants. Plant Cell **13:** 2333-2347

Kondo T, Ishiura M (2000) The circadian clock of cyanobacteria. Bioessays **22:** 10-15

Kucho K, Okamoto K, Tabata S, Fukuzawa H, Ishiura M (2005) Identification of novel clock-controlled genes by cDNA macroarray analysis in Chlamydomonas reinhardtii. Plant Molecular Biology **57:** 889-906

Lakin-Thomas PL, Bell-Pedersen D, Brody S (2011) The Genetics of Circadian Rhythms in Neurospora. *In* S Brody, ed, Genetics of Circadian Rhythms, Vol 74. Elsevier Academic Press Inc, San Diego, pp 55-103

Lecharny A, Schwall M, Wagner E (1985) Stem Extension Rate in Light-Grown Plants: Effects of Photo- and Thermoperiodic Treatments on the Endogenous Circadian Rhythm in Chenopodium rubrum. Plant Physiology **79:** 625-629

Legnaioli T, Cuevas J, Mas P (2009) TOC1 functions as a molecular switch connecting the circadian clock with plant responses to drought. Embo Journal **28:** 3745-3757

Leivar P, Quail PH (2011) PIFs: pivotal components in a cellular signaling hub. Trends in Plant Science **16:** 19-28

Liu T, Carlsson J, Takeuchi T, Newton L, Farre EM (2013) Direct regulation of abiotic responses by the Arabidopsis circadian clock component PRR7. Plant Journal **76:** 101-114

Mackey SR, Golden SS, Ditty JL (2011) The Itty-Bitty Time Machine: Genetics of the Cyanobacterial Circadian Clock. *In* S Brody, ed, Genetics of Circadian Rhythms, Vol 74, pp 13-53

Makino S, Kiba T, Imamura A, Hanaki N, Nakamura A, Suzuki T, Taniguchi M, Ueguchi C, Sugiyama T, Mizuno T (2000) Genes encoding pseudo-response regulators: Insight into His-to-Asp phosphorelay and circadian rhythm in Arabidopsis thaliana. Plant and Cell Physiology **41:** 791-803

Makino S, Matsushika A, Kojima M, Yamashino T, Mizuno T (2002) The APRR1/TOC1 quintet implicated in circadian rhythms of Arabidopsis thaliana: 1. Characterization with APRR1-overexpressing plants. Plant and Cell Physiology **43:** 58-69

Matsuo T, Ishiura M (2010) New insights into the circadian clock in Chlamydomonas. *In* KW Jeon, ed, International Review of Cell and Molecular Biology, Vol 280, Vol 280. Elsevier Academic Press Inc, San Diego, pp 281-314

Matsushika A, Imamura A, Yamashino T, Mizuno T (2002) Aberrant expression of the light-inducible and circadian-regulated APRR9 gene belonging to the circadian-associated APRR1/TOC1 quintet results in the phenotype of early flowering in Arabidopsis thaliana. Plant and Cell Physiology **43:** 833-843

McClung CR (2013) Beyond Arabidopsis: The circadian clock in non-model plant species. Seminars in Cell and Developmental Biology **24:** 430-436

Michael TP, Mockler TC, Breton G, McEntee C, Byer A, Trout JD, Hazen SP, Shen RK, Priest HD, Sullivan CM, Givan SA, Yanovsky M, Hong FX, Kay SA, Chory J (2008) Network discovery pipeline elucidates conserved time-of-day-specific cis-regulatory modules. PLoS Genetics **4**

Millar AJ, Carre IA, Strayer CA, Chua NH, Kay SA (1995) Circadian clock mutants in Arabidopsis identified by luciferase imaging. Science **267:** 1161-1163

Mizuno T, Nomoto Y, Oka H, Kitayama M, Takeuchi A, Tsubouchi M, Yamashino T (2014) Ambient temperature signal feeds into the circadian clock transcriptional circuitry through the EC night-time repressor in Arabidopsis thaliana. Plant and Cell Physiology **55:** 958-976

Mizuno T, Yamashino T (2008) Comparative transcriptome of diurnally oscillating genes and hormone-responsive genes in Arabidopsis thaliana: Insight into circadian clock-controlled daily responses to common ambient stresses in plants. Plant and Cell Physiology **49:** 481-487

Nakajima M, Imai K, Ito H, Nishiwaki T, Murayama Y, Iwasaki H, Oyarna T, Kondo T (2005) Reconstitution of circadian oscillation of cyanobacterial KaiC phosphorylation in vitro. Science **308:** 414-415

Nakamichi N (2011) Molecular Mechanisms Underlying the Arabidopsis Circadian Clock. Plant and Cell Physiology **52:** 1709-1718

Nakamichi N, Kiba T, Henriques R, Mizuno T, Chua NH, Sakakibara H (2010) PSEUDO-RESPONSE REGULATORS 9, 7, and 5 Are Transcriptional Repressors in the Arabidopsis Circadian Clock. Plant Cell **22:** 594-605

Nakamichi N, Kiba T, Kamioka M, Suzuki T, Yamashino T, Higashiyama T, Sakakibara H, Mizuno T (2012) Transcriptional repressor PRR5 directly regulates clock-output pathways. Proceedings of the National Academy of Sciences of the United States of America **109:** 17123-17128

Nakamichi N, Kita M, Ito S, Sato E, Yamashino T, Mizuno T (2005) The Arabidopsis pseudo-response regulators, PRR5 and PRR7, coordinately play essential roles for circadian clock function. Plant and Cell Physiology **46:** 609-619

Nakamichi N, Kita M, Niinuma K, Ito S, Yamashino T, Mizoguchi T, Mizuno T (2007) Arabidopsis clock-associated pseudo-response regulators PRR9, PRR7 and PRR5 coordinately and positively regulate flowering time through the canonical CONSTANS-dependent photoperiodic pathway. Plant and Cell Physiology **48:** 822-832

Nakamichi N, Kusano M, Fukushima A, Kita M, Ito S, Yamashino T, Saito K, Sakakibara H, Mizuno T (2009) Transcript Profiling of an Arabidopsis PSEUDO RESPONSE REGULATOR Arrhythmic Triple Mutant Reveals a Role for the Circadian Clock in Cold Stress Response. Plant and Cell Physiology **50:** 447-462

Niinuma K, Someya N, Kimura M, Yamaguchi I, Hamamoto H (2005) Circadian rhythm of circumnutation in inflorescence stems of Arabidopsis. Plant and Cell Physiology **46:** 1423-1427

Nozue K, Covington MF, Duek PD, Lorrain S, Fankhauser C, Harmer SL, Maloof JN (2007) Rhythmic growth explained by coincidence between internal and external cues. Nature **448:** 358-361

Nusinow DA, Helfer A, Hamilton EE, King JJ, Imaizumi T, Schultz TF, Farre EM, Kay SA (2011) The ELF4-ELF3-LUX complex links the circadian clock to diurnal control of hypocotyl growth. Nature **475:** 398-402

O'Neill JS, van Ooijen G, Dixon LE, Troein C, Corellou F, Bouget FY, Reddy AB, Millar AJ (2011) Circadian rhythms persist without transcription in a eukaryote. Nature **469:** 554-558

Para A, Farre EM, Imaizumi T, Pruneda-Paz JL, Harmon FG, Kay SA (2007) PRR3 is a vascular regulator of TOC1 stability in the Arabidopsis circadian clock. Plant Cell **19:** 3462-3473

Pattanayak GK, Phong C, Rust MJ (2014) Rhythms in Energy Storage Control the Ability of the Cyanobacterial Circadian Clock to Reset. Current Biology **24:** 1934-1938

Penfield S, Hall A (2009) A Role for Multiple Circadian Clock Genes in the Response to Signals That Break Seed Dormancy in Arabidopsis. Plant Cell **21:** 1722-1732

Perales M, Mas P (2007) A functional link between rhythmic changes in chromatin structure and the Arabidopsis biological clock. Plant Cell **19:** 2111-2123

Peschel N, Helfrich-Forster C (2011) Setting the clock - by nature: Circadian rhythm in the fruitfly Drosophila melanogaster. Febs Letters **585:** 1435-1442

Pruneda-Paz JL, Breton G, Para A, Kay SA (2009) A Functional Genomics Approach Reveals CHE as a Component of the Arabidopsis Circadian Clock. Science **323:** 1481-1485

Rawat R, Takahashi N, Hsu PY, Jones MA, Schwartz J, Salemi MR, Phinney BS, Harmer SL (2011) REVEILLE8 and PSEUDO-REPONSE REGULATOR5 form a negative feedback loop within the Arabidopsis circadian clock. PLoS Genetics **7**

Robinson I, Reddy AB (2014) Molecular mechanisms of the circadian clockwork in mammals. Febs Letters **588:** 2477-2483

Sanchez SE, Petrillo E, Beckwith EJ, Zhang X, Rugnone ML, Hernando CE, Cuevas JC, Godoy Herz MA, Depetris-Chauvin A, Simpson CG, Brown JW, Cerdan PD, Borevitz JO, Mas P, Ceriani MF, Kornblihtt AR, Yanovsky MJ (2010) A methyl transferase links the circadian clock to the regulation of alternative splicing. Nature **468:** 112-116

Sawa M, Kay SA (2011) GIGANTEA directly activates Flowering Locus T in Arabidopsis thaliana. Proceedings of the National Academy of Sciences of the United States of America **108:** 11698-11703

Sawa M, Nusinow DA, Kay SA, Imaizumi T (2007) FKF1 and GIGANTEA complex formation is required for day-length measurement in Arabidopsis. Science **318:** 261-265

Somers DE, Webb AAR, Pearson M, Kay SA (1998) The short-period mutant, toc1-1, alters circadian clock regulation of multiple outputs throughout development in Arabidopsis thaliana. Development **125:** 485-494

Suarez-Lopez P, Wheatley K, Robson F, Onouchi H, Valverde F, Coupland G (2001) CONSTANS mediates between the circadian clock and the control of flowering in Arabidopsis. Nature **410:** 1116-1120

Takahashi JS, Hong HK, Ko CH, McDearmon EL (2008) The genetics of mammalian circadian order and disorder: implications for physiology and disease. Nature Reviews Genetics **9:** 764-775

Takase T, Ishikawa H, Murakami H, Kikuchi J, Sato-Nara K, Suzuki H (2011) The Circadian Clock Modulates Water Dynamics and Aquaporin Expression in Arabidopsis Roots. Plant and Cell Physiology **52:** 373-383

Takeuchi T, Newton L, Burkhardt A, Mason S, Farre EM (2014) Light and the circadian clock mediate time-specific changes in sensitivity to UV-B stress under light/dark cycles. Journal of Experimental Botany **65:** 6003-6012

Tataroglu O, Emery P (2014) Studying circadian rhythms in Drosophila melanogaster. Methods **68:** 140-150

Thain SC, Vandenbussche F, Laarhoven LJJ, Dowson-Day MJ, Wang ZY, Tobin EM, Harren FJM, Millar AJ, Van Der Straeten D (2004) Circadian rhythms of ethylene emission in Arabidopsis. Plant Physiology **136:** 3751-3761

Valverde F, Mouradov A, Soppe W, Ravenscroft D, Samach A, Coupland G (2004) Photoreceptor regulation of CONSTANS protein in photoperiodic flowering. Science **303:** 1003-1006

Wang L, Fujiwara S, Somers DE (2010) PRR5 regulates phosphorylation, nuclear import and subnuclear localization of TOC1 in the Arabidopsis circadian clock. Embo Journal **29:** 1903-1915

Wang L, Kim J, Somers DE (2013) Transcriptional corepressor TOPLESS complexes with pseudoresponse regulator proteins and histone deacetylases to regulate circadian transcription. Proceedings of the National Academy of Sciences of the United States of America **110:** 761-766

Wang W, Barnaby JY, Tada Y, Li H, Tor M, Caldelari D, Lee DU, Fu XD, Dong XN (2011) Timing of plant immune responses by a central circadian regulator. Nature **470:** 110-114

Wang Y, Wu JF, Nakamichi N, Sakakibara H, Nam HG, Wu SH (2011) LIGHT-REGULATED WD1 and PSEUDO-RESPONSE REGULATOR9 Form a Positive Feedback Regulatory Loop in the Arabidopsis Circadian Clock. Plant Cell **23:** 486-498

Warren DM, Wilkins MB (1961) An Endogenous Rhythm in the Rate of Dark-Fixation of Carbon Dioxide in Leaves of *Bryophyllum Fedtschenkoi*. Nature **191:** 686-688

Williams JA, Sehgal A (2001) Molecular components of the circadian system in drosophila. Annual Review of Physiology **63:** 729-755

Woelfle MA, Yan OY, Phanvijhitsiri K, Johnson CH (2004) The adaptive value of circadian clocks: An experimental assessment in cyanobacteria. Current Biology **14:** 1481-1486

Xu XD, Hotta CT, Dodd AN, Love J, Sharrock R, Lee YWG, Xie Q, Johnson CH, Webb AAR (2007) Distinct light and clock modulation of cytosolic free Ca2+ oscillations and rhythmic CHLOROPHYLL A/B BINDING PROTEIN2 promoter activity in Arabidopsis. Plant Cell **19:** 3474-3490

Yanovsky MJ, Kay SA (2003) Living by the calendar: How plants know when to flower. Nature Reviews Molecular Cell Biology **4:** 265-275

Yazdanbakhsh N, Sulpice R, Graf A, Stitt M, Fisahn J (2011) Circadian control of root elongation and C partitioning in Arabidopsis thaliana. Plant Cell and Environment **34:** 877-894

Yeom M, Kim H, Lim J, Shin AY, Hong S, Kim JI, Nam HG (2014) How Do Phytochromes Transmit the Light Quality Information to the Circadian Clock in Arabidopsis? Molecular Plant **7:** 1701-1704

Yerushalmi S, Green RM (2009) Evidence for the adaptive significance of circadian rhythms. Ecology Letters **12:** 970-981

Yerushalmi S, Yakir E, Green RM (2011) Circadian clocks and adaptation in Arabidopsis. Molecular Ecology **20:** 1155-1165

CHAPTER 2

Direct regulation of abiotic responses by the Arabidopsis circadian clock component PRR7

The work presented in this chapter has been published:

Liu Tiffany*, Carlsson Jenny*, Takeuchi Tomomi, Newton Linsey, Farré Eva M. (2013)

Plant Journal 10.1111/tpj.12276

(*) Contributed equally to the work.

ABSTRACT

Up to 30% of the plant transcriptome is circadian regulated in different species. However, we still lack a good understanding of the mechanisms involved in these genome-wide oscillations in gene expression. Here we show that PSEUDO-RESPONSE REGULATOR 7 (PRR7), a central component of the Arabidopsis clock, is directly involved in the repression of master regulators of plant growth, light signaling and stress responses. The expression levels of most PRR7 target genes peak around dawn, in an antiphasic manner to PRR7 protein levels and were repressed by PRR7. These findings indicate that PRR7 is important for cyclic gene expression by repressing the transcription of morning-expressed genes. In particular we found an enrichment in genes involved in abiotic stress responses and in accordance, we observed that PRR7 is involved in the oxidative stress response and the regulation of stomata conductance.

INTRODUCTION

A diverse range of organisms have evolved time-keeping mechanisms known as circadian clocks (Bell-Pedersen et al., 2005). Circadian rhythms have an approximately 24 h period, persist under constant conditions and are entrained by light and temperature. The ability to anticipate environmental changes enable organisms to regulate biological processes in a timely order to optimize their growth and development (McClung, 2011). In the plant model organism *Arabidopsis thaliana*, the circadian clock regulates approximately 30% of the transcriptome (Covington et al., 2008; Michael et al., 2008), while about 90% of Arabidopsis genes display oscillations in expression levels under diel conditions (Michael et al., 2008). Circadian regulated transcription is involved in many plant processes including metabolism, light signaling and floral development (Doherty and Kay, 2010). It also plays a key role in the regulation of stress

responses, such as cold, drought, oxidative stress and pathogen attack (Doherty and Kay, 2010; Lai et al., 2012). Recent results show that the circadian regulated expression of a significant number of genes is conserved across different plant species (Khan et al., 2010; Filichkin et al., 2011).

In the Arabidopsis circadian clock, several components form interlocking feedback loops, which are a common feature of circadian clocks in eukaryotes (Bell-Pedersen et al., 2005). Two homologous MYB transcription factors, CIRCADIAN CLOCK ASSOCIATED 1 (CCA1) and LATE ELONGATED HYPOCOTYL (LHY), peak close to dawn and activate the expression of *PSEUDO-RESPONSE REGULATOR 9* (*PRR9*) and *PRR7* (Farre et al., 2005). PRR9, PRR7 and PRR5 protein levels peak between the middle and the end of the day to repress *CCA1* and *LHY* expression (Farre and Kay, 2007; Nakamichi et al., 2010). In addition to activating gene expression, CCA1 and LHY repress the transcription of the evening-expressed genes *TIMING OF CAB EXPRESSION 1/ PSEUDO-RESPONSE REGULATOR 1* (*TOC1/ PRR1*), *EARLY FLOWERING 3* (*ELF3*), *ELF4* and *LUX ARRYTHMO* (*LUX*) (Nakamichi, 2011). In turn, these genes regulate the expression of *CCA1* and *LHY* indirectly by repressing *PRR9, PRR7* and/or *PRR5* expression (Pruneda-Paz et al., 2009; Dixon et al., 2011; Gendron et al., 2012; Huang et al., 2012; Pokhilko et al., 2012). In addition, TOC1 has also recently been shown to repress *CCA1* and *LHY* expression directly (Gendron et al., 2012; Huang et al., 2012). Mutant analyses indicate that PRR9, PRR7 and PRR5 are necessary for rhythmicity and play partly overlapping roles in the regulation of both the circadian clock and clock output processes (Farre et al., 2005; Nakamichi et al., 2005; Nakamichi et al., 2007; Nakamichi et al., 2009; Nakamichi et al., 2010). Circadian-regulated PRRs contain a pseudo-receiver domain, similar to the receiver domains of response regulators, and a CCT (CONSTANS, CONSTANS-like, and TOC1) motif. The PRRs

have been found to be associated with specific promoter regions *in vivo* and are able to bind DNA *in vitro* (Pruneda-Paz et al., 2009; Nakamichi et al., 2010; Gendron et al., 2012; Nakamichi et al., 2012). For example, PRR9, PRR7, and PRR5 associate to the promoter regions of *CCA1* and *LHY* to repress their transcription (Nakamichi et al., 2010). Mutations in any of these *PRR*s also result in alterations of numerous physiological and developmental processes, and these changes are exacerbated in higher order mutants. When compared to the wild type, the *prr5prr7prr9* triple mutant (*prr579)* is photoperiod insensitive and displays a very late flowering phenotype under long day conditions (Nakamichi et al., 2007). This triple mutant is also more drought and cold tolerant and has perturbed metabolite levels, including an elevated abscisic acid (ABA) content (Fukushima et al., 2009; Nakamichi et al., 2009).

In order to understand the role of PRR7 in the regulation of plant growth and development, we identified genome-wide PRR7 targets in Arabidopsis by conducting chromatin immunoprecipitation combined with high-throughput sequencing (ChIP-Seq). Using this approach, we were able to identify 73 high-confidence PRR7 binding sites. Putative PRR7 target genes were enriched in morning-expressed circadian regulated genes and included master regulators of growth, light signaling and stress responses. In accordance, we found that PRR7 is involved in the oxidative stress responses and the regulation of stomata opening in Arabidopsis.

RESULTS

Identification of PRR7 target genes using ChIP-seq

Mutant expression analyses have shown that PRR7 influences numerous physiological processes in Arabidopsis. In order to identify the direct targets of PRR7 transcriptional regulation we

carried out two ChIP-Seq experiments using lines expressing HA-PRR7 under the control of its endogenous promoter that complement the long period circadian phenotype of *prr7-3* (*prr7*) (Farre and Kay, 2007). The ChIP-Seq data were analyzed using QuEST, a statistical package used to determine transcription factor binding sites (Valouev et al., 2008) (Dataset S2.1), and we identified 73 high-confidence binding sites in common between the two experiments (Dataset S2.1). Putative PRR7 target genes were defined as genes with binding sites located within 1000 bp upstream of a transcriptional start site to 1000 bp downstream of a transcriptional stop. Based on these criteria, of the 73 HA-PRR7 specific binding sites, 17 binding sites did not associate with any annotated gene, whereas the remaining 56 binding sites associated with 83 genes (Dataset S2.1). Of these 83 putative PRR7 target genes, each gene associated with one binding site except for AT1G22767, for which we identified two sites (Dataset S2.1). For 90% of the genes, the location of the PRR7 binding sites identified in Experiments I and II differed by no more than 100 bp (Figure 2.1a). Our data confirmed the association of PRR7 with genomic regions close to the transcriptional start sites of *CCA1* and *LHY* (Figure S2.1a-d) (Nakamichi et al., 2010).

We further tested and confirmed the binding of PRR7 to 12 out of 19 binding sites identified in both Experiment I and Experiment II in a PRR7 overexpressing line (*PRR7ox*) using three independent ChIP-quantitative PCR assays (ChIP-qPCR) (Figure S2.1). Using this independent assay, we also tested and confirmed PRR7 binding to 20 out of 32 binding sites identified in one of the two ChIP-seq experiments (Dataset S2.1, Figure S2.1e-f). These target genes were selected based on their potential role in the phenotypes observed in *prr* mutants and/or were members of gene families identified in the common set. Downstream analyses were performed on a total of 93 sites, composed of 73 identified in both ChIP-Seq experiments and the 20 sites

that were independently confirmed. We will subsequently refer to these binding sites as PRR7 binding sites. These sites were associated with a total of 113 genes, which we will refer to as putative PRR7 targets (Dataset S2.1). The majority of PRR7 binding sites were located within 1000 bp upstream of a transcriptional start site and 54% lie within 300 bp of a transcriptional start site (Figure 2.1b).

PRR7 represses the expression of target genes by binding to regions close to their transcriptional start sites

In order to study the effect of PRR7 on its target genes we used publicly available data on gene expression in the *prr579* mutant (Nakamichi et al., 2009) and analyzed RNA levels in *PRR7ox* (Farre and Kay, 2007) and *prr579* by reverse transcription-qPCR (RT-qPCR) (Figure 2.2, Figure S2.2, Dataset S2.1). We found an enrichment of genes upregulated in *prr579* among PRR7 targets (Fisher's exact test, $p<0.0001$) (Figure 2.1c). We observed a further enrichment of genes upregulated in *prr579* among genes that contain PRR7 binding sites upstream of their transcriptional start sites when compared to putative PRR7 targets with intragenic or downstream binding sites (Figure 2.1c; Fisher's exact test, $p<0.05$). These results indicate that PRR7 associates with regions close to transcriptional start sites to repress transcription. Among the PRR7 binding sites, 16 are associated with the upstream region of one gene and the downstream region of another gene. In 64% of the cases analyzed (7/11), the gene with the PRR7 binding site closer to the transcriptional start site was upregulated in *prr579* in the subjective evening and downregulated in the *PRR7ox* line in the subjective morning (Figure S2.2a-h), suggesting repression by PRR7. We also identified a few genes with a PRR7 binding site in their downstream region displaying changes in expression in either the *prr579* mutant or the *PRR7ox*

line (Figure S2.2a-c, e, g). Since these genes show circadian oscillations, these effects might be caused indirectly by other clock components. In order to further study the role of the position of PRR7 binding sites on PRR7 regulation of gene expression, we identified PRR7 binding sites that were located upstream of the transcriptional start sites of two genes. In five of the six pairs analyzed, only one gene from each pair appeared to be repressed by PRR7 (Dataset S2.1, Figure S2.2i-k).

Of the PRR7 targets with an upstream binding site, 71% cycle under light/dark conditions compared to 31% genome-wide (Fisher's exact test, $p<0.0001$; Figure 2.1d) (Michael et al., 2008). In addition, 71% cycle under constant light conditions compared to 23% genome-wide, revealing an enrichment in circadian-regulated genes among PRR7 targets (Fisher's exact test, $p<0.0001$; Figure 2.1d) (Michael et al., 2008). Most of the PRR7 cycling target genes displayed a peak in expression between the end of the night and early morning under both light/dark cycles and constant light conditions (Figure 2.1e-f). This pattern of expression is antiphasic to PRR7 protein levels that peak at the end of the day (Farre and Kay, 2007) and agrees with the recent results showing that PRR7 can act as a transcriptional repressor (Nakamichi et al., 2010). In general, *PRR7* overexpression resulted in decreased peak RNA levels of PRR7 target genes, whereas the expression levels of PRR7 targets were elevated in the *prr579* mutant at the troughs compared to the wild type (Figure S2.2). This pattern of changes in expression is similar to what occurs in overexpressing and mutant lines of other clock components that act as repressors such as TOC1 (Huang et al., 2012), CCA1 and LHY (Wang and Tobin, 1998; Mizoguchi et al., 2002; Pruneda-Paz et al., 2009), ELF3, ELF4 and LUX (Dixon et al., 2011; Nusinow et al., 2011).

PRR7 regulates the expression of other clock components and regulators of developmental processes

Functional analysis of PRR7 target genes showed an enrichment in transcriptional regulators (Figure 2.2a). These transcriptional regulators include other clock components as well as factors involved in plant growth, development, light signaling and stress responses (Figure 2.3). In addition to *CCA1* and *LHY*, we found that PRR7 associated with the promoter of *PRR9* (Dataset S2.1). The expression level of *PRR9* is strongly reduced in the *PRR7ox* (Figure 2.3). Moreover, the *prr579* triple mutant displays a long hypocotyl phenotype under several growth conditions (Kunihiro et al., 2011). Consistent with this phenotype, PRR7 targets include *PHYTOCHROME INTERACTING FACTOR 4* (*PIF4*) and *PIF5* (Dataset S2.1). These two genes encode for bHLH transcription factors that promote hypocotyl growth in the dark and integrate both the clock and light to regulate hypocotyl growth in a diurnal pattern (Nozue et al., 2007; Nusinow et al., 2011; Kinmonth-Schultz et al., 2013). Thus, the long hypocotyls observed in the *prr579* mutant may be attributed to the derepression of both *PIF4* and *PIF5* by PRR7 (Figure 2.3). In addition, PRR7 also represses the expression of the myb-like transcription factors *REVEILLE 1* (*RVE1*), *RVE2* and *RVE7* (Dataset S2.1, Figure 2.3). These proteins are involved in the regulation of processes downstream of the circadian clock such as hypocotyl growth and flowering (Kuno et al., 2003; Zhang et al., 2007; Rawat et al., 2009), and their elevated expression in the *prr579* mutant could contribute to its long hypocotyl phenotype as well (Figure 2.3). Under both short-day and long-day conditions, the *prr579* triple mutant exhibits an extremely late flowering phenotype, suggesting that the PRRs may play a role in the photoperiodic control of flowering time (Nakamichi et al., 2007). Indeed, this mutant displays elevated transcript levels of *CYCLING DOF FACTORS* (*CDFs*), which are negative regulators of *CONSTANS* gene expression (Nakamichi et

al., 2007; Song et al., 2010). We found that PRR7 targets include *CDF2* and *CDF5* and that their expression is reduced in the *PRR7ox* and elevated in the *prr579* triple mutant (Figure 2.3).

Among PRR7 targets, we identified several genes involved in light signaling (Dataset S2.1, Figure 2.3). For example, the expression of both *LONG HYPOCOTYL 5* (*HY5*) and *HY5-HOMOLOG* (*HYH*) is elevated in the *prr579* triple mutant, although only *HYH* is repressed in the *PRR7ox* line (Figure 2.3). These proteins encode homologous bZIP transcription factors shown to mediate light responses and promote photomorphogenesis (Chattopadhyay et al., 1998; Holm et al., 2002). In addition, we found that PRR7 represses *ATTENUATED FAR-RED RESPONSE* (*AFR*), an F-box protein involved in phyA light signaling (Harmon and Kay, 2003), as well as *SALT TOLERANCE* (*STO*) and *SALT TOLERANCE-HOMOLOGUE* (*STH*), which are B-box transcription factors involved in red light dependent hypocotyl elongation (Indorf et al., 2007; Kumagai et al., 2008) (Figure 2.3). Moreover, light regulated genes were enriched among PRR7 targets (Fisher's exact test, $p<0.0001$) (Figure 2.4a) (Nozue et al., 2011) (Dataset S2.2). Accordingly, most PRR7 target genes contained a G-box motif in their promoter regions (Figure 2.4b). G-box elements are overrepresented in light regulated genes, and several proteins involved in light signaling are known to bind to these DNA elements (Chattopadhyay et al., 1998; Hudson and Quail, 2003; Yadav et al., 2005; Oh et al., 2009). To look for potential *cis*-regulatory elements directly involved in PRR7 function, we search for conserved motifs in regions ± 50 bp from the PRR7 upstream binding sites. Using the software packages MEME (Bailey et al., 2006) and Weeder (Pavesi et al., 2004) we only found a G-box containing motif enriched in regions close to PRR7 binding sites (Figure 2.4d). The analysis of regions ± 100 bp and ± 250 bp from the PRR7 upstream binding sites also identified a G-box containing motif (Figure S2.3). These findings suggest that a G-box is involved in the regulation of gene expression by PRR7.

In order to identify potential co-regulators of PRR7 targets, we compared them with the genome-wide targets of transcriptional regulators involved in light signaling. We found that a significant number of PRR7 targets are also regulated by the G-box binding factors PIF1/PIL5 and/or HY5, as well as FAR-RED ELONGATED HYPOCOTYL3 (FHY3) (Figure 2.4c; Fisher's exact test, $p<0.0001$) (Lee et al., 2007; Oh et al., 2009; Ouyang et al., 2011) (Dataset S2.2). These results could explain the enrichment of genes involved in red and far-red light responses among putative PRR7 target genes (Figure 2.2a) and indicate that they might be co-regulated by different light signaling components. Finally, PRR5 and TOC1 transcriptional targets have recently been described and comparative analysis show that their target genes overlap significantly with the PRR7 targets identified in this study (Figure 2.4e) (Fisher's exact test, $p<0.0001$) (Huang et al., 2012; Nakamichi et al., 2012).

PRR7 is involved in the regulation of cold regulated gene expression

The *prr579* triple mutant has been shown to be more cold and drought stress tolerant than wild type plants (Nakamichi et al., 2009). Consistent with these findings, PRR7 targets include *C-REPEAT/DRE BINDING FACTOR 1* (*CBF1), CBF2,* and *CBF3,* which are AP2 domain-containing transcriptional activators in the cold response pathway (Dataset S2.1) (Gilmour et al., 1998). The levels of *CBF2* and *CBF3* are constitutively upregulated in *prr579* and repressed in the *PRR7ox* (Figure 2.3). The *prr579* triple mutant also displays constitutively higher induction of the three *CBF*s upon transfer to cold (Nakamichi et al., 2009). Moreover, analyses of cold stress microarrays (Kilian et al., 2007) revealed that 73% of PRR7 targets are differentially regulated in response to cold compared to 39% genome-wide (Fisher's exact test, $p<0.0001$) (Dataset S2.2). None of the PRR7 target genes are upregulated in CBF overexpressing lines

(Fowler and Thomashow, 2002). This indicates that the upregulation of cold responsive genes in the *prr579* mutant is not only caused by the effect of these pseudo-response regulators on *CBF* expression, but also suggests a wider role of the circadian clock in cold responses than previously thought (Dong et al., 2011).

PRR7 regulates drought and abscisic acid responsive genes

We observed an enrichment in drought responsive genes among the putative PRR7 targets and found that 80% are drought responsive compared to 45% genome-wide (Fisher's exact test, $p<0.0001$) (Kilian et al., 2007) (Dataset S2.2). Furthermore, one PRR7 target is *ABA DEFICIENT 1* (*ABA1*) (Dataset1), which encodes a zeaxanthin epoxidase involved in ABA biosynthesis (Xiong et al., 2002). The upregulation of *ABA1* (Figure 2.5) could explain the elevated levels of ABA observed in the *prr579* triple mutant (Fukushima et al., 2009). In addition, general functional annotation analysis indicated an enrichment of ABA regulated genes (Figure 2.2a) and we showed that 28% of PRR7 targets are regulated by ABA (Fisher's exact test, $p<0.0001$) using data from reference (Nemhauser et al., 2006) (Dataset S2.2). Consistent with this finding, more than one third of the PRR7 target genes contain ABA-responsive Elements (ABRE) in their upstream regions (Figure 2.4b). The ABA regulated genes comprise about half of the drought and cold responsive PRR7 targets (Figure 2.2b). Moreover, most of the PRR7 target genes that are drought responsive are also cold responsive and *vice versa*. These results suggest that PRR7 may regulate cold and drought responses in coordination with an ABA dependent mechanism. We further investigated the role of PRR7 on ABA-regulated gene expression in PRR7 mutants and overexpressors. Genes induced by ABA, such as *CDF1* and *ABA1* were less induced in the seedlings overexpressing PRR7 (Figure 2.5). We also investigated

the physiological effects of PRR7 on ABA regulated genes. The *prr579* mutants displayed a significant reduction in stomata conductance under well-watered conditions (Figure 2.6a). In order to test whether PRR7 could affect the plant sensitivity to ABA we analyzed the water loss of wild type and PRR7 misexpressing lines treated with this hormone. All plants including PRR7 overexpressors responded to the ABA treatment. ABA treated overexpressors lost more water and the *prr579* mutant lost less water than ABA treated wild type plants after root detachment (Figure 2.6b). This suggests that factors other than ABA content affect water loss in PRR7 misexpressing plants.

It has been shown that ABA affects the period length of the circadian clock under constant light conditions (Hanano et al., 2008). Therefore, we tested if PRR7 could affect the sensitivity of the clock towards ABA. Under our experimental conditions, ABA addition led to a small reduction in the period length of wild type seedlings but to a stronger reduction in *prr7* mutants (Figure 2.7a-c). After treatment with exogenous ABA, *prr7* mutants became short period with respect to the wild type (Figure 2.7c). The *prr57* and *prr79* double mutants also displayed a small reduction in period length after the addition of ABA. In contrast to the effects of ABA on *TOC1* (Legnaioli et al., 2009) (Figure S2.4), we did not observe any effect of exogenous ABA on *PRR7* gene expression (Figure 2.7d). However, the expression of *PRR7* was reduced in the ABA deficient *npq2-1* mutant (Figure 2.7d).

PRR7 is involved in the adaptation to iron excess

PRR7 targets also included three *FERRITINS*, *FER1*, *FER3* and *FER4*. These genes are part of the few PRR7 targets with peaks of expression in the evening in wild type seedlings (Figure 2.8). The RNA levels of *FER1*, *FER3* and *FER4* are reduced in *PRR7ox*, while their expression is

elevated during the subjective day in the *prr579* mutant (Figure 2.8). Ferritins have been proposed to protect plants against oxidative stress caused by excess iron (Briat et al., 2010) and the *fer134* triple mutant displays increased sensitivity towards excess iron when grown on soil (Ravet et al., 2009). Therefore, we tested whether misexpression of PRR7 would lead to a defect in the adaptation to iron excess media. PRR7 overexpressing lines were more sensitive to iron-excess and displayed a significant reduction in chlorophyll content when grown under high iron conditions (Figure 2.9a). In contrast, higher order *prr* mutants appeared almost insensitive to iron addition (Figure 2.9a). Under the conditions tested, the *fer134* mutant did not display an increased sensitivity towards excess iron indicating that other mechanisms mediate the role of PRRs in oxidative stress (Figure 2.9b). It has recently been shown that CCA1 and LHY regulate the levels of reactive oxygen species (Lai et al., 2012). Since PRR7 represses the expression of *CCA1* and *LHY* (Farre and Kay, 2007, Nakamichi, 2010 #402), we analyzed the sensitivity of the *cca1lhy* mutant and the *CCA1ox* line to excess iron. In agreement with the role of CCA1 and LHY in protecting against reactive oxygen species, the *cca1lhy* mutant was significantly more sensitive to iron-excess than the wild type (Figure 2.9c). We therefore assessed the iron sensitivity of *prr79* mutants with reduced levels of *CCA1* and *LHY* (Salome and McClung, 2005). In spite of their decrease in *CCA1* and *LHY* expression (Figure S2.5) these lines still displayed a decreased sensitivity to iron-excess (Figure 2.9d), suggesting an independent role of PRRs under oxidative stress.

DISCUSSION

PRR7 is a repressor of gene expression

Our results suggest that PRR7 represses gene expression by binding to regions close to transcriptional start sites. We did not find any evidence for PRR7 acting as a transcriptional activator. These findings suggest that the mechanism of transcriptional regulation by PRR7 could be the same for all of its target genes. PRR5, PRR7 and PRR9 contain a partially conserved amino acid sequence shown to be necessary for repressing transcription in yeast (Nakamichi et al., 2010). This conserved EAR (ethylene-responsive element binding factor-associated amphiphilic repression) motif is located in the variable domain of these PRRs, between the highly conserved pseudo-receiver and CCT domains. It has recently been shown that PRR5, PRR7 and PRR9 associate with the plant Groucho/Tup1 co-repressor family, TOPLESS/TOPLESS-RELATED, via the EAR motif to repress the transcription of *CCA1* and *LHY* (Wang et al., 2013). The CCT domain shares some sequence similarity with the DNA binding domain of yeast HEME ACTIVATOR PROTEIN 2 (HAP2), which is a subunit of the HAP2/HAP3/HAP5 trimeric complex that binds to CCAAT boxes in eukaryotic promoters (Wenkel et al., 2006). The CCT domain of PRR5 is necessary for association to the DNA *in vivo* (Nakamichi et al., 2012), and the CCT domain of several circadian regulated PRRs, including PRR7, has also been shown to bind DNA directly *in vitro* (Gendron et al., 2012). However, the DNA binding specificity of the PRRs remains unknown. The transcriptional regulation activity of the PRRs might also be mediated by their interaction with DNA binding transcriptional regulators. For example, TOC1 has been shown to interact with CHE1 and several bHLH transcription factors (Yamashino et al., 2003; Kidokoro et al., 2009; Pruneda-Paz et al., 2009).

Our results indicate that a G-box motif is enriched in regions very close to the PRR7 binding sites. This finding suggests that PRR7 could mediate regulation directly or through G-box binding proteins. The G-box is also enriched in regions close to PRR5 and TOC1 binding sites (Huang et al., 2012; Nakamichi et al., 2012) indicating that these three pseudo-response regulators might be binding to the same promoter regions. Moreover, G-box like promoter elements mediate light and ABA signaling processes (Jiao et al., 2007; Cutler et al., 2010). The combinatorial effect of PRR7 and these signaling pathways are likely to cause the differences in the phase of expression of PRR7 target genes between constant light and light/dark cycles (Figure 2.1e,f).

PRR7 represses the expression of other clock proteins and master regulators of plant growth, development and response to abiotic stress

Other clock genes were identified among the strongest bound targets in our experiments. We found that PRR7 directly regulates morning-expressed *PRR9* in addition to *CCA1* and *LHY*. Similar experiments on the mammalian clock component BMAL1 have also shown stronger binding to other clock components than to clock output genes (Rey et al., 2011). These differences in binding could reflect differences in tissue specific expression, tissue specific association and/or overall binding affinity. Among PRR7 targets, we found a significant enrichment of transcription factors. The presence of a large number of transcription factors among first order circadian regulated genes indicates that the circadian clock regulates output processes in a hierarchical fashion. However, as has been shown for BMAL1 in mice (Rey et al., 2011), PRR7 also regulates a significant number of non-regulator targets. The identified direct targets of PRR7 can explain most of the observed phenotypes of the *prr579* triple mutant such as

cold and drought tolerance, long hypocotyl and late flowering. Since PRR5 and PRR9 are also able to directly regulate the expression of *CCA1* and *LHY*, it was expected that their target promoters would also overlap significantly with PRR7 targets. PRR5 transcriptional targets have recently been identified using a ChIP-seq approach and they include a significant number of genes also regulated by PRR7. Among these common targets are key transcription factors, such as *RVE1* and *RVE7*, *CDF2* and *CDF5*, *PIF4* and *PIF5* and *CBF1/2/3*. Interestingly, PRR7 and PRR5 also share a large number of target genes with TOC1 (Figure 2.4e). Most of PRR5, PRR7 and TOC1 regulated genes peak in the morning in an antiphasic manner to late day/dusk expression of these proteins. The consecutive expression of PRR7, PRR5 and TOC1 therefore leads to the repression of their targets during a wide window between the late day and early night period.

PRR7 modulates ABA regulated gene expression

A significant number of PRR7 target genes are regulated by ABA and we observed that changes in PRR7 levels influence the response of these genes to the hormone (Figure 2.5). Interestingly, even under the exogenous application of ABA, the expression of *CDF1* cycles in wild type seedlings under constant light conditions with little or no activation observed at dusk (Figure 2.5), which coincides with the peak of PRR7 protein levels. Our analysis of PRR7 mutants and overexpressors indicate that PRR7 is at least partly responsible for that time dependent response to ABA. In spite of the effects of PRR7 on ABA-mediated expression changes, PRR7 mutants and overexpressors still responded to the ABA promotion of stomata closing (Figure 2.6b). Moreover, PRR7 is associated with the upstream regions of several genes involved in ABA signaling such as *HY5* (Chen et al., 2008), *GENOMES UNCOUPLED 5* (*GUN5*) (Du et al.,

2012) and *ABI FIVE BINDING PROTEIN 4* (*AFP4*) (Garcia et al., 2008). *GUN5* is also directly repressed by TOC1, and TOC1 overexpressors display changes in ABA sensitivity in stomata closing. A possible explanation for this difference in response to ABA between TOC1 and PRR7 misexpressing lines might be due to differences in tissue specific expression among the PRRs. Although PRR5, PRR7, PRR9 and TOC1 are expressed in the phloem, only TOC1 is significantly expressed in the stomata (Figure S2.6) (Mustroph et al., 2009). Finally, we observed that *prr7* mutant period length was more sensitive to exogenous ABA than the wild type (Figure 2.7a-c). ABA affects *TOC1* expression (Legnaioli et al., 2009; Huang et al., 2012) (Figure S2.4) but not *PRR7* RNA levels (Figure 2.7d) under constant light conditions and therefore the mechanism behind this difference in ABA sensitivity of the *prr7* mutants remains to be studied.

PRR7 mediates sensitivity against oxidative stress

PRR7 overexpressors and *prr579* triple mutants displayed changes in sensitivity to oxidative stress caused by excess iron. Our results indicate that this is not caused solely by the role of PRRs on *CCA1* and *LHY* expression, which have recently been shown to play a direct role in the time dependent protection against reactive oxygen species (Lai et al., 2012). In addition to three ferritin genes that have been shown to be involved in the protection against excess iron (Ravet et al., 2009), PRR7 targets also include a superoxide dismutase family protein (At3g56350). It has been shown that the overexpression of Arabidopsis CBF1 in transgenic tomato also leads to an increased tolerance against oxidative damage (Hsieh et al., 2002). Therefore, the strong changes in *CBF1/2/3* expression in PRR7 mutants and overexpressors could also be partly responsible for these changes in sensitivity to oxidative stress.

In conclusion, our studies show that PRR7 directly regulates a significant number of genes involved in the response to abiotic stimuli. Most PRR7 targets are expressed in the morning and are co-regulated by light, drought and/or cold signaling pathways as well as by other clock components. Taken together, these results establish the role of clock components directly regulating multiple signaling pathways in a time dependent manner.

EXPERIMENTAL PROCEDURES

Plant Materials

The Arabidopsis lines *prr7-3, prr9-1, prr79* (*prr7-3prr9*-1), *prr79 CCR2::LUC* (Farre et al., 2005), *prr7-3 PRR7::HA-PRR7* #151 (Farre and Kay, 2007), *35S::HA-PRR7* #54 (Farre and Kay, 2007), *35S::PRR7 #5* (Farre and Kay, 2007), *CCA1ox* (*35S::CCA1 #*34) (Wang and Tobin, 1998), *cca1lhy* (*cca1-11 lhy-21*,CS9380) (Dong et al., 2011), *npq2-1*(Niyogi et al., 1998), *fer123* (Ravet et al., 2009) were previously described. The lines *prr7,prr9 (prr7,9)* and *prr7,9* amiR-*CCA1-LHY* are in the Col-2 *CCA1::LUC* background (Salome and McClung, 2005). The lines *prr57* (*prr5-1prr7-3)* and *prr579* (*prr5-1prr7-3prr9-1)* were generated by crossing. *prr57 CCR2::LUC* was generated by transformation (Strayer et al., 2000).

Growth conditions

For gene expression and ChIP experiments, seedlings were grown on Murashige and Skoog (MS) medium (Murashige and Skoog, 1962) with 0.8% agar and 2% sucrose under 70 µmol $m^{-2}s^{-1}$ and a 12 h light/12 h dark regime at 22 ºC for two weeks. For the analysis of ABA regulated gene expression, plants were treated with 10 µM ABA or ethanol control in 0.01% silwett at ZT24 and transferred to constant light. For the iron excess experiments sterilized seeds were

germinated on plates containing (MS) medium without sucrose and were grown for three weeks under a 70 µmol $m^{-2}s^{-1}$ and a 12 h light/12 h dark regime. The seedlings were then transferred to a new MS media plate (100 µM iron), or MS medium supplemented with iron EDTA to achieve a final iron concentration of 600 µM. The plates were moved to constant light (70 µmol $m^{-2}s^{-1}$) the next day at ZT0 and were kept in constant light for 4 to 7 days before the analysis of chlorophyll content. For stomata conductance seeds were sown on soil in Ray Leach "Cone-tainers" (Stuewe & Sons, Tangent, OR, USA). After a 3-day imbibition at 4°C, the wild type, *prr7* mutant, and PRR7 overexpressors were grown under a 120 µmol $m^{-2}s^{-1}$, 8 h light/16 h dark short day at 24 °C light/20 °C dark for 7 weeks until the gas exchange experiments were performed. For *prr579* triple mutant, the plants were grown under a 120 µmol $m^{-2}s^{-1}$, 16 h light/8 h dark long-day regime at 24 °C light/20 °C dark for 6 weeks, and the plants were transferred to an aforementioned short-day regime 10 days before the gas exchange measurements were performed. The rosette leaves of the triple mutant remained otherwise too small for single-leaf conductance analysis under short-day growth conditions. For the water loss assays, four-week-old plants grown on soil under 100 µmol $m^{-2}s^{-1}$, 16 h light/8 h dark at 22°C were treated with either 10 µM ABA in water or water with methanol as control at ZT1. Three hours later at ZT4.5 rosettes were detached and the weight loss was measured over a 2 h period.

Chromatin Immunoprecipitation, Library Preparation and Sequencing

Chromatin immunoprecipitation was carried out by a modified protocol based on Sawa et al. (2007). Details are described in Method S1. Arabidopsis seedlings were harvested at ZT12. For each ChIP we used ~120 µg of DNA. The protocol for library preparation for sequencing is described in the Method S2. For each library, we pooled 5 (Experiment I) and 12 (Experiment II)

individual immunoprecipitated DNA and respective input DNA using QIAquick^{R} PCR Purification Kit (Qiagen, Hilden, Germany). Adapter sequences are described in Dataset S2.3. The DNA size and quality was controlled using the BioAnalyser DNA high sensitivity kit (Agilent, Santa Clara, CA, USA) and Fluorometer Qubit (Invitrogen, Carlsbad, CA, USA). Single end Illumina sequencing-by-synthesis was performed by the Michigan State University Research Technology Support Facility.

Analysis of Enrichment of Immunoprecipitated DNA by quantitative PCR

1.5 µl of DNA were used for PCR amplification by qPCR using an Eppendorf single-color real-time PCR detection system (Master Cycle Realplex^{2}). Two technical replicates were analyzed for each sample. Quantification was carried out by PCR base line subtracted curve fit with the provided Realplex software. Primers are described in Dataset S2.3. The intron of *ACT2* (AT5G09810) was used as a negative control. Details on the use of different HA-PRR7 expressing lines are described in Method S3.

Expression Analysis by RT-qPCR

RNA was extracted using the Plant RNA Kit according to the manufacturer's recommendations (Omega). The iScript cDNA synthesis kit (Bio-Rad) was used for reverse transcriptase-mediated PCR. The cDNA was diluted five times with water, and 1.5 µl were used for PCR amplification by real-time PCR as described for the detection of immunoprecipitated DNA. Two technical replicates were analyzed for each sample. Primers are described in Dataset S2.3. The gene *IPP2* (AT3G02780) was used as a normalization control.

ChIP-Seq Data Analysis

Sequences were preprocessed using the FASTX toolkit (http://hannonlab.cshl.edu/fastx_toolkit/) and aligned to the Arabidopsis TAIR10 genome using Bowtie (Langmead et al., 2009). QuEST (Valouev et al., 2008) was used to identify binding sites and determine the false discovery rates (FDR). In Experiment I, each immunoprecipitated sample from *prr7-3 PRR7::HA-PRR7* and *prr7-3* were compared to their respective inputs as negative controls. After discarding 11 binding sites common between the two sets, we identified 674 sites specific to *prr7-3 PRR7::HA-PRR7.* In Experiment II, we compared the immunoprecipitated *prr7-3 PRR7::HA-PRR7* to the immunoprecipitated *prr7-3* as a negative control and identified 298 binding sites (Figure S2.7). We defined common binding sites between the two experiments as binding sites located within 500 bp and identified 73 PRR7 binding sites. The binding sites determined by QuEST were compared to TAIR10 genes to associate binding sites to putative target genes. Genes were associated to binding sites located within 1000 bp upstream of the transcriptional start site to 1000 bp downstream of the transcriptional stop. Details are described in Method S4.

Identification of Common DNA Elements in Regions Close to PRR7 Binding Sites

Flanking sequences around each binding site were acquired using a publicly available script (http://www.stanford.edu/%7evalouev/QuEST/output_genomic_regions_from_calls.pl.gz). Overrepresented motifs were identified using MEME (Mustroph et al., 2009) and Weeder (Pavesi et al., 2006). Significant motifs were defined as having an E-value less than 0.001. We used positional weight matrices (PWM) to search for specific motifs of interest, including the G-BOX (CACGTG), ABA responsive element (C/T)ACGTGGC), evening element (AAAATATCT), and CCA1 binding site (AA(A/C)AATCT) (Zou et al., 2011). The mapping p-

value was set at $<10^{-4}$, the mapping score threshold was set to 0.9, and the background AT and GC frequency was specified as 0.33 and 0.17, respectively. We looked for these elements in the promoter region (1000 bp upstream of the transcriptional start site) for the 79 out of 113 genes that had a PRR7 binding site located in the upstream region, and compared them to genome-wide data. We specifically searched for the LUX binding site (GAT[A/T]CG) since a PWM had not been generated for this motif.

Comparison of PRR7 Target Genes and other Data Sets

The Fisher's exact test implemented in R (fisher.test) was used to determine enrichment of PRR7 targets in different datasets. Functional analysis of PRR7 targets was performed using DAVID (Huang da et al., 2009). Cycling gene expression was analyzed using PHASER (Michael et al., 2008). Genes were defined as cycling if the mbpma > 0.8.

Determination of chlorophyll content

Chlorophylls were extracted from the 4-week-old seedlings with 4 seedlings/1 mL of 80% acetone in the dark (Mackinney, 1941). The chlorophyll contents were then measured using a spectrophotometer at wavelengths of 645 and 663 nm with 80% acetone as a blank. Chlorophyll content was calculated as micrograms of chlorophyll per mg of fresh leaves using the following equation: Chlorophyll a+b (mg gFW^{-1}) = (8.02 x A_{663} + 20.20 x A_{645}) x (1/W); where W indicates the fresh weight of seedlings in milligrams.

Stomata conductance measurements

Stomata conductance was measured using an open infrared gas analysis system, LI-COR 6400.

For all lines, fully expanded, 7-week old rosette leaves were used in a standard single leaf chamber (chamber area = 6 cm^2). An air mixture consisting of 20% O_2 and 80% N_2 were fed to the leaves, and the CO_2 levels were set to 400 ppm in the reference cell. The leaves were illuminated under a photosynthetic photon flux density (PPFD) of 400 μmol $m^{-2}s^{-1}$. Leaf temperature was held between 22 to 23 ^oC, and the dew points within the chamber were kept at 14 $^oC \pm 1.0\ ^oC$. Before the start of each experiment, the leaves or the plants were acclimated to the conditions inside the chamber for at least 20 min under 400 μmol $m^{-2}s^{-}$ of light. Measurements were carried out between ZT2 and ZT9.

Analysis of circadian rhythms

Ten-day old seedlings growing on MS/0.8% agar/2% sucrose media at 12 h light/12 h dark and 22°C were transferred to a 96-well white plate with ~50μl of the same media. 20 μl of 5 mM luciferin in 0.01% silwett was added to each seedling. The plate was transferred the next day to constant light conditions and bioluminescence was detected using a Berthold LB960XS3 luminometer. For the ABA treatment, 30 μl of 25 μM ABA or methanol (diluent control) in 0.01% silwett was added to the seedlings at ZT29.

ACKNOWLEDGEMENTS

We thank K. Childs and other members of the Buell lab for help with data analysis, the Shiu lab for advice on the analysis of promoter elements and P. Salome, S. Matsubara and F. Gaymard for the provision of Arabidopsis lines. We are grateful to N. Bolduc and S. Hake, for the provision of an initial library preparation protocol, and the Howe and Thomashow labs for primers. We also thank S. Weise and T. Sharkey for help with the conductance measurements. We also thank

S. Hoffmann-Benning, B. Montgomery, and S. Shiu for critically reading the manuscript and the MSU Research Technology Support Facility for sequencing. This work was supported by the National Science Foundation (IOS 1054243) and Michigan State University. T.L. was supported by the US Department of Energy and the Michigan Agricultural Experiment Station (DE-FG02-91ER20021).

APPENDIX

SUPPLEMENTARY INFORMATION

Dataset S2.1. PRR7 binding site identification using ChIP-seq (digital file).

Dataset S2.2. PRR7 target genes identified in other experiments (digital file).

Dataset S2.3. Primers used in this study (digital file).

SUPPLEMENTARY METHODS

Chromatin Immunoprecipitation

15-day-old Arabidopsis seedlings were harvested at ZT 12 and vacuum infiltrated in 0.4 M sucrose and 1% formaldehyde for 4 x 5 minutes at room temperature. Glycine was added to a final concentration of 0.133 M and vacuum infiltrated for an additional 5 minutes. The seedlings were then rinsed 5 times in excess volumes of water, frozen in liquid N_2 and ground in liquid N_2 to a fine powder. Nuclei were extracted in Extraction Buffer 1 (400 mM sucrose, 10 mM Tris-HCl, pH 8, 5 mM β-ME, 1 mM PMSF, 1 x protease inhibitor cocktail (Complete Mini, EDTA-free, Roche, Basel, Switzerland), 5 mM benzamidine) for 5 minutes on ice. The extract was filtered through miracloth and centrifuged for 20 minutes at 3200g at +4°C. The supernatant was removed and the pellet was resuspended in 1 ml Extraction Buffer 2 [250 mM sucrose, 10 mM Tris-Hcl, pH 8, 10 mM $MgCl_2$, 1 % Triton-X-100, 5 mM β-ME, 1 mM PMSF, 1 x protease inhibitor cocktail, 5 mM benzamidine] and subsequently centrifuged at maximum speed in a microfuge for 10 minutes at +4°C. The supernatant was removed and the pellet was resuspended in 500 µl Extraction Buffer 3 [1.7 M sucrose, 10 mM Tris-HCl, pH 8, 2 mM $MgCl_2$, 0.15 % Triton-X-100, 5 mM β-ME, 1 mM PMSF, 1 x protease inhibitor cocktail, 5 mM Benzamidine,

50 µM MG132] at +4°C. 500 µl Extraction Buffer 3 was added to a clean and empty 1.5 ml tube and the resuspended pellet was layered on top. The sample was centrifuged for 1 hour at maximum speed in a microfuge at +4°C. The supernatant was removed and the chromatin-enriched pellet was resuspended in 500 µl Nuclei Lysis Buffer [50 mM Tris-Hcl, pH 8, 10 mM EDTA, 1% SDS, 1 mM PMSF, 1 x protease inhibitor cocktail, 5 mM Benzamidine, 50 µM MG132]. The chromatin solution was sonicated on ice and then centrifuged for 10 minutes at maximum speed in microfuge at +4°C. The supernatant was transferred to a 0.45 µm filter tube (Pall, Port Washington, NY, USA) and centrifuged for additional 10 minutes at +4°C. The filtrate was divided into 150 µl aliquots. The aliquots were stored at -80°C or immunoprecipitated (see below).

Immunoprecipitation was performed with Dynabeads ProteinG (Invitrogen Dynal AS, Oslo, Norway). Each sample contained ~120 µg of DNA. Beads were pretreated with anti-HA high affinity rat IgG monoclonal antibody (clone 3F10, Roche, Basel, Switzerland, 10 µg/ 50 µl beads), rabbit anti-GFP polyclonal antibody (Ab290, Abcam, Cambridge, MA; 4 µg/ 50µl beads), or rat IgG (mock control, Jackson Immuno Research, West Grove, PA, USA, 10 µg/ 50 µl beads). Chromatin extracts were diluted 1:10 with ChIP Dilution Buffer [16.7 mM Tris-HCl, pH 8, 1.2 mM EDTA, 167 mM NaCl, 1.1 % Triton-X-100, 1 mM PMSF, 1 x protease inhibitor cocktail, 5 mM Benzamidine, 50 µM MG132]. 1200 µl of diluted chromatin solution was immunoprecipitated with anti-HA beads for 2 hours at +4°C under rotation. 120 µl of the chromatin suspension was used as Input Control. The beads were then washed once with low salt wash buffer [20 mM Tris-HCl, pH 8, 2 mM EDTA, 150 mM NaCl, 0.5 % Triton-X-100, 0.2 % SDS], once with high salt wash buffer [20 mM Tris-HCl, pH 8, 2 mM EDTA, 500 mM NaCl, 0.5

% Triton-X-100, 0.2 % SDS], once with LiCl wash buffer [20 mM Tris-HCl, pH 8, 2 mM EDTA, 0.25 M LiCl, 1 % NP40, Igepal, 0.5 % Deoxycholate], and twice with TE [50 mM Tris-HCl, pH8, 10 mM EDTA]. After the wash, the chromatin was eluted twice with 100 µl Elution Buffer [50 mM Tris-HCl, pH 8, 10 mM EDTA, 1 % SDS], whereas the Input control sample was diluted 1:2 with Elution Buffer. After incubating at +65°C overnight, the DNA was treated with Proteinase K (0.2mg/ml, Roche, Basel, Switzerland) for 2 hours at +65°C. The DNA was purified using the QIAquick PCR Purification kit (Qiagen, Hilden, Germany) and eluted in 50 µl of the Qiagen EB.

Confirmation of PRR7 binding by ChIP-qPCR

For the confirmation of PRR7 binding to the targets identified in our ChIP-Seq experiments we used the line *35S::HA-PRR7* #54 (Farre and Kay, 2007). We have carried out ChIP-qPCR experiments on *CCA1* and *LHY* promoters using the *prr7 PRR7::HA-PRR7* #151 line and observed almost identical IP/Input ratios as the ones measured using *35S::HA-PRR7* #54 shown in Figure S1. For example, using *prr7 PRR7::HA-PRR7* the IP/input value for region 6 on the *CCA1* promoter was 0.013 ± 0.0085 (average ± range, n=2) and for region 3 on the *LHY* promoter 0.0048 ± 0.00025 (average ± range, n=2). These values are very close to the ones shown on Figure S1 measured using the *35S::HA-PRR7* line. Therefore, we found it acceptable to use the *35S::HA-PRR7* plants for our validation experiments.

Library preparation for sequencing

For each library, we pooled 5 (Experiment I) and 12 (Experiment II) individual immunoprecipitated DNA and respective input DNA using QIAquick^{R} PCR Purification Kit

(Qiagen, Hilden, Germany). The pooled DNA-samples were first end-repaired using the End-It™ DNA End-Repair Kit (Epicentre® Biotechnologies, Madison, WI, USA) according to manufacturer protocol. The samples were incubated at room temperature for 45 minutes. The DNA was purified using QIAquick® PCR Purification Kit (Qiagen, Hilden, Germany) and eluted in 36 µl EB. ATP was added to the 3′ ends using Klenow (3′→5′ exo$^-$) (New England BioLabs, Ipswich, MA, USA). 34 µl end-repaired DNA was mixed with 5 µl 10 x NEBuffer 2/Klenow buffer (final conc. 1 x), 10 µl 1 mM dATP and 1 µl Klenow (3′→5′ exo$^-$) (5U/µl) and incubated for 30 minutes at +37°C. The DNA was purified using MinElute® PCR Purification Kit (Qiagen, Hilden, Germany) and eluted in 13 µl EB.

Adapters were ligated to the DNA with A-overhang using LigaFast™ Rapid DNA Ligation System (Promega, Madison, WI, USA). For adapter sequences see Dataset S3. 11 µl DNA was mixed with 15 µl 2 x Rapid Ligation Buffer/DNA ligase buffer, 1 µl Adapter oligo mix (diluted 1:50), 3 µl T4 DNA ligase (3U/µl) and incubated for 15 min at room temperature. The DNA was purified using MinElute® PCR Purification Kit (Qiagen, Hilden, Germany) and eluted in 25 µl EB.

The DNA was PCR-amplified using Finnzymes Phusion® Flash High-Fidelity PCR Master Mix (New England BioLabs, Ipswich, MA, USA) and primers 1.1 and 2.1 (Dataset S2). 23 µl DNA was mixed with 25 µl 2x master mix Phusion® Flash DNA polymerase and 1.75 µl primer mix (12.5 µM each) and amplified: 30 seconds at +98°C; 18 cycles of 10 seconds at +98°C, 30 seconds at +65°C and 30 seconds at +72°C; with a final extension of 15 minutes at +72°C.

The amplified DNA was separated using a 2% low melting point agarose gel (Agarose Low Melt from USB). A band in the range of 150-300 bp was excised with a clean razor blade. The DNA

was purified using QIAquick^{R} Gel Extraction Kit (Qiagen, Hilden, Germany) and eluted in 50 μl EB. The DNA size and quality was controlled using the BioAnalyser DNA high sensitivity kit (Agilent, Santa Clara, CA, USA) and Fluorometer Qubit (Invitrogen, Carlsbad, CA, USA). Single end Illumina sequencing-by-synthesis was performed by the Michigan State University Research Technology Support Facility.

ChIP-Seq Data Analysis

Sequences were preprocessed using the FASTX toolkit (http://hannonlab.cshl.edu/fastx_toolkit/) to filter out adapter sequences (fastx_clipper) and low quality reads (fastq_quality_trimmer). The minimum read length was set at 30 bp and the minimum quality threshold was set at 20. Reads that failed to meet the above criteria were not analyzed further. The preprocessed reads were aligned to the Arabidopsis TAIR10 genome using Bowtie (Langmead et al., 2009) with the -m option to exclude reads that can align more than once to the genome. The rest of the Bowtie parameters were set to default. SAMtools (Li et al., 2009) was used to visualize the Bowtie alignments in the Integrative Genomics Viewer (Robinson et al., 2011). To analyze sequences that successfully aligned to the Arabidopsis genome, QuEST (Valouev et al., 2008) was used to identify binding sites and determine the false discovery rate (FDR). The type of experiment was specified as a "transcription factor with defined motif and narrow (punctate) binding site resulting in regions of enrichment 100-300 bp wide." The binding site calling parameters were set to the relaxed option and the peak shift lower threshold was set at 10. The rest of the QuEST parameters were set to default.

In Experiment I, each immunoprecipitated sample from *prr7-3 PRR7::HA-PRR7* and *prr7-3* were compared to their respective inputs as negative controls. 685 binding sites were identified

in *prr7-3 PRR7::HA-PRR7* and 143 binding sites in *prr7-3* with FDRs of 6.1% and 1.2%, respectively. We defined common binding sites as those located within 500 bp, and found 11 binding sites in common between the two sets, resulting in 674 sites specific to *prr7-3 PRR7::HA-PRR7* (Dataset S1, Figure S7). A comparison of the immunoprecipitated *prr7-3 PRR7::HA-PRR7* to the immunoprecipitated *prr7-3* as a negative control resulted in the identification of 644 sites with an FDR of 45% in Experiment I (Figure S7). Although we did not use this comparison for downstream studies, both types of analyses led to an almost identical set of binding sites; a comparison of the 674 sites to the 644 sites resulted in 611 binding sites in common between the two sets of analyses (Figure S7). Based on this data, we found it sufficient to compare the immunoprecipitated *prr7-3 PRR7::HA-PRR7* to the immunoprecipitated *prr7-3* as a negative control for Experiment II. In Experiment II, reads were randomly discarded from the immunoprecipitated *prr7-3 PRR7::HA-PRR7* until the total number closely matched the total number of reads from the immunoprecipitated *prr7-3* negative control in order for QuEST to calculate FDR values. 298 *prr7-3 PRR7::HA-PRR7* specific binding sites were identified in Experiment II with a 2.7% FDR (Dataset S1).

We observed a higher percentage of putative PRR7 targets upregulated in the *prr579* mutant in Experiment II than Experiment I (Figure S7b). The percentage of genes displaying cycling gene expression in Experiment I was closer to the genome-wide percentage than for genes associated with common binding sites (Figure S7c). Experiment I did not display an enrichment of binding sites in upstream regions close to transcriptional start sites as we observed for Experiment II and the common binding sites (Figure 1, Figure S7 d-e). These observations suggest that a large number of false positive binding sites are present in Experiment I, and therefore, we took a conservative approach by further studying sites identified in both Experiments I and II.

QuEST generated wig files to visualize binding sites in the Integrative Genomics Viewer (Robinson et al., 2011). The binding sites determined by QuEST were compared to TAIR10 genes to associate binding sites to putative target genes. Genes were associated to binding sites located within 1000 bp upstream of the transcriptional start site to 1000 bp downstream of the transcriptional stop. Multiple peaks associated with one gene or multiple genes associated with one peak were retained. Common targets from Experiment I and II, along with the independently confirmed binding sites, were used for further analysis. To analyze the distribution of binding sites, we binned their location every 50 bp, up to 1000 bp upstream from the transcriptional start or 1000 bp downstream from the transcriptional stop. For the binding sites located in the intragenic region, we determined which intron or exon the binding site was located based on TAIR10.

FIGURES

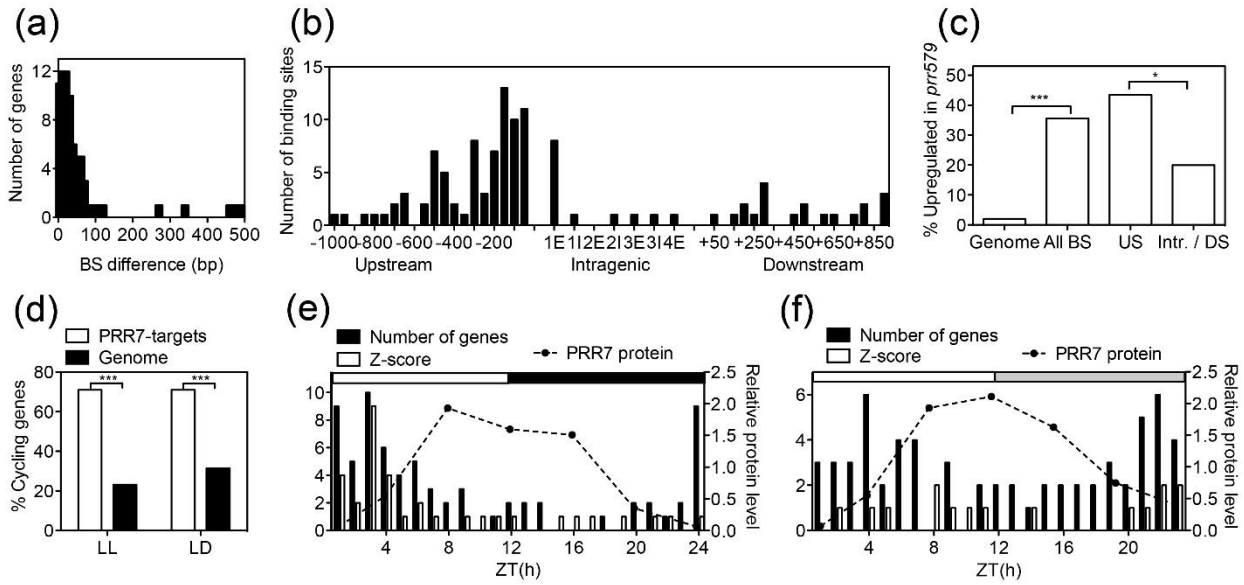

Figure 2.1. Location of PRR7 binding sites and expression patterns of putative PRR7 target genes. (a) Differences in binding site location between Experiment I and Experiment II. (b) PRR7 binding sites location in Experiment II. These binding sites include sites in common between Experiment I and Experiment II and the independently confirmed binding sites. (c) Percentage of genes that display increased expression levels in the *prr579* mutant. (d) Percentage of genes with an upstream PRR7 binding site that display cycling expression levels. Data is from (Edwards et al., 2006) for LL (constant light) and from (Blasing et al., 2005) for LD (light/dark). Cycling gene expression was analyzed using PHASER (Michael et al., 2008). Genes were defined as cycling if the mbpma (model-based, pattern-matching algorithm) > 0.8. Phase of cycling expression of genes associated with PRR7 binding sites under light/dark cycles (e) and under constant light conditions (f), as well as HA-PRR7 protein levels in *PRR7::HA-PRR7* expressing seedlings from (Farre and Kay, 2007). E, exon; I, intron; LD, light/dark; LL, constant light; BS, binding site; US, upstream (-1/-1000 from transcriptional start); DS, downstream

Figure 2.1. (cont'd)

(+1/+1000 from transcriptional stop); Intr., intragenic. Fisher's exact test: *, p<0.05; **, p<0.001; ***, p<0.0001.

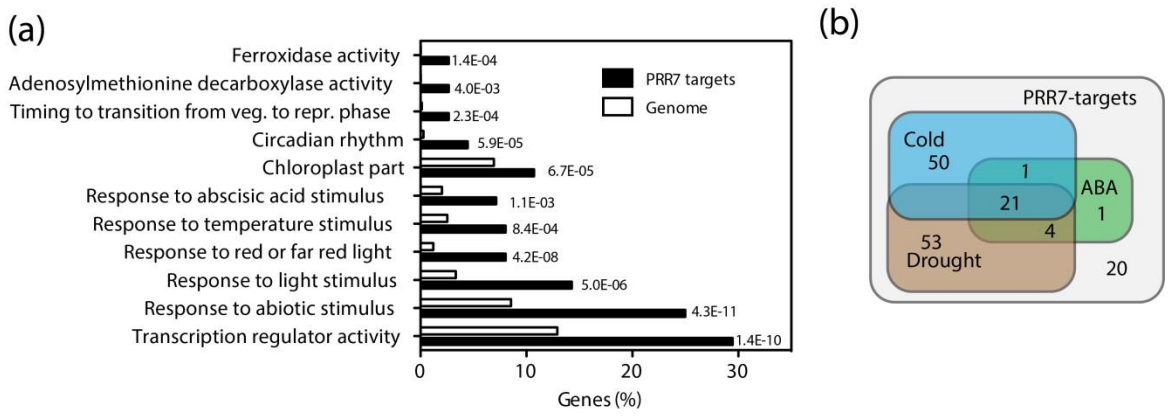

Figure 2.2. Analysis of putative PRR7 target genes. (a) Enrichment of selected Gene Ontology categories in PRR7 target genes. Numbers on the top are p-values for EASE score modified Fisher's exact test (Huang da et al., 2009). (b) Distribution of PRR7 targets among drought, cold and abscisic acid regulated genes.

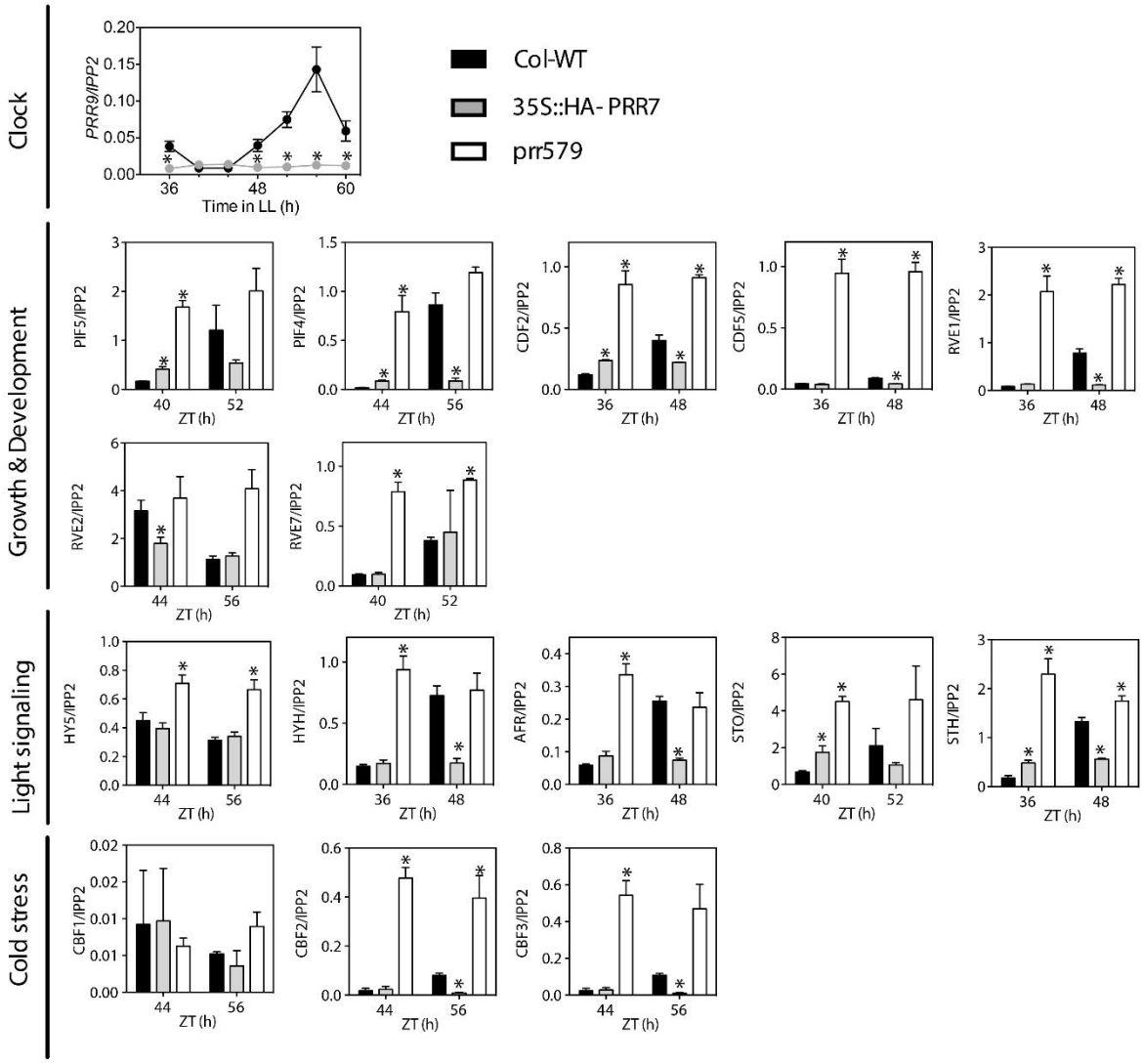

Figure 2.3. PRR7 directly regulates master regulators of the circadian clock, development and stress responses. Expression analysis of these PRR7 target genes in wild type (Col-WT), PRR7 overexpressing line (*35S::HA-PRR7*) and the *prr579* triple mutant. Data are the average ± standard error of 2-3 biological replicates. Expression level was analyzed by RT-qPCR and normalized to *IPP2*. (*) Indicate significant differences with the wild type (*t*-test, $p<0.05$). *IPP2, ISOPENTENYL PYROPHOSPHATE:DIMETHYLALLYL PYROPHOSPHATE ISOMERASE 2; PRR9, PSUEDO-RESPONSE REGULATOR 9; PIF5, PHYTOCHROME INTERACTING FACTOR 5; PIF4, PHYTOCHROME INTERACTING FACTOR 4; CDF2, CYCLING DOF*

Figure 2.3. (cont'd)

FACTOR 2; CDF5, CYCLING DOF FACTOR 5; RVE1, REVEILLE 1; RVE2, REVEILLE 2; RVE 7, REVEILLE 7; HY5, ELONGATED HYPOCOTYL 5; HYH, HY5-HOMOLOG; AFR, ATTENUATED FAR-RED RESPONSE; STO, SALT TOLERANCE; STH, SALT TOLERANCE HOMOLOGUE; CBF1, C-REPEAT/DRE BINDING FACTOR 1; CBF2, C-REPEAT/DRE BINDING FACTOR 2; CBF3, C-REPEAT/DRE BINDING FACTOR 3.

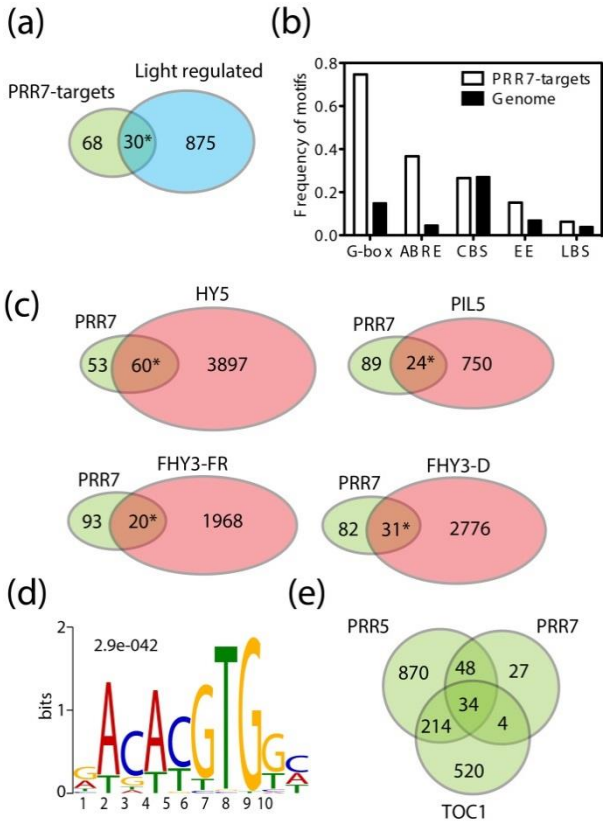

Figure 2.4. PRR7 target genes are light regulated. (a) Venn diagram showing the overlap of PRR7 targets and light regulated genes as defined by Nozue et al. (2011). (b) Enrichment of known motifs in the upstream regions of PRR7 target genes. (c) Venn diagrams showing the overlap of PRR7 targets with HY5 (Lee et al., 2007), PIL5 (Oh et al., 2009), and FHY3

Figure 2.4. (cont'd)

(Ouyang et al., 2011) target genes. ABRE, ABA-responsive Element; CBS, CCA1 binding site; EE, Evening Element; LBS, LUX binding site; FR, far-red; D, dark. (d) A G-box motif was identified as the only statistically overrepresented motif in the 100 bp (50 bp on either side) regions surrounding PRR7 binding sites located upstream of a gene. Regions surrounding the PRR7 binding location from the common and independently confirmed binding sites were used as input for MEME analysis. (e) Venn diagrams showing the overlap of PRR7 targets with PRR5 (Nakamichi et al., 2012) and TOC1 target genes (Huang et al., 2012). (*), Fisher's exact test, $p<0.0001$.

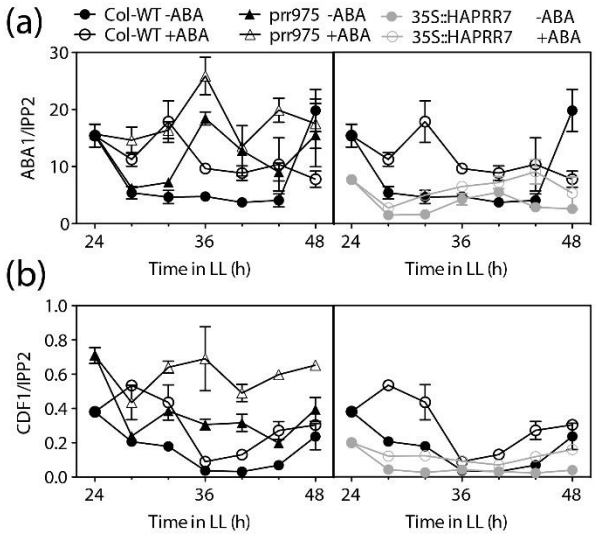

Figure 2.5. PRR7 modulates ABA regulated gene expression. Expression analysis of ABA regulated PRR7 target genes in wild type (Col-WT), PRR7 overexpressing line (*35S::HA-PRR7*) and the *prr579* triple mutant in the presence of ABA. Seedlings were treated with 10 µM ABA at ZT0. Data are the average ± standard error of 2-3 biological replicates. Expression level was analyzed by RT-qPCR and normalized to *IPP2*.

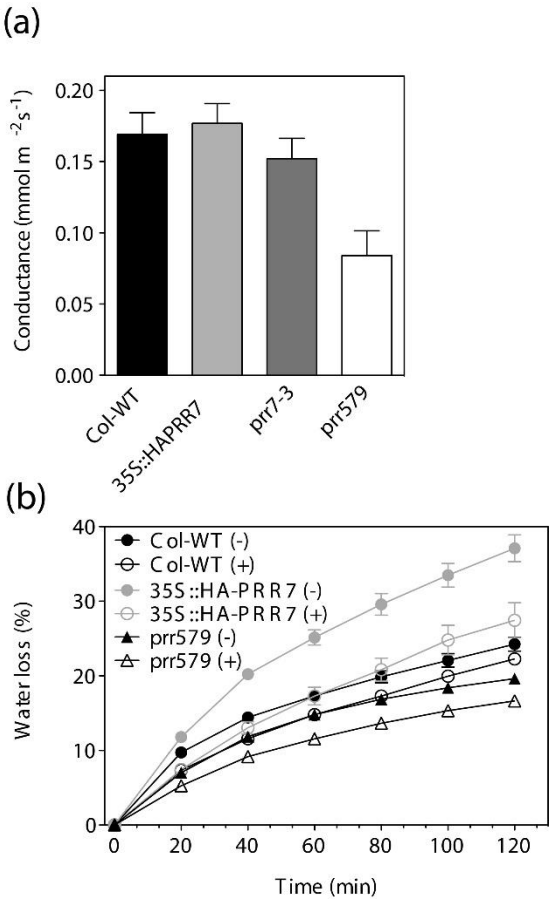

Figure 2.6. PRR7 affects leaf stomata conductance. (a) Stomata conductance of 7-week old plants. Data represents the average ± standard error of 4-6 plants. (b) Rates of water-loss of detached rosettes. Plants were treated with either 10 µM ABA in water (+) or water with methanol (-) as control at ZT1. Three hours later at ZT4.5 rosettes were detached and the weight loss was measured over a 2 h period. Data represents the mean ± standard error of five rosettes per genotype and treatment. Both experiments were performed twice with similar results.

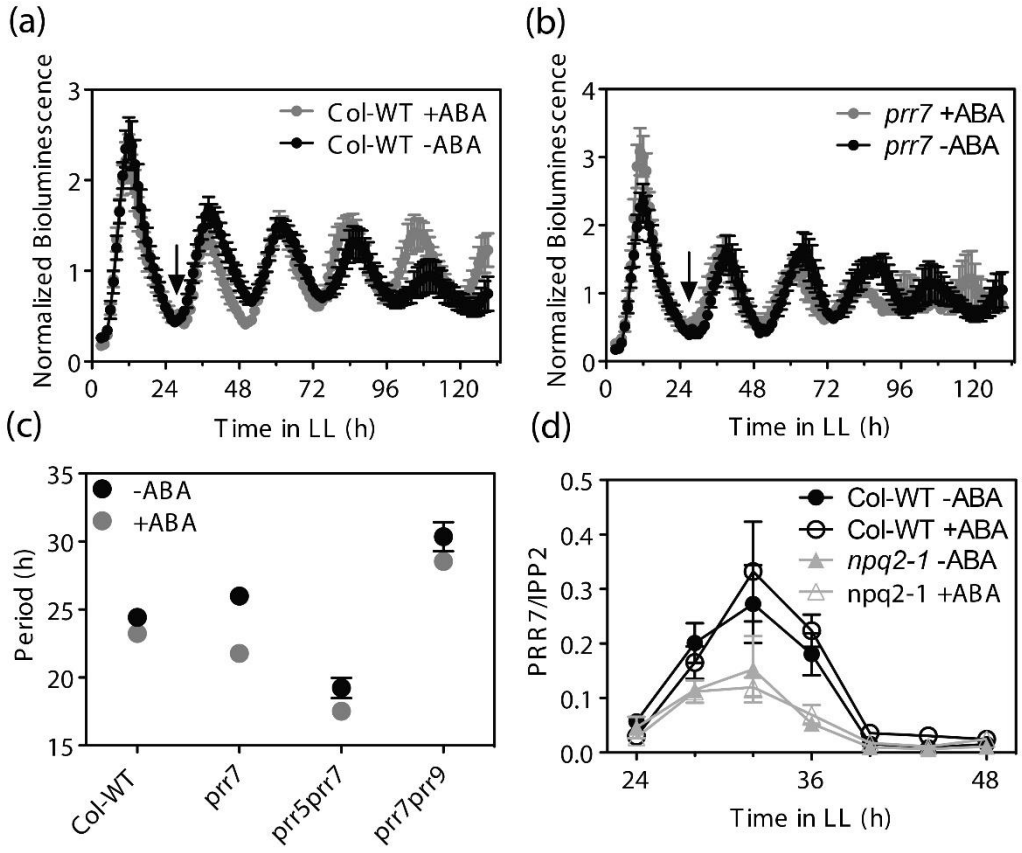

Figure 2.7. ABA affects the period length of *prr7* mutants under constant light conditions. *CCR2:LUC* bioluminescence rhythms in wild type (a) or *prr7* mutants (b) in the presence or absence of exogenous ABA. Arrow indicates time of treatment. (c) Period length estimates of the *CCR2::LUC* bioluminescence rhythms shown in (a) and (b), and in the *prr57* and *prr79* double mutants. (d) *PRR7* RNA levels in the presence or absence of exogenous ABA. Seedlings were treated with 10 µM ABA at ZT0. Data are the average ± standard error of 3 biological replicates. Expression level was analyzed by RT-qPCR and normalized to *IPP2*.

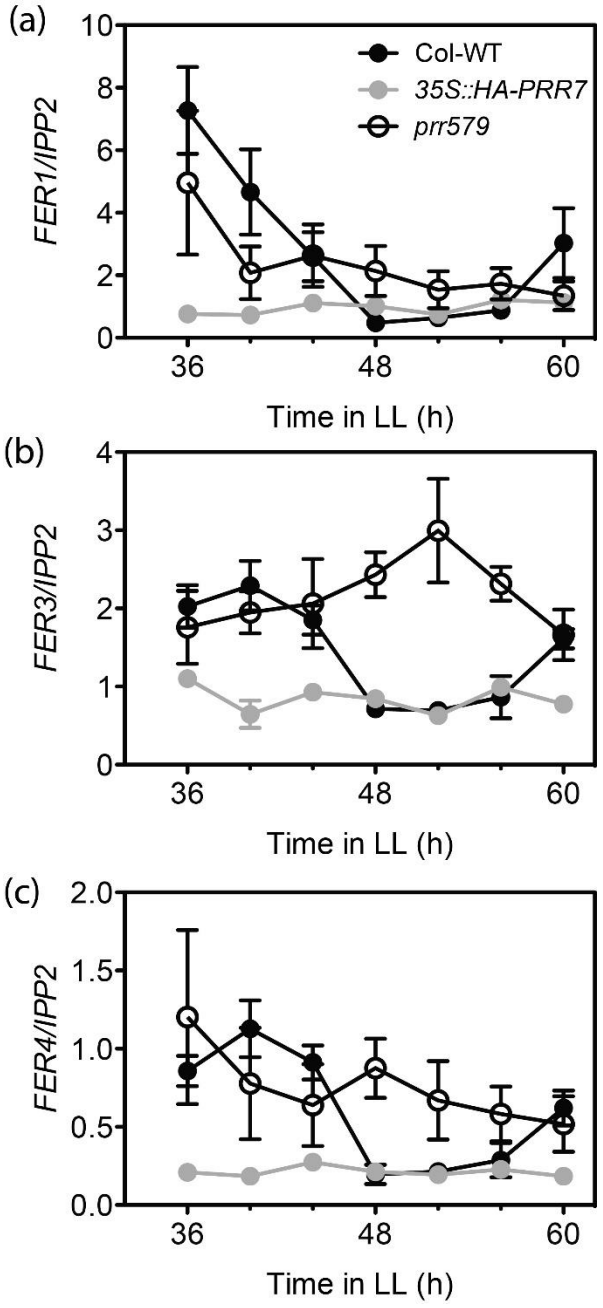

Figure 2.8. PRR7 directly regulates ferritin gene expression. RNA levels of *FER1* (a), *FER3* (b) and *FER4* (c) in wild type (Col-WT), PRR7 overexpressing line (*35S::HA-PRR7*) and the *prr579* triple mutant. Data are the average ± standard error of 2-3 biological replicates. Expression level was analyzed by RT-qPCR and normalized to *IPP2*.

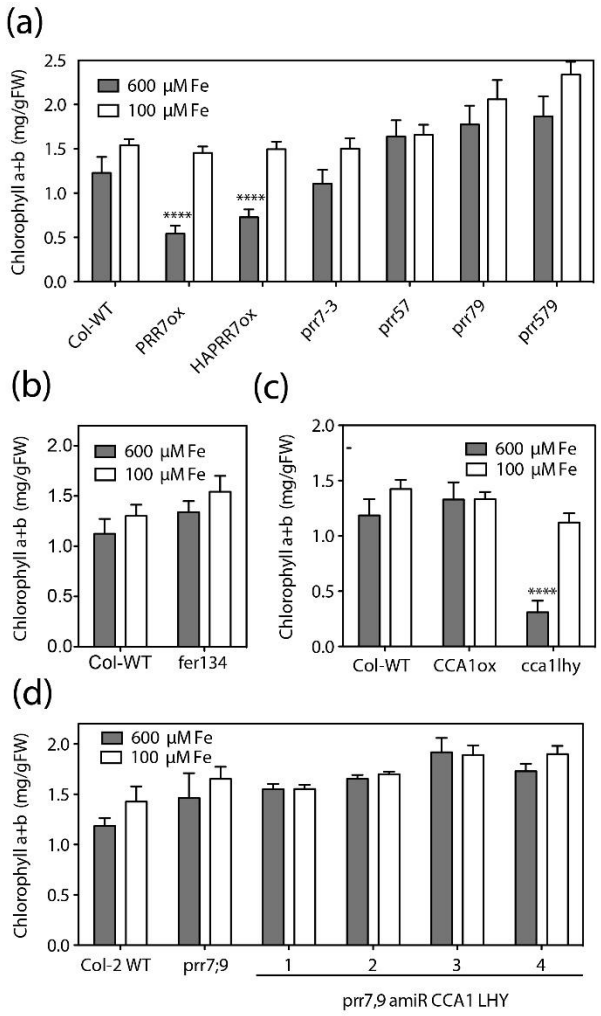

Figure 2.9. PRR7 affects sensitivity to iron excess. Seedlings were grown for three weeks in MS without sucrose media (100 µM iron) before being transferred to MS without sucrose media supplemented with 500 µM iron EDTA (total iron concentration of 600 µM) for 4-7 days before the analysis of chlorophyll content. FW, fresh weight. Data represents the averages ± standard error of 4-12 biological replicates from 2-3 independent experiments.

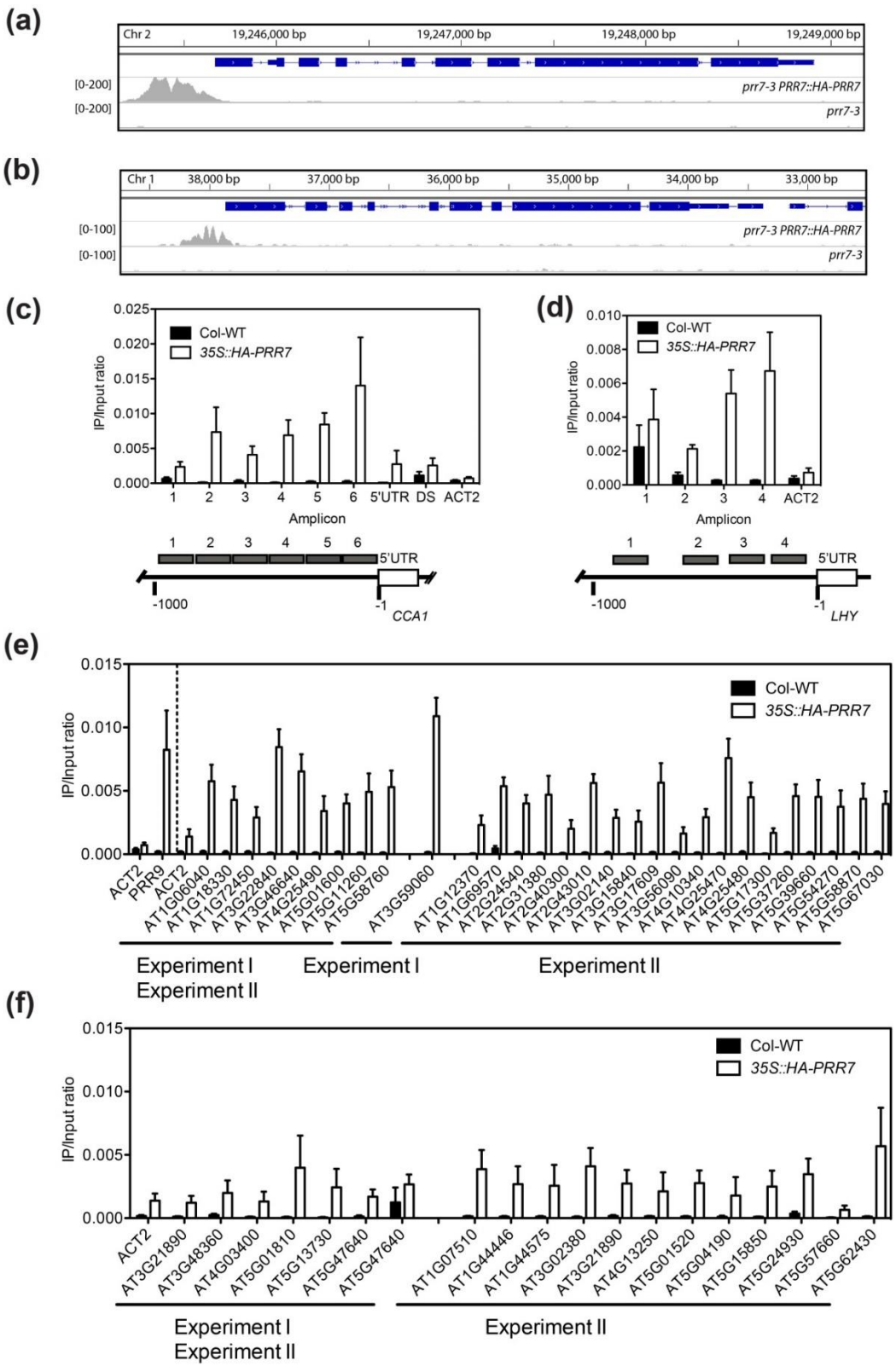

Figure S2.1. ChIP-Seq confirms the binding of PRR7 to the promoters of *CCA1* and *LHY*.

Figure S2.1. (cont'd)

Mapped ChIP-Seq reads in Experiment II in the (a) *CCA1* and (b) *LHY* promoter regions and their respective gene structures in *prr7-3 PRR7::HA-PRR7* and *prr7-3* immunoprecipitated samples. Numbers in brackets on the left-hand side indicate the scale shown. Analysis of the association of PRR7 to specific regions in the (c) *CCA1* and (d) *LHY* promoters by ChIP-qPCR using *35S::HA-PRR7* lines. Data are the average of 3-7 biological replicates ± standard error. (e) and (f) show the analysis of PRR7 binding to other putative targets identified by ChIP-Seq using ChIP-qPCR with the *35S::HA-PRR7 #54* line. Data represents the average ± standard error of three biological replicates. The enrichments in *HA-PRR7* samples were significantly different from the wild type in (e) (Student's t-test, $p<0.05$) but not in (f). The *ACT2* intron was used as a control. Also indicated are the ChIP-Seq experiments from which the binding sites were initially identified.

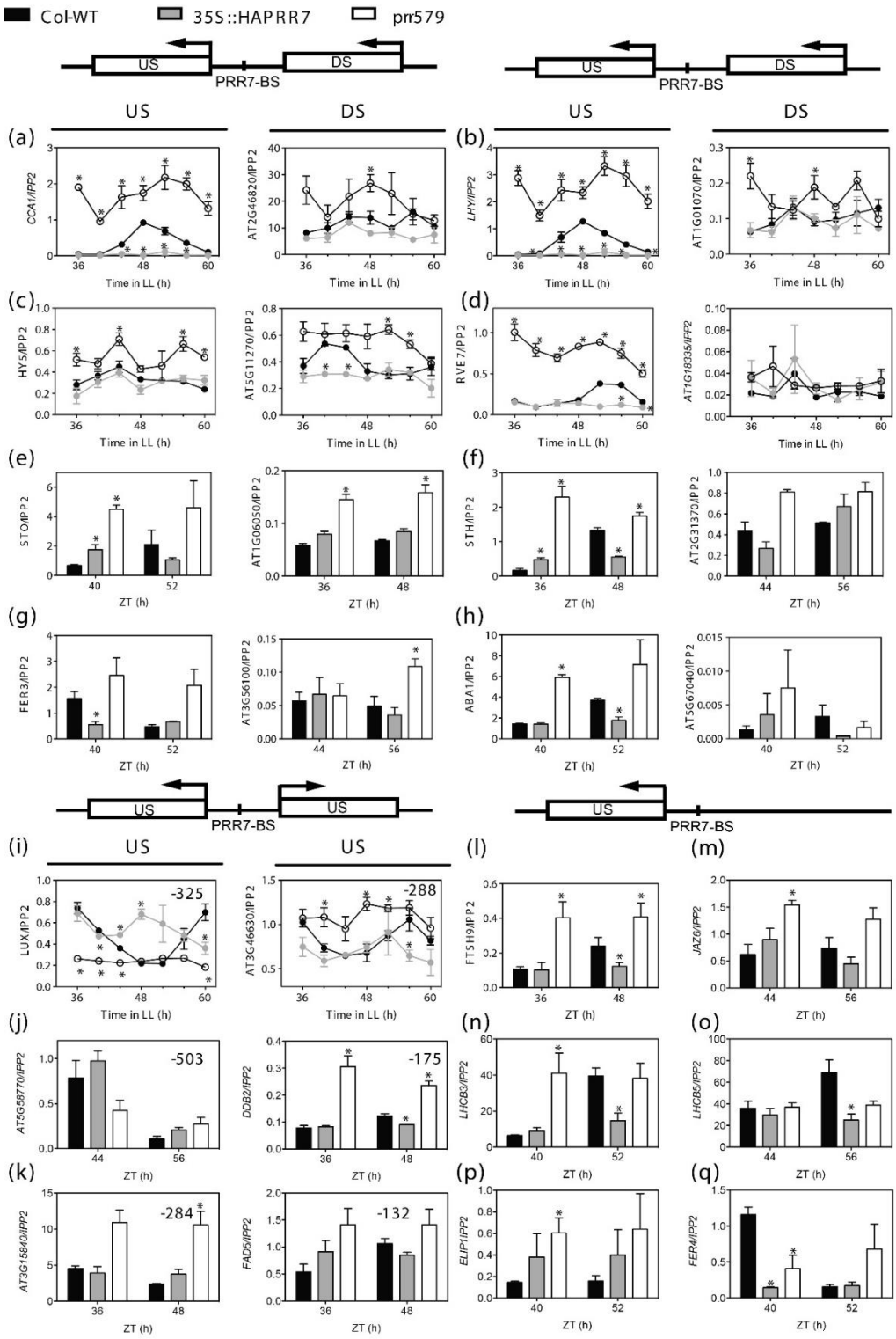

Figure S2.2. Expression of putative genes associated with PRR7 binding sites in wild type (Col-WT), *PRR7* overexpressor (*PRR7ox, 35S::HA-PRR7 #54*) and the *prr579* triple

Figure S2.2. (cont'd)

mutant. (a-h) Analysis of pairs of genes associated with one binding site for which the binding site is located upstream (US, -1/-1000 from transcriptional start) of one of the genes and one downstream (DS, +1/+1000 from transcriptional stop) of the other one. (i-k) Analysis of pairs of genes associated with one binding site for which the binding site is located upstream (US, -1/-1000 from transcriptional start) of both genes. The number in the top right corner of each panel represents the PRR7 binding site location (the average of both ChIP-Seq experiments or in case of (k), the location in Experiment II). (l-q) Expression of genes with a PRR7 binding site in their US region (l, m, o, p, q) or 5'UTR region (n). Binding site rank number in Experiment II for the sites analyzed as reported in Dataset S2.1: (a) R-2; (b) R-25; (b) R-31; (d) R-42; (e) R-44; (f) R-315; (g) R-110; (h) R-383; (i) R-47; (j) R-5; (k) R-319. The data are the average of 2-3 biological replicates ± standard error. Expression level was analyzed by RT-qPCR and normalized to *IPP2*. (*) Indicate significant differences with the wild type (t-test, $p<0.05$). The diagrams indicate the relative position of the binding sites (PRR7-BS) with respect to transcriptional start sites of associated genes.

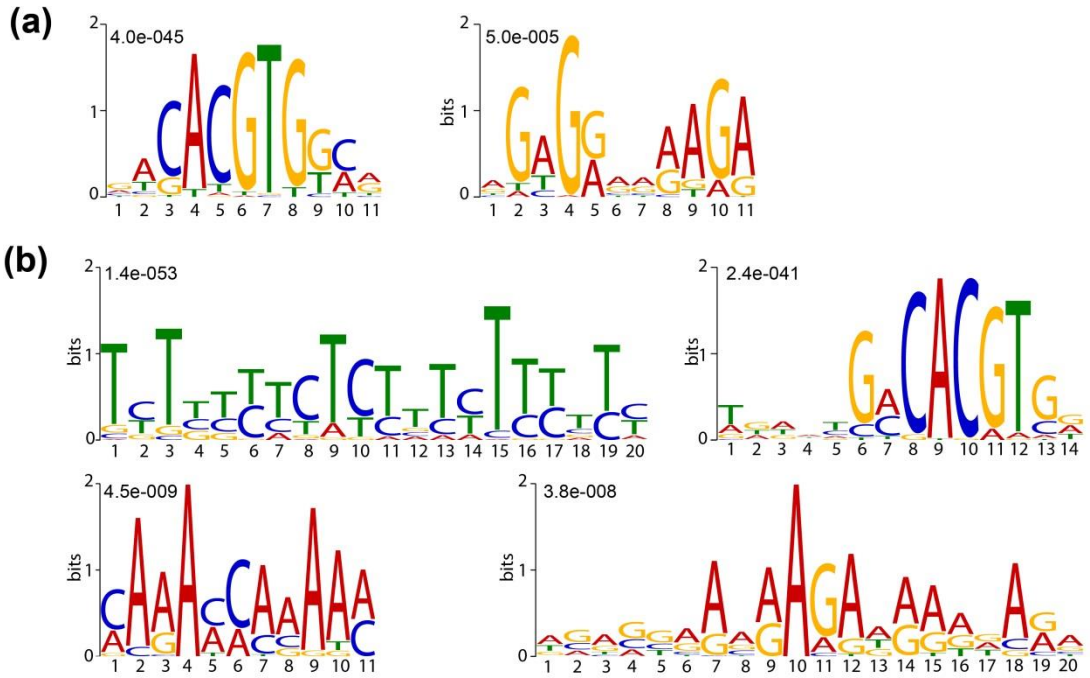

Figure S2.3. Motifs significantly enriched at the common and independently confirmed PRR7 binding sites located upstream of a gene. (a) Regions of 200 bp (100 bp on either side) and (b) 500 bp (250 bp on either side) surrounding the PRR7 binding sites were used as input into MEME. Numbers on top of the logos are the E-values for each of the different motifs.

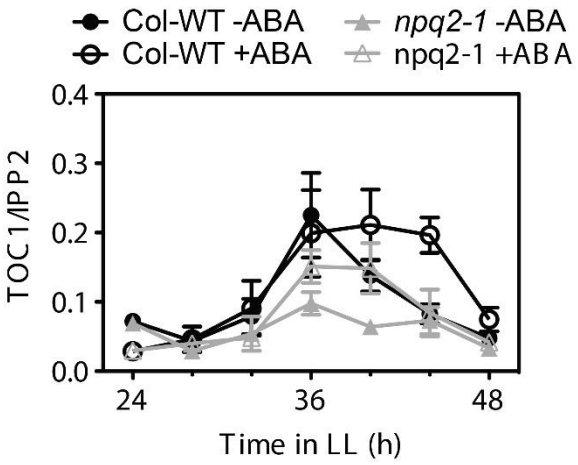

Figure S2.4. TOC1 RNA levels in the presence or absence of exogenous ABA. Seedlings were treated with 10 µM ABA at ZT0. Data are the average ± standard error of 3 biological replicates. Expression level was analyzed by RT-qPCR and normalized to *IPP2*.

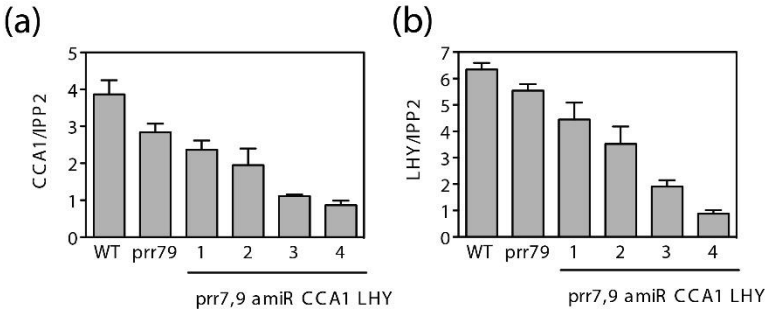

Figure S2.5. *CCA1* (a) and *LHY* (b) expression level in *prr7,9 amiR CCA1 LHY* lines. Seedlings were harvested at ZT0 and expression level was analyzed by RT-qPCR and normalized to *IPP2*. Data are the average ± standard error of 3 biological replicates.

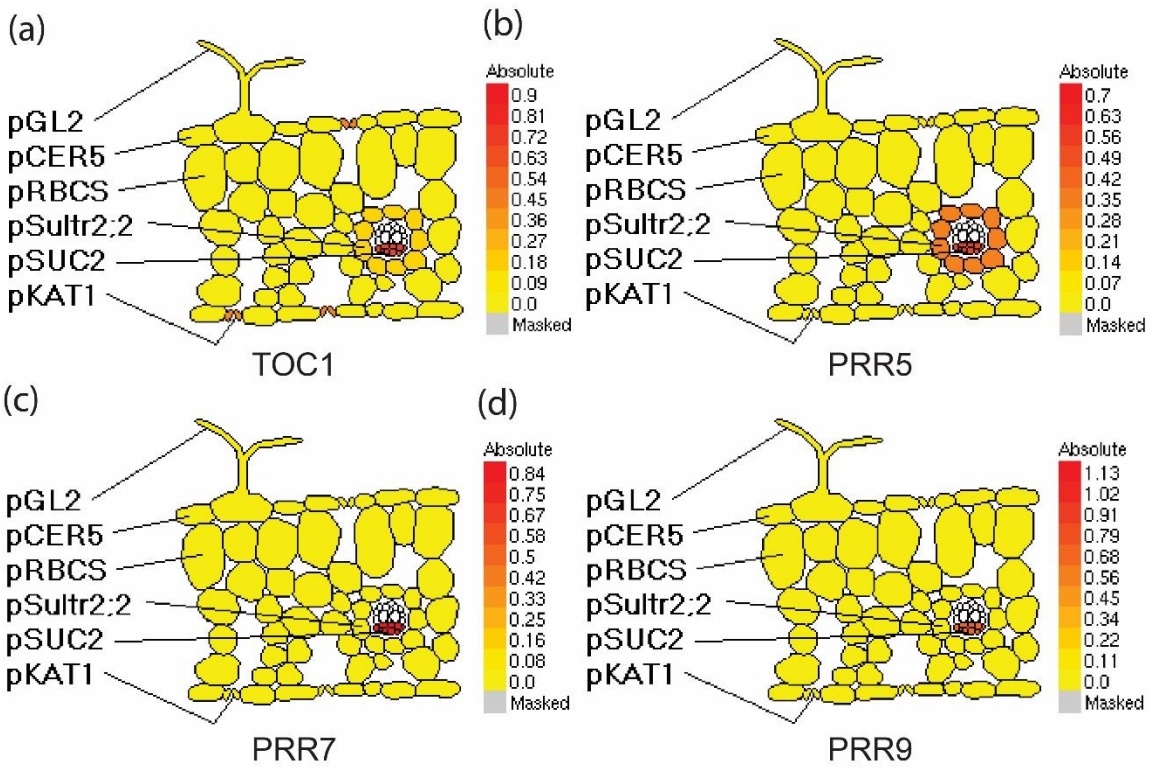

Figure S2.6. Translatome data for (a) TOC1, (b) PRR5, (c) PRR7 and (d) PRR9. Data are derived from microarray studies of RNA bound to polysomes (http://efp.ucr.edu) (Mustroph et al., 2009). Analysis is based on co-immunoprecipitation with tagged ribosomes expressed under the control of different cell specific promoters: pGL.2 for trichomes, pCER5 for epidermis, pRBCS for mesophyll, pSULTR2.2 for bundle sheath, pSUC2 for companion cells and pKAT1 for guard cells. The colors refer to expression levels, with yellow indicating low levels of expression and red corresponding to high levels of expression. Data are from plants grown under 16 h light/8 h dark photoperiods, and harvested at ZT18 after 2 h of low light (Mustroph et al., 2009).

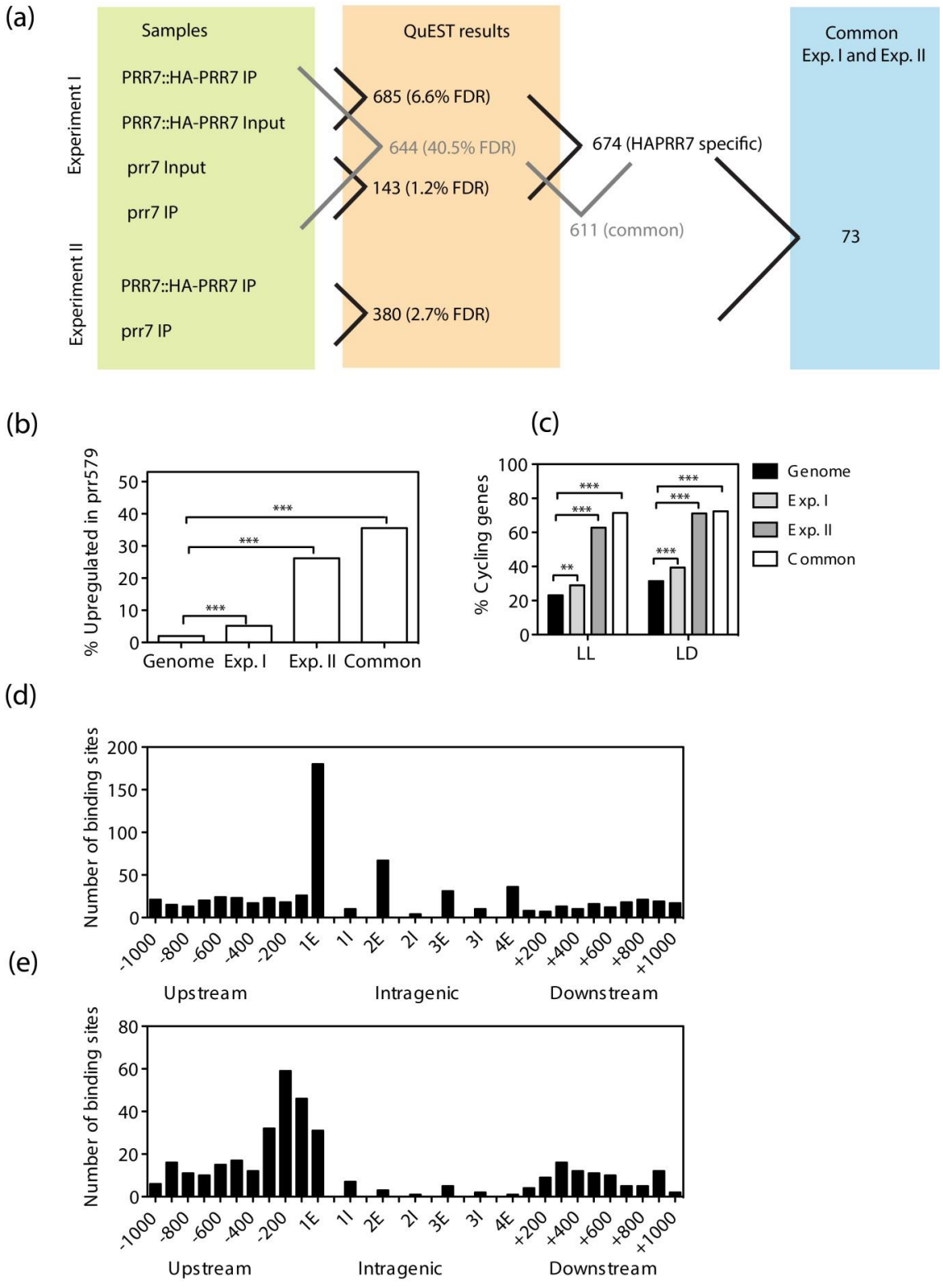

Figure S2.7. Schematic representation of sample comparisons for binding site identification using QuEST and analysis of target genes identified in Experiment I and/or Experiment II.

Figure S2.7. (cont'd)

(a) Schematic representation of samples compared for binding site identification in Experiment I and Experiment II using QuEST. Numbers indicate number of binding sites. Bold labels indicate samples that were used as controls for QuEST analysis. Lines and numbers in gray are comparisons that were not used for further studies. (b) Percentage of genes that display increased expression levels in the *prr579* mutant at ZT12 based on microarray analysis from reference (Nakamichi et al., 2009). (c) Percentage of genes that display cycling expression levels. Data is from (Edwards et al., 2006) for LL (constant light) and (Blasing et al., 2005) for LD (light/dark). Cycling gene expression was analyzed using PHASER (Michael et al., 2008). Genes were defined as cycling if the mbpma > 0.8. (d) PRR7 binding site location in Experiment I. (e) PRR7 binding site location in Experiment II. FDR, false discovery rate; E, exon; I, intron; Genome, all genes; Exp. I, genes associated with binding sites identified in Experiment I; Exp. II, genes associated with binding sites identified in Experiment II; Common, genes identified in both experiments in addition to genes identified in only one experiment but confirmed by ChIP-qPCR. Fisher's-exact test: **, $p<0.001$; ***, $p<0.0001$.

REFERENCES

REFERENCES

Bailey TL, Williams N, Misleh C, Li WW (2006) MEME: discovering and analyzing DNA and protein sequence motifs. Nucleic Acids Research **34:** W369-W373

Bell-Pedersen D, Cassone VM, Earnest DJ, Golden SS, Hardin PE, Thomas TL, Zoran MJ (2005) Circadian rhythms from multiple oscillators: Lessons from diverse organisms. Nature Reviews Genetics **6:** 544-556

Blasing OE, Gibon Y, Gunther M, Hohne M, Morcuende R, Osuna D, Thimm O, Usadel B, Scheible WR, Stitt M (2005) Sugars and circadian regulation make major contributions to the global regulation of diurnal gene expression in Arabidopsis. Plant Cell **17:** 3257-3281

Briat JF, Ravet K, Arnaud N, Duc C, Boucherez J, Touraine B, Cellier F, Gaymard F (2010) New insights into ferritin synthesis and function highlight a link between iron homeostasis and oxidative stress in plants. Annals of Botany **105:** 811-822

Chattopadhyay S, Ang LH, Puente P, Deng XW, Wei N (1998) Arabidopsis bZIP protein HY5 directly interacts with light-responsive promoters in mediating light control of gene expression. Plant Cell **10:** 673-683

Chen H, Zhang J, Neff MM, Hong SW, Zhang H, Deng XW, Xiong L (2008) Integration of light and abscisic acid signaling during seed germination and early seedling development. Proceedings of the National Academy of Sciences of the United States of America **105:** 4495-4500

Covington MF, Maloof JN, Straume M, Kay SA, Harmer SL (2008) Global transcriptome analysis reveals circadian regulation of key pathways in plant growth and development. Genome Biology **9**

Cutler SR, Rodriguez PL, Finkelstein RR, Abrams SR (2010) Abscisic acid: emergence of a core signaling network. Annual Review of Plant Biology **61:** 651-679

Dixon LE, Knox K, Kozma-Bognar L, Southern MM, Pokhilko A, Millar AJ (2011) Temporal Repression of Core Circadian Genes Is Mediated through EARLY FLOWERING 3 in Arabidopsis. Current Biology **21:** 120-125

Doherty CJ, Kay SA (2010) Circadian Control of Global Gene Expression Patterns. *In* A Campbell, M Lichten, G Schupbach, eds, Annual Review of Genetics, Vol 44. Annual Reviews, Palo Alto, pp 419-444

Dong MA, Farre EM, Thomashow MF (2011) CIRCADIAN CLOCK-ASSOCIATED 1 and LATE ELONGATED HYPOCOTYL regulate expression of the C-REPEAT BINDING

FACTOR (CBF) pathway in Arabidopsis. Proceedings of the National Academy of Sciences of the United States of America **108:** 7241-7246

Du SY, Zhang XF, Lu Z, Xin Q, Wu Z, Jiang T, Lu Y, Wang XF, Zhang DP (2012) Roles of the different components of magnesium chelatase in abscisic acid signal transduction. Plant Molecular Biology **80:** 519-537

Edwards KD, Anderson PE, Hall A, Salathia NS, Locke JC, Lynn JR, Straume M, Smith JQ, Millar AJ (2006) FLOWERING LOCUS C mediates natural variation in the high-temperature response of the Arabidopsis circadian clock. Plant Cell **18:** 639-650

Farre EM, Harmer SL, Harmon FG, Yanovsky MJ, Kay SA (2005) Overlapping and distinct roles of PRR7 and PRR9 in the Arabidopsis circadian clock. Current Biology **15:** 47-54

Farre EM, Kay SA (2007) PRR7 protein levels are regulated by light and the circadian clock in Arabidopsis. Plant Journal **52:** 548-560

Filichkin SA, Breton G, Priest HD, Dharmawardhana P, Jaiswal P, Fox SE, Michael TP, Chory J, Kay SA, Mockler TC (2011) Global Profiling of Rice and Poplar Transcriptomes Highlights Key Conserved Circadian-Controlled Pathways and cis-Regulatory Modules. PLoS One **6**

Fowler S, Thomashow MF (2002) Arabidopsis transcriptome profiling indicates that multiple regulatory pathways are activated during cold acclimation in addition to the CBF cold response pathway. Plant Cell **14:** 1675-1690

Fukushima A, Kusano M, Nakamichi N, Kobayashi M, Hayashi N, Sakakibara H, Mizuno T, Saito K (2009) Impact of clock-associated Arabidopsis pseudo-response regulators in metabolic coordination. Proceedings of the National Academy of Sciences of the United States of America **106:** 7251-7256

Garcia ME, Lynch T, Peeters J, Snowden C, Finkelstein R (2008) A small plant-specific protein family of ABI five binding proteins (AFPs) regulates stress response in germinating Arabidopsis seeds and seedlings. Plant Molecular Biology **67:** 643-658

Gendron JM, Pruneda-Paz JL, Doherty CJ, Gross AM, Kang SE, Kay SA (2012) Arabidopsis circadian clock protein, TOC1, is a DNA-binding transcription factor. Proceedings of the National Academy of Sciences of the United States of America **109:** 3167-3172

Gilmour SJ, Zarka DG, Stockinger EJ, Salazar MP, Houghton JM, Thomashow MF (1998) Low temperature regulation of the Arabidopsis CBF family of AP2 transcriptional activators as an early step in cold-induced COR gene expression. Plant Journal **16:** 433-442

Hanano S, Stracke R, Jakoby M, Merkle T, Domagalska MA, Weisshaar B, Davis SJ (2008) A systematic survey in Arabidopsis thaliana of transcription factors that modulate circadian parameters. Bmc Genomics **9**

Harmon FG, Kay SA (2003) The F box protein AFR is a positive regulator of phytochrome A-mediated light signaling. Current Biology **13:** 2091-2096

Holm M, Ma LG, Qu LJ, Deng XW (2002) Two interacting bZIP proteins are direct targets of COP1-mediated control of light-dependent gene expression in Arabidopsis. Genes & Development **16:** 1247-1259

Hsieh TH, Lee JT, Yang PT, Chiu LH, Charng YY, Wang YC, Chan MT (2002) Heterology expression of the Arabidopsis C-repeat/dehydration response element binding factor 1 gene confers elevated tolerance to chilling and oxidative stresses in transgenic tomato. Plant Physiology **129:** 1086-1094

Huang da W, Sherman BT, Lempicki RA (2009) Bioinformatics enrichment tools: paths toward the comprehensive functional analysis of large gene lists. Nucleic Acids Research **37:** 1-13

Huang da W, Sherman BT, Lempicki RA (2009) Systematic and integrative analysis of large gene lists using DAVID bioinformatics resources. Nature Protocols **4:** 44-57

Huang W, Pérez-García P, Pokhilko A, Millar AJ, Antoshechkin I, Riechmann JL, Mas P (2012) Mapping the Core of the Arabidopsis Circadian Clock Defines the Network Structure of the Oscillator. Science **336:** 75-79

Hudson ME, Quail PH (2003) Identification of promoter motifs involved in the network of phytochrome A-regulated gene expression by combined analysis of genomic sequence and microarray data. Plant Physiology **133:** 1605-1616

Indorf M, Cordero J, Neuhaus G, Rodriguez-Franco M (2007) Salt tolerance (STO), a stress-related protein, has a major role in light signalling. Plant Journal **51:** 563-574

Jiao Y, Lau OS, Deng XW (2007) Light-regulated transcriptional networks in higher plants. Nature Reviews Genetics **8:** 217-230

Khan S, Rowe SC, Harmon FG (2010) Coordination of the maize transcriptome by a conserved circadian clock. Bmc Plant Biology **10:** 1-15

Kidokoro S, Maruyama K, Nakashima K, Imura Y, Narusaka Y, Shinwari ZK, Osakabe Y, Fujita Y, Mizoi J, Shinozaki K, Yamaguchi-Shinozaki K (2009) The phytochrome-interacting factor PIF7 negatively regulates DREB1 expression under circadian control in Arabidopsis. Plant Physiology **151:** 2046-2057

Kilian J, Whitehead D, Horak J, Wanke D, Weinl S, Batistic O, D'Angelo C, Bornberg-Bauer E, Kudla J, Harter K (2007) The AtGenExpress global stress expression data set: protocols, evaluation and model data analysis of UV-B light, drought and cold stress responses. Plant Journal **50:** 347-363

Kinmonth-Schultz HA, Golembeski GS, Imaizumi T (2013) Circadian clock-regulated physiological outputs: Dynamic responses in nature. Seminars in Cell and Developmental Biology **24:** 407-413

Kumagai T, Ito S, Nakamichi N, Niwa Y, Murakami M, Yamashino T, Mizuno T (2008) The common function of a novel subfamily of B-box zinc finger proteins with reference to circadian-associated events in Arabidopsis thaliana. Bioscience Biotechnology and Biochemistry **72:** 1539-1549

Kunihiro A, Yamashino T, Nakamichi N, Niwa Y, Nakanishi H, Mizuno T (2011) PHYTOCHROME-INTERACTING FACTOR 4 and 5 (PIF4 and PIF5) Activate the Homeobox ATHB2 and Auxin-Inducible IAA29 Genes in the Coincidence Mechanism Underlying Photoperiodic Control of Plant Growth of Arabidopsis thaliana. Plant and Cell Physiology **52:** 1315-1329

Kuno N, Moller SG, Shinomura T, Xu XM, Chua NH, Furuya M (2003) The novel MYB protein EARLY-PHYTOCHROME-RESPONSIVE1 is a component of a slave circadian oscillator in Arabidopsis. Plant Cell **15:** 2476-2488

Lai AG, Doherty CJ, Mueller-Roeber B, Kay SA, Schippers JH, Dijkwel PP (2012) CIRCADIAN CLOCK-ASSOCIATED 1 regulates ROS homeostasis and oxidative stress responses. Proceedings of the National Academy of Sciences of the United States of America **109:** 17129-17134

Langmead B, Trapnell C, Pop M, Salzberg SL (2009) Ultrafast and memory-efficient alignment of short DNA sequences to the human genome. Genome Biology **10**

Lee J, He K, Stolc V, Lee H, Figueroa P, Gao Y, Tongprasit W, Zhao HY, Lee I, Deng X (2007) Analysis of transcription factor HY5 genomic binding sites revealed its hierarchical role in light regulation of development. Plant Cell **19:** 731-749

Legnaioli T, Cuevas J, Mas P (2009) TOC1 functions as a molecular switch connecting the circadian clock with plant responses to drought. EMBO Journal **28:** 3745-3757

Mackinney G (1941) Absorption of light by chlorophyll solutions. Journal of Biological Chemistry **140:** 315-322

McClung CR (2011) The Genetics of Plant Clocks. *In* S Brody, ed, Genetics of Circadian Rhythms, Vol 74. Elsevier Academic Press Inc, San Diego, pp 105-139

Michael TP, Mockler TC, Breton G, McEntee C, Byer A, Trout JD, Hazen SP, Shen R, Priest HD, Sullivan CM, Givan SA, Yanovsky M, Hong F, Kay SA, Chory J (2008) Network discovery pipeline elucidates conserved time-of-day-specific cis-regulatory modules. PLoS Genetics **4:** e14

Mizoguchi T, Wheatley K, Hanzawa Y, Wright L, Mizoguchi M, Song HR, Carre IA, Coupland G (2002) LHY and CCA1 are partially redundant genes required to maintain circadian rhythms in Arabidopsis. Developmental Cell **2:** 629-641

Murashige T, Skoog F (1962) A revised medium for rapid growth and bio assays with tobacco tissue cultures. Physiologia Plantarum **15:** 473-497

Mustroph A, Zanetti ME, Jang CJ, Holtan HE, Repetti PP, Galbraith DW, Girke T, Bailey-Serres J (2009) Profiling translatomes of discrete cell populations resolves altered cellular priorities during hypoxia in Arabidopsis. Proceedings of the National Academy of Sciences of the United States of America **106:** 18843-18848

Nakamichi N (2011) Molecular Mechanisms Underlying the Arabidopsis Circadian Clock. Plant and Cell Physiology **52:** 1709-1718

Nakamichi N, Kiba T, Henriques R, Mizuno T, Chua NH, Sakakibara H (2010) PSEUDO-RESPONSE REGULATORS 9, 7, and 5 Are Transcriptional Repressors in the Arabidopsis Circadian Clock. Plant Cell **22:** 594-605

Nakamichi N, Kiba T, Kamioka M, Suzuki T, Yamashino T, Higashiyama T, Sakakibara H, Mizuno T (2012) Transcriptional repressor PRR5 directly regulates clock-output pathways. Proceedings of the National Academy of Sciences of the United States of America **109:** 17123-17128

Nakamichi N, Kita M, Ito S, Sato E, Yamashino T, Mizuno T (2005) The Arabidopsis pseudo-response regulators, PRR5 and PRR7, coordinately play essential roles for circadian clock function. Plant and Cell Physiology **46:** 609-619

Nakamichi N, Kita M, Niinuma K, Ito S, Yamashino T, Mizoguchi T, Mizuno T (2007) Arabidopsis clock-associated pseudo-response regulators PRR9, PRR7 and PRR5 coordinately and positively regulate flowering time through the canonical CONSTANS-dependent photoperiodic pathway. Plant and Cell Physiology **48:** 822-832

Nakamichi N, Kusano M, Fukushima A, Kita M, Ito S, Yamashino T, Saito K, Sakakibara H, Mizuno T (2009) Transcript Profiling of an Arabidopsis PSEUDO RESPONSE REGULATOR Arrhythmic Triple Mutant Reveals a Role for the Circadian Clock in Cold Stress Response. Plant and Cell Physiology **50:** 447-462

Nemhauser JL, Hong FX, Chory J (2006) Different plant hormones regulate similar processes through largely nonoverlapping transcriptional responses. Cell **126:** 467-475

Niyogi KK, Grossman AR, Bjorkman O (1998) Arabidopsis mutants define a central role for the xanthophyll cycle in the regulation of photosynthetic energy conversion. Plant Cell **10:** 1121-1134

Nozue K, Covington MF, Duek PD, Lorrain S, Fankhauser C, Harmer SL, Maloof JN (2007) Rhythmic growth explained by coincidence between internal and external cues. Nature **448:** 358-361

Nozue K, Harmer SL, Maloof JN (2011) Genomic Analysis of Circadian Clock-, Light-, and Growth-Correlated Genes Reveals PHYTOCHROME-INTERACTING FACTOR5 as a Modulator of Auxin Signaling in Arabidopsis. Plant Physiology **156:** 357-372

Nusinow DA, Helfer A, Hamilton EE, King JJ, Imaizumi T, Schultz TF, Farre EM, Kay SA (2011) The ELF4-ELF3-LUX complex links the circadian clock to diurnal control of hypocotyl growth. Nature **475:** 398-402

Oh E, Kang H, Yamaguchi S, Park J, Lee D, Kamiya Y, Choi G (2009) Genome-Wide Analysis of Genes Targeted by PHYTOCHROME INTERACTING FACTOR 3-LIKE5 during Seed Germination in Arabidopsis. Plant Cell **21:** 403-419

Ouyang XH, Li JG, Li G, Li BS, Chen BB, Shen HS, Huang X, Mo XR, Wan XY, Lin RC, Li SG, Wang HY, Deng XW (2011) Genome-Wide Binding Site Analysis of FAR-RED ELONGATED HYPOCOTYL3 Reveals Its Novel Function in Arabidopsis Development. Plant Cell **23:** 2514-2535

Pavesi G, Mereghetti P, Mauri G, Pesole G (2004) Weeder Web: discovery of transcription factor binding sites in a set of sequences from co-regulated genes. Nucleic Acids Research **32:** W199-W203

Pavesi G, Mereghetti P, Zambelli F, Stefani M, Mauri G, Pesole G (2006) MoD Tools: regulatory motif discovery in nucleotide sequences from co-regulated or homologous genes. Nucleic Acids Research **34:** W566-570

Pokhilko A, Fernandez AP, Edwards KD, Southern MM, Halliday KJ, Millar AJ (2012) The clock gene circuit in Arabidopsis includes a repressilator with additional feedback loops. Molecular Systems Biology **8**

Pruneda-Paz JL, Breton G, Para A, Kay SA (2009) A Functional Genomics Approach Reveals CHE as a Component of the Arabidopsis Circadian Clock. Science **323:** 1481-1485

Ravet K, Touraine B, Boucherez J, Briat JF, Gaymard F, Cellier F (2009) Ferritins control interaction between iron homeostasis and oxidative stress in Arabidopsis. Plant Journal **57:** 400-412

Rawat R, Schwartz J, Jones MA, Sairanen I, Cheng YF, Andersson CR, Zhao YD, Ljung K, Harmer SL (2009) REVEILLE1, a Myb-like transcription factor, integrates the circadian clock and auxin pathways. Proceedings of the National Academy of Sciences of the United States of America **106:** 16883-16888

Rey G, Cesbron F, Rougemont J, Reinke H, Brunner M, Naef F (2011) Genome-Wide and Phase-Specific DNA-Binding Rhythms of BMAL1 Control Circadian Output Functions in Mouse Liver. PLoS Biology **9**

Salome PA, McClung CR (2005) PSEUDO-RESPONSE REGULATOR 7 and 9 are partially redundant genes essential for the temperature responsiveness of the Arabidopsis circadian clock. Plant Cell **17:** 791-803

Sawa M, Nusinow DA, Kay SA, Imaizumi T (2007) FKF1 and GIGANTEA complex formation is required for day-length measurement in Arabidopsis. Science **318:** 261-265

Song YH, Ito S, Imaizumi T (2010) Similarities in the circadian clock and photoperiodism in plants. Current Opinion in Plant Biology **13:** 594-603

Strayer C, Oyama T, Schultz TF, Raman R, Somers DE, Mas P, Panda S, Kreps JA, Kay SA (2000) Cloning of the Arabidopsis clock gene TOC1, an autoregulatory response regulator homolog. Science **289:** 768-771

Valouev A, Johnson DS, Sundquist A, Medina C, Anton E, Batzoglou S, Myers RM, Sidow A (2008) Genome-wide analysis of transcription factor binding sites based on ChIP-Seq data. Nature Methods **5:** 829-834

Wang L, Kim J, Somers DE (2013) Transcriptional corepressor TOPLESS complexes with pseudoresponse regulator proteins and histone deacetylases to regulate circadian transcription. Proceedings of the National Academy of Sciences of the United States of America **110:** 761-766

Wang ZY, Tobin EM (1998) Constitutive expression of the CIRCADIAN CLOCK ASSOCIATED 1 (CCA1) gene disrupts circadian rhythms and suppresses its own expression. Cell **93:** 1207-1217

Wenkel S, Turck F, Singer K, Gissot L, Le Gourrierec J, Samach A, Coupland G (2006) CONSTANS and the CCAAT box binding complex share a functionally important domain and interact to regulate flowering of Arabidopsis. Plant Cell **18:** 2971-2984

Xiong LM, Lee HJ, Ishitani M, Zhu JK (2002) Regulation of osmotic stress-responsive gene expression by the LOS6/ABA1 locus in Arabidopsis. Journal of Biological Chemistry **277:** 8588-8596

Yadav V, Mallappa C, Gangappa SN, Bhatia S, Chattopadhyay S (2005) A basic helix-loop-helix transcription factor in Arabidopsis, MYC2, acts as a repressor of blue light-mediated photomorphogenic growth. Plant Cell **17:** 1953-1966

Yamashino T, Matsushika A, Fujimori T, Sato S, Kato T, Tabata S, Mizuno T (2003) A Link between circadian-controlled bHLH factors and the APRR1/TOC1 quintet in Arabidopsis thaliana. Plant and Cell Physiology **44:** 619-629

Zhang X, Chen Y, Wang Z-Y, Chen Z, Gu H, Qu L-J (2007) Constitutive expression of CIR1 (RVE2) affects several circadian-regulated processes and seed germination in Arabidopsis. Plant Journal **51:** 512-525

Zou C, Sun K, Mackaluso JD, Seddon AE, Jin R, Thomashow MF, Shiu SH (2011) Cis-regulatory code of stress-responsive transcription in Arabidopsis thaliana. Proceedings of the National Academy of Sciences of the United States of America **108:** 14992-14997

CHAPTER 3

A G-box-like motif is necessary for transcriptional regulation by circadian pseudo-response regulators in Arabidopsis

The work presented in this chapter has been published:

Tiffany L. Liu*, Linsey Newton*, Ming-Jung Liu, Shin-Han Shiu and Eva M. Farré (2015)

Plant Physiology 10.1104/pp.15.01562

(*) Contributed equally to the work.

ABSTRACT

PSEUDO-RESPONSE REGULATORs (PRRs) play overlapping and distinct roles in maintaining circadian rhythms and regulating diverse biological processes, including the photoperiodic control of flowering, growth, and abiotic stress responses. PRRs act as transcriptional repressors and associate with chromatin via their conserved C-terminal CCT (CONSTANS, CONSTANS-like, and TIMING OF CAB EXPRESSION 1 (TOC1/PRR1)) domains by a still poorly understood mechanism. Here we identified genome-wide targets of PRR9 using chromatin immunoprecipitation followed by high-throughput sequencing (ChIP-seq) and compared them with PRR7, PRR5, and TOC1/PRR1 ChIP-seq data. We found that PRR binding sites are located within genomic regions of low nucleosome occupancy and high DNase I hypersensitivity. Moreover, conserved noncoding regions among Brassicaceae species are enriched around PRR binding sites, indicating that PRRs associate with functionally relevant *cis*-regulatory regions. The PRRs shared a significant number of binding regions and our results indicate that they coordinately restrict the expression of target genes to around dawn. A G-box-like motif was overrepresented at PRR binding regions and we showed that this motif is necessary for mediating transcriptional regulation of *CCA1* and *PRR9* by the PRRs. Our results further our understanding of how PRRs target specific promoters and provides an extensive resource for studying circadian regulatory networks in plants.

INTRODUCTION

Eukaryotic circadian clocks consist of complex transcriptional-translational regulatory networks that sustain rhythms with a period length of ~24 hours (Bell-Pedersen et al., 2005). This biochemical oscillator confers a fitness advantage by enabling organisms to anticipate daily and

seasonal changes in the environment (Woelfle et al., 2004; Dodd et al., 2005; Yerushalmi and Green, 2009; Yerushalmi et al., 2011). PSEUDO-RESPONSE REGULATORS (PRRs) are key components of green alga and plant circadian networks (Farre and Liu, 2013). These proteins are characterized by sharing a conserved N-terminal pseudo-receiver domain and C-terminal CCT (CONSTANS, CONSTANS-like, and TIMING OF CAB EXPRESSION 1 (TOC1/PRR1)) domain. The protein levels of the five PRRs in *Arabidopsis thaliana* peak sequentially throughout the day, starting with PRR9 3-4 h after dawn, followed by PRR7, PRR5 and PRR3, and TOC1/PRR1 peaking 1-3 h after dusk (Fujiwara et al., 2008). PRR9, PRR7, PRR5, and TOC1 have been shown to act as transcriptional repressors and associate with chromatin via their CCT domains by a still poorly understood mechanism (Nakamichi et al., 2010; Gendron et al., 2012; Nakamichi et al., 2012).

Within the Arabidopsis circadian clock, PRRs are involved in several transcriptional-translational feedback loops. PRR9, PRR7, PRR5, and TOC1 repress clock components *CIRCADIAN CLOCK ASSOCIATED 1* (*CCA1*) and *LATE ELONGATED HYPOCOTYL* (*LHY*), both of which are expressed at dawn (Nakamichi et al., 2010; Gendron et al., 2012). In turn, CCA1 and LHY activate the expression of *PRR9* and *PRR7*, as well as repress the expression of *TOC1* and probably *PRR5* (Farre et al., 2005; Nagel et al., 2015). REVEILLE 8 (RVE8), which belongs to a subfamily of MYB-domain-containing transcription factors that includes CCA1 and LHY, acts as an activator for *TOC1* and *PRR5* (Farinas and Mas, 2011; Rawat et al., 2011; Hsu et al., 2013). In addition, a protein complex consisting of LUX ARRHYTHMO, EARLY FLOWERING 4 (ELF4) and ELF3 transcriptionally represses *PRR9* and *PRR7* during the night period (Dixon et al., 2011; Helfer et al., 2011; Herrero et al., 2012; Mizuno et al., 2014).

Mutant analyses have shown that PRRs play overlapping and distinct functions in maintaining circadian rhythms and regulating diverse biological processes (Farre and Liu, 2013). The identification of PRR7, PRR5, and TOC1 binding regions using chromatin immunoprecipitation followed by high-throughput sequencing (ChIP-seq) have shown that these proteins are involved in the direct regulation of growth, abiotic stress responses, and the photoperiodic control of flowering (Huang et al., 2012; Nakamichi et al., 2012; Liu et al., 2013). In order to further understand the role of PRRs in regulating gene expression, we identified PRR9 putative target genes using ChIP-seq and performed a comprehensive analysis of PRR bound regions. We observed that PRRs share a large number of binding sites and associate with conserved *cis*-regulatory regions in open chromatin. We also showed that a G-box related motif enriched in PRR binding regions is necessary for transcriptional regulation by the PRRs. Since so far there is no evidence that PRRs are able to bind directly to G-box motifs, these results suggest that PRRs associate with other transcription factors to regulate gene expression.

RESULTS

Genome-wide identification of PRR9 binding regions

In order to dissect the contribution of each PRR in regulating transcription, we generated a PRR9 ChIP-seq dataset to compare with available ChIP-seq data for PRR7, PRR5, and TOC1 (Huang et al., 2012; Nakamichi et al., 2012; Liu et al., 2013). The complemented line *prr9-1 PRR9::HA-PRR9 CCR2::LUC* (Figure S3.1A, Figure S3.1B) was grown in cycling 12 h light/12 h dark for two weeks and harvested four hours after dawn (Zeitgeber, ZT4), the time at which PRR9 protein levels peak (Fujiwara et al., 2008). Three independent PRR9 ChIP experiments were

pooled for sequencing and their quality was confirmed by quantitative PCR, showing an enrichment of PRR9 binding at the *CCA1* promoter (Figure S3.1C) (Nakamichi et al., 2010). We identified 150 PRR9 binding regions using the MACS2 algorithm (Zhang et al., 2008), associated each binding region with the nearest transcriptional start site, and defined these genes as putative targets. PRR9 putative targets included *CCA1* and *LHY*, known to be regulated by PRR9 (Nakamichi et al., 2010). Approximately 34% of PRR9 putative targets were differentially expressed in the *prr5prr7prr9* (*prr579)* triple mutant compared to wild type (Dataset S3.1) (Nakamichi et al., 2009) and all 45 differentially expressed genes, with the exception of one, displayed elevated RNA levels in *prr579* (Fisher's exact test, *p-value* < 0.0001). These findings are consistent with PRR9 functioning as a transcriptional repressor (Dataset S3.1). In addition, approximately 77% of PRR9 putative target genes cycle under constant light conditions (Figure 3.1A) and ~72% of these cycling genes exhibit peak expression around dawn, similar to what has been observed for the putative targets of PRR7, PRR5, and TOC1 (Figure 3.1B) (Huang et al., 2012; Nakamichi et al., 2012; Liu et al., 2013).

PRRs bind to the same DNA regions to regulate common target genes

To compare the binding regions of different PRRs, raw data from PRR7, PRR5, and TOC1 ChIP-seq experiments (Huang et al., 2012; Nakamichi et al., 2012; Liu et al., 2013) were uniformly processed in parallel to PRR9. Between 37-52% of PRR binding summits were located within 500 bp of transcriptional start sites (Figure S3.2A-D). Most PRR9 (86%), PRR7 (80.7%), and to a lesser degree PRR5 (61%) binding summits were located upstream, whereas a large number of TOC1 (30.4%) binding summits were located in the first exon (Figure S3.2E-H). We then asked whether the PRRs bind to the same regions of DNA. To determine shared binding

events, we performed pairwise analyses of the proximity between PRR binding regions using IntervalStats (Chikina and Troyanskaya, 2012). Focusing on the top ranked 150 binding regions for each of the PRRs, we observed that PRR9, PRR7, and PRR5 have the most binding events in common (p-value < 0.05) (Figure 3.2A). TOC1 was more distinct and shared fewer binding events with each of the other PRRs (Figure 3.2A). This difference might be due to the preferential association of TOC1 to exonic regions (Figure S3.2H). We also calculated the distance between binding summits of PRRs with shared target genes. The median distance between binding summits in each of the PRR pairwise comparisons ranged from 23 – 53 bp (Figure 3.2B). To compare these values with values for proteins that bind to the same *cis*-regulatory regions, we analyzed the positions of mouse BMAL1 (Brain and Muscle ARNT-like 1) and CLOCK (Circadian Locomotor Output Cycles Kaput) binding summits determined by ChIP-seq. These clock components are bHLH transcription factors that form heterodimers to regulate gene expression by associating with the same *cis*-regulatory element (Ko and Takahashi, 2006; Hatanaka et al., 2010; Yoshitane et al., 2014) (Figure 3.2B). The median distance between BMAL1 and CLOCK binding summits is 23 bp, which is comparable to the values calculated for the PRR pairwise comparisons, particularly PRR9-PRR7 (28 bp) and PRR7-PRR5 (23 bp). Taken together, our results indicate that PRRs associate with the same regions of DNA to regulate shared target genes.

Although only 27 putative target genes were shared among all four PRRs, a larger percentage of genes were shared among three or two PRRs (Figure 3.3A). For example, 75% of PRR9 putative target genes were in common with PRR7 and PRR5, and of these genes, 38.4% were upregulated in *prr579* (Dataset S3.2). Moreover, pairwise comparisons showed that 95.4% of PRR7 and

89.8% of TOC1 putative target genes were in common with PRR5 (Dataset S3.2). Among all four PRRs, common enriched biological process gene ontology (GO) terms were related to flowering and responses to various abiotic stresses (Figure S3.3.3A, Dataset S3.3). The PRRs were also significantly enriched for molecular function GO terms associated with DNA binding and transcription factor activity (Figure S3.3.3B, Dataset S3.3), reflecting the role of PRRs in orchestrating rhythmic transcription.

The *prr579* triple mutant is arrhythmic, late flowering, resistant to cold and drought, and has a long hypocotyl (Nakamichi et al., 2007; Nakamichi et al., 2009; Niwa et al., 2009). Accordingly, we found that PRR9, PRR7, and PRR5 were bound to regions upstream of *CYCLING DOF FACTOR 2* (*CDF2*), which encodes a repressor of *CONSTANS* (Fornara et al., 2009), a key component in the photoperiodic control of flowering. We also found these PRRs associated with multiple sites in the CBF (*C-REPEAT/DRE BINDING)* regulon (Figure 3.3B) and to the promoter of a gene involved in abscisic acid (ABA) biosynthesis *ABA DEFICIENT 1* (*ABA1*). Moreover, master regulators of growth and development, such as *ELONGATED HYPOCOTYL 5* (*HY5*), *HY5 HOMOLOG* (*HYH*), *PHYTOCHROME INTERACTING FACTOR 4* (*PIF4*), and *PIF5* were also targets of multiple PRRs (Dataset S3.1).

Our results demonstrate a tight interconnected network between members of several families of circadian clock related genes, such as the PRRs, CCA1/LHY/RVEs, and LNKs (NIGHT LIGHT-INDUCIBLE AND CLOCK-REGULATED). All four PRRs associated with the promoters of *CCA1* and *LHY*, along with the promoters of at least two other PRRs (Dataset S3.1). Due to the presence of a small open reading frame in the *PRR9* promoter (AT2G46787), *PRR9* was not

initially identified as a PRR target in the ChIP-seq datasets, but its RNA level is reduced in PRR overexpressing lines (Makino et al., 2002; Sato et al., 2002; Liu et al., 2013). We found that PRR9, PRR7, and PRR5 were also bound within 500 bp of the transcriptional start sites of *RVE8*, *RVE1*, *RVE2/EPR1* (*EARLY-PHYTOCHROME-RESPONSIVE 1),* and *RVE7*. The expression of *RVE8*, *RVE1*, and *RVE7* is upregulated in *prr579* and the expression of *RVE2* is repressed in a PRR7 overexpressing line (Rawat et al., 2011; Liu et al., 2013), indicating that the association is functional. In turn, it has been shown that CCA1/LHY/RVE transcription factors regulate the expression of several *PRR*s (Figure 3.3C) (Alabadi et al., 2001; Farre et al., 2005; Rawat et al., 2011; Hsu et al., 2013). Finally, we observed PRR9 and other PRRs at the promoters of various *LNK* genes. LNK proteins associate with CCA1/LHY/RVE to regulate gene expression (Xie et al., 2014). For example, LNK1 and LNK2 are necessary for RVE8 activation of *PRR5* (Xie et al., 2014). The expression of all four *LNK* genes is upregulated in the *prr579* mutant (Dataset S3.1) (Nakamichi et al., 2010) and the RNA levels of *LNK1* and *LNK2* are elevated in *toc1* mutants (Rugnone et al., 2013). These results indicate strong reciprocal regulation among families of transcription regulators involved in circadian control.

PRRs associate with conserved *cis*-regulatory regions

It is unknown whether PRRs bind to *cis*-regulatory regions to influence gene expression. The positions of active *cis*-regulatory sites correlate with sections of open chromatin and low nucleosome occupancy in plants and animals (Bell et al., 2011). To investigate whether the PRRs associate with regulatory sites, we examined the chromatin landscape of PRR binding regions. We first quantified nucleosome occupancy around PRR binding summits using MNase-seq (micrococcal nuclease digestion combined with sequencing) data on plants harvested at ZT4 (Liu

et al., 2015). Our analyses revealed that PRR binding summits coincide with regions of low nucleosome occupancy compared to background (Figure 3.4A). In addition, open chromatin is susceptible to DNase I cleavage, and DNase I hypersensitive sites (DHSs) also correlate with transcription factor bound DNA in eukaryotes, including plants (Bell et al., 2011; Jiang, 2015). Analysis of recently published DHS data on seedlings grown in light/dark cycles (Sullivan et al., 2014) showed that PRR binding summits are located within DHSs, further establishing that PRRs bind to regulatory regions of DNA (Figure 3.4B).

PRRs are conserved among plants (Farre and Liu, 2013) and many orthologous genes in angiosperms exhibit similar diurnal and circadian gene expression patterns (Filichkin et al., 2011). Therefore, we hypothesized that functionally relevant PRR binding regions would display a high degree of conservation. We examined publicly available data on conserved noncoding sequences (CNSs) among nine Brassicaceae species and compared regions surrounding the PRR binding summits to the same coordinates of randomly selected genes (Haudry et al., 2013). Conserved noncoding sequences are enriched around PRR binding summits (Figure 3.4C), further supporting that PRRs associate with regulatory regions of DNA.

G-boxes are necessary for transcriptional regulation by PRRs

Uncovering the *cis*-regulatory elements (CREs) necessary for PRR association to DNA will provide insight on how PRRs directly target genes to regulate their expression. We identified CREs *de novo* using MEME (Machanick and Bailey, 2011) by analyzing binding regions located upstream of transcriptional start sites. As previously observed for PRR7, PRR5, and TOC1 (Huang et al., 2012; Nakamichi et al., 2012; Liu et al., 2013), a G-box (CACGTG) related motif

was also the most enriched element found at PRR9 binding regions (Figure 3.5A). To determine the similarity between each of the G-box motifs, a distance measure of 1-PCC (Pearson Correlation Coefficient) was calculated for each pair of PRR associated motifs. We found that the motifs identified for each of the PRRs were significantly more similar to each other than randomly expected (Figure 3.3C).

We observed a statistically significant enrichment of G-box-like elements at PRR binding regions located upstream of transcriptional start sites. However, a large percentage of TOC1 binding regions are located in exons (Figure S3.2). When we performed motif enrichment analyses using TOC1 binding regions located within genes, we did not identify any overrepresented motifs. Therefore, we hypothesize that TOC1 binding within genes may represent a different mechanism of regulation as opposed to the mechanism mediated by G-box-like elements located in the upstream regions.

To investigate the role of G-boxes in mediating transcriptional regulation by PRRs, we focused on the promoters of *PRR9* and *CCA1*, which were bound by all four PRRs (Figure 3.5B, C). In Arabidopsis, the *PRR9* promoter contains two G-box motifs (-286, -214), whereas the *CCA1* promoter contains one G-box motif (-296). These sequences are located within DHSs and the *CCA1* G-box is located within a CNS (Figure 3.5B, C). The G-boxes in the *PRR9* and *CCA1* promoters, along with other circadian associated motifs, are conserved across different Brassicaceae species (Figure S3.4).

We used *CCA1* and *PRR9* promoter fragments driving a luciferase reporter gene in Arabidopsis protoplasts to investigate the role of G-boxes *in vivo*. A short fragment of the *PRR9* promoter (-287/-1 bp) was sufficient to mediate repression by full length PRR7 (Dataset S3.6A, B). This activity was reduced when the G-boxes were mutated. In order to provide further evidence that PRR7 directly regulates gene expression, we used the PRR7-CCT domain fused to the herpes simplex viral protein 16 (VP16) trans-activation domain in our transfection assays. The CCT domain by itself cannot mediate transcriptional repression but can be converted to an activator when fused to the VP16 domain (Nakamichi et al., 2012). Therefore, if the transcriptional regulation by the PRRs is direct, we expect to see opposite activities between the full length protein (repression) and the CCT-VP16 fusion protein (activation). Accordingly, the PRR7-CCT domain fused to the VP16 trans-activation domain led to transcriptional activation in a G-box dependent manner (Dataset S3.6C), indicating that this effect may be direct. The *PRR9* G-box located at the -286 position appeared to mediate most of the activity, since the absence of this motif in the -279/-1 fragment caused the same loss of activity as mutations in both G-boxes (Dataset S3.6C). Notably, this G-box is conserved in the promoter of a putative PRR9 ortholog that displays a morning phase of expression in the distantly related *Carica papaya* (Figure S3.4A) (Zdepski et al., 2008). Moreover, a -337/-1 fragment of the *CCA1* promoter (Dataset S3.6D) was also sufficient to mediate activation by PRR7-CCT-VP16 and PRR9-CCT-VP16 in a G-box dependent manner (Dataset S3.6E, F).

We also analyzed plants expressing *PRR9* promoter reporter constructs harboring wild type or mutated G-boxes. The -287/-1 constructs retained strong rhythmicity under constant light with a phase slightly later than a longer *PRR9* promoter construct (-1108/+225) that includes the 5'

UTR (Para et al., 2007) (Dataset S3.6G). The absence of G-boxes in the context of the -287/-1 fragment led to a slight delay in phase, a higher expression level during the end of the day under light/dark cycles, and overall higher expression under constant light conditions (Dataset S3.6G, F). These results indicate that these G-boxes mediate the association of a transcriptional repressor during the end of the day.

DISCUSSION

We performed a comprehensive analysis of PRR binding regions showing that the PRRs share a large number of target genes. Our findings provide an explanation of their partially redundant functions in regulating the circadian clock, growth, development, and responses to abiotic stimuli. Most PRR binding regions are shared by at least two PRRs, which could explain the similarity between the overall phase distributions among the target genes of different PRRs (Figure 3.3A) (Huang et al., 2012; Nakamichi et al., 2012; Liu et al., 2013). As recently reported for CCA1 (Nagel et al., 2015), we also found non-cycling genes among PRR targets. This could be due to differences in the phase of expression in different tissues or masking of transcriptional regulation caused by changes in RNA stability (Gutierrez et al., 2002; Endo et al., 2014). However, it may also reflect a broader role of clock components as modulators of signaling processes. For example, one of the genes bound by PRR9, PRR7, and PRR5 is *ELIP1* (*EARLY LIGHT INDUCED PROTEIN 1*), which is upregulated in the *prr579* mutant, but does not cycle in constant light (Edwards et al., 2006; Nakamichi et al., 2010). *ELIP1* is also directly regulated by CCA1 (Nagel et al., 2015) and the Evening Complex, which is composed of LUX, ELF4, and ELF3 (Takeuchi et al., 2014). In addition, *ELIP1* RNA levels cycle under light/dark conditions and are induced by visible (Harari-Steinberg et al., 2001) and UV-B light (Takeuchi et al., 2014).

Thus, in some cases, regulation by clock components may be restricted to provide a gated response to light signals.

Our results show that there is a tight regulatory network among PRR, CCA1/RVE and LNK protein families. The PRRs are conserved among the green lineage and a single feedback loop between a PRR and a CCA1-like gene forms the basis of the clock in the green algae, *Ostreococcus tauri* (Corellou et al., 2009). The PRR and CCA1 families of transcription regulators have expanded in Angiosperms (Takata et al., 2009; Takata et al., 2010) and some of these genes have retained their function as circadian clock components, such as the PRRs, CCA1, LHY, RVE8, RVE4, and RVE6 (Hsu and Harmer, 2014). However, others have lost their role in the regulation of circadian rhythms, such as RVE1, which has been shown to regulate auxin biosynthesis (Rawat et al., 2011). The recently characterized LNK proteins act as transcriptional co-regulators with RVE8 and possibly CCA1 and LHY (Rugnone et al., 2013; Xie et al., 2014). We observed several PRRs bound to the promoters of *CCA1/LHY/RVE* and *LNK* genes (Dataset S3.1). In turn, CCA1 has been found to associate with promoter regions of several *PRR*s, *LNK3, RVE1*, *RVE2*, *RVE7*, *LHY*, and its own promoter (Nagel et al., 2015). These results show that transcriptional regulation has been maintained during the expansion of these gene families in spite of some functional divergence. Moreover, they confirm our observation that genes tend to maintain cyclic regulation after duplication (Panchy et al., 2014) and emphasize the importance of cyclic expression for gene function.

We observed that the PRRs were bound to conserved regions in open chromatin, indicating that they associate with specific regulatory sites. Our results also suggest that PRRs are able to bind

to the same *cis*-regulatory regions and therefore, might compete for certain binding sites. Differences in time and tissue-specific expression could reduce the direct competition for binding at the cellular level between the PRRs. Some differences in tissue-specific expression of the PRRs have been reported (Para et al., 2007; Endo et al., 2014) but the implications for the regulation of target gene expression are not well understood. PRR binding to target promoters appear to correlate with protein abundance (Nakamichi et al., 2010; Huang et al., 2012). However, the lack of correlation between PRR5 and PRR7 protein abundance and their binding to the *CCA1* and *LHY* promoters at certain times of day (Nakamichi et al., 2010) indicate that other factors might influence PRR association to DNA.

The mechanism by which PRRs associate with target promoters is poorly understood. It has been shown that the C-terminal CCT domain is necessary and sufficient for PRR association to DNA (Gendron et al., 2012; Nakamichi et al., 2012). CCT domains share homology with the DNA binding domain of HEME ACTIVATOR PROTEIN 2 (HAP2) (Wenkel et al., 2006). HAP2 is able to bind DNA when forming a complex with other HAP proteins in yeast (Olesen et al., 1987; Forsburg and Guarente, 1988) and the CCT domain containing protein CONSTANS binds HAP proteins in Arabidopsis (Wenkel et al., 2006). The interaction of PRRs with HAP proteins remains to be studied. It has been shown that the CCT domains of TOC1, PRR5, PRR7, and PRR9 are able to bind a region within the *CCA1* gene *in vitro* (Gendron et al., 2012). However, we showed that a different region located in the *CCA1* promoter is sufficient to maintain cyclic expression and regulation by PRRs *in vivo*. It is possible that tethering or co-binding of the PRRs with other transcription factors might be sufficient for transcriptional activity at specific promoters.

G-box-containing elements are enriched among PRR target genes and we showed that these elements are necessary to mediate PRR transcriptional regulation of *PRR9* and *CCA1* promoters. PRRs share a significant number of target genes with G-box binding factors, including HY5 and PIF1, and both PRR7 and PRR5 share binding regions with PIF4 and PIF5 (Liu et al., 2013; Heyndrickx et al., 2014). In addition, PRRs have been shown to interact with some G-box binding proteins, such as TOC1 with PIF7 (Kidokoro et al., 2009). However, not all PRR binding regions contain G-box-like motifs (Figure 3.5A). In a similar manner, a recent study of Arabidopsis transcription factors showed that single motifs are rarely present in more than half of transcription factor binding regions determined by ChIP-seq (Heyndrickx et al., 2014). This study also showed that some PRR5 and PRR7 binding regions contain FHY3 (FAR RED ELONGATED HYPOCOTYLS 3) and FAR1 (FAR RED-IMPAIRED RESPONSE) binding sites, in agreement with significant overlaps in PRR5 and PRR7 with FHY3 target genes (Heyndrickx et al., 2014). Future analyses of PRR interactions with other transcription factors will aid in understanding the role of different *cis*-regulatory sites for determining promoter specificity.

MATERIALS AND METHODS

Generation of *prr9-1 PRR9::HA-PRR9* lines

The construct pENTR HA-PRR9 containing the PRR9 coding sequence was used to introduce HA-PRR9 into pMDC32 (Curtis and Grossniklaus, 2003) via Gateway technology. The primers 5'-caccatgtacccatacgatgttccagattacgctatgggggagattgtggttt-3' and 5'-tgattttgtagacgcgtctga-3' were used to amplify the PRR9 coding region and introduce an HA-tag at the amino-terminus of

PRR9. The *PRR9* promoter/5'UTR (-1332/+225) was amplified using the primers 5'-cactcctgcaggtcaaccaagaatccgttca-3' and 5'-catcggtaccagactcagacctcaaaaca-3' and cloned into the pCRBlunt II and pMDC32 HA-PRR9 vector using *Sse*8387I and BamHI to exchange the 35S promoter. The final *PRR9::HA-PRR9* construct was used to transform *prr9-1 CCR2::LUC* (*prr9*) (Farre et al., 2005). Circadian rhythms were monitored as described previously (Liu et al., 2013) and analyzed using FFT-NLLS implemented in BRASS (http://millar.bio.ed.ac.uk/Downloads.html)(Plautz et al., 1997). Three independent lines that displayed similar RNA levels to wild type were selected (Figure S3.1A). Gene expression was determined as described previously (Liu et al., 2013). The line *PRR9::HA-PRR9 #109* (HA9) complemented the long period phenotype of *prr9* under constant light (Figure S3.1B) and was chosen for further studies.

Chromatin immunoprecipitation, library preparation, and sequencing

Plants were grown on MS medium with 0.8% agar and 2% sucrose under cycling 12 h light (70 µmol m^{-2} s^{-1} white light)/12 h dark at 22°C for two weeks before harvesting at four hours after the onset of light. ChIPs were performed on the complemented *HA9* line and *prr9* parental control as described earlier (Liu et al., 2013). We pooled three independent ChIPs and confirmed their quality via qPCR of DNA from the immunoprecipitated (IP) fraction normalized to the input control using previously described primers to check the *CCA1* promoter (Figure S3.1C) (Liu et al., 2013). The Research Technology Sequencing Facility at Michigan State University prepared the libraries using the ThruPLEX-FD Prep Kit (Rubicon Genomics) following the manufacturer's protocol for multiplexing. The DNA size and quality was checked using the BioAnalyser DNA high sensitivity kit (Agilent, Santa Clara, CA, USA) and Fluorometer Qubit

(Invitrogen, Carlsbad, CA, USA). DNA sequencing of 50 bp, single-end reads with the Illumina Hi-Seq 2500 yielded a depth of coverage of 4.8 for the HA9 input and 9.5 for the HA9 IP.

ChIP-seq data analysis

The NCBI SRA Toolkit (www.ncbi.nlm.nih.gov/Traces/sra/sra.cgi?view=software) was used to convert PRR5 and TOC1 ChIP-seq data acquired from the NCBI Gene Expression Omnibus to fastq format. ChIP-seq data for PRR9 and PRR7 were generated in our lab and were already in fastq format. All sequences were preprocessed using the fastx_quality_trimmer from the FASTX toolkit (http://hannonlab.cshl.edu/fastx_toolkit/) with a quality score threshold of 20 (-t 20) and a minimum length of 30 nucleotides (-l 30). Quality filtered reads were aligned to the Arabidopsis TAIR10 genome using Bowtie with the option of suppressing all alignments for reads with more than 1 reportable alignment (-m 1) (Langmead et al., 2009). Alignments were visualized using Samtools (Li et al., 2009) and the Integrative Genomics Viewer (Robinson et al., 2011). MACS2 (Zhang et al., 2008) was used to identify binding regions with the broad peak calling parameter (-broad). In each experiment, the immunoprecipitated (IP) sample was compared to their respective input as the negative control, except for the PRR7 ChIP-seq experiment, in which the *prr7-3 PRR7::HA-PRR7* IP was compared to the *prr7-3* IP as the negative control. ChIPpeakAnno (Zhu et al., 2010) was used to associate binding regions to the nearest transcriptional start site as well as for the Gene Ontology enrichment tests (Benjamini Hochberg adjusted *p-value* < 0.05). Binding regions located between 5 kbp upstream to 500 bp downstream of genes on chromosomes 1-5 captured more than 90% of PRR binding regions and were used for further analysis. Bedtools (Quinlan and Hall, 2010) was used to acquire DNA sequences based on bed files. Sequence motifs were identified *de novo* using MEME-ChIP (Machanick and

Bailey, 2011) on PRR binding regions located upstream. The JASPAR CORE Plantae 2014 database (Mathelier et al., 2014) was used for TOMTOM (Gupta et al., 2007) to find known motifs and CentriMo (Bailey and Machanick, 2012) (-db JASPAR_CORE_2014_plants.meme) to examine the distribution of the best matched known motif. Each PRR had one significantly enriched motif, and FIMO (Grant et al., 2011) was used to determine the percentage of upstream PRR binding regions that contained at least one instance of the corresponding PRR motif. The MEME position weight matrices were converted to TAMO format using meme2tamo.py from the Fraenkel Lab (Gordon et al., 2005). Pearson correlation coefficient (PCC) distance (1-PCC) (Zou et al., 2011) was used to determine the extent to which the position weight matrices of PRR motifs differ (Zou et al., 2011). The threshold (0.38) was determined using the 5th percentile of the distances between binding motifs from different families of transcription factors (Franco-Zorrilla et al., 2014).

Expression analysis

Data on cyclic expression are from (Mockler et al., 2007), and genes with an mbpma (model-based, pattern-matching algorithm) > 0.8 were defined as cycling. LD data are from (Blasing et al., 2005) and LL data from (Edwards et al., 2006). PHASER (Michael et al., 2008) was used to analyze peak gene expression of cycling genes with an mbpma > 0.8. The *prr5prr7prr9* (*prr579)* expression data compared to wild type is from (Nakamichi et al., 2009), the PRR5-VP16 expression data is from (Nakamichi et al., 2012), and the alcohol inducible *ALC::TOC1* expression data is from (Gendron et al., 2012).

Analysis of nucleosome occupancy, DNase I hypersensitive sites, and conserved noncoding regions

Nucleosome occupancy (NOC) data are from (Liu et al., 2015), DNase I hypersensitive sites (DHS) data from (Sullivan et al., 2014), and conserved noncoding sequences (CNS) data from (Haudry et al., 2013). Normalized values represent the $\log_2$ ratio of the average (NOC) or median (DHS and CNS) score per base from -1 kbp upstream to +1 kbp downstream of the binding summit, to the average (NOC) or median (DHS and CNS) score at the same coordinates of randomly selected genes. For the CNS reference file, the presence of a CNS was given a value of one, whereas the absence of a CNS was given a value of zero. In order to focus on binding regions located in noncoding regions, binding summits located in exons were omitted for the CNS analyses.

Generation of constructs for protoplast transformation

The PRR full length or CCT domain coding sequence was amplified and cloned into pENTR/D-TOPO (Invitrogen) and transferred into pRTL2-35S-GW or pRTL2-GW-VP64, respectively. The PRR7 CCT domain was amplified using the primers 5'-caccatgaataagatctctcaaagggaa-3' and 5'-gctatcctcaatgttttttatgt-3' and the PRR9 CCT domain using 5'-caccatgtggagtagaagccagagag-3' and 5'-tgattttgtagacgcgtctgaatt-3'. To generate the pRTL2-35S-GW vector the gateway cassette was amplified from pESpyce (Berendzen et al., 2012) using the primers XhoI-GW-F 5'-cacactcgagacaagtttgtacaaaaaagc-3' and GWs-XbaI-R 5'-tgtgtctagattaaaccactttgtac-3' and inserted into vector pRTL2-35S-NYFP (Strayer et al., 2000) using the XhoI and XbaI sites. The pRTL2-35S-GW-VP64 vector was used to express the PRR-CCT domains fused to four copies of the VP16 transactivation domain. The GW-VP64 insert was amplified from pB7WG2-VP64 (Helfer

et al., 2011) using the primers XhoI-GW-F and VP64s-XbaI-R 5'- tgtgtctagattagttaattaacatatcg-3' and cloned into pRTL2-NYFP using XhoI and XbaI. In both cases the NYFP was removed from pRTL2.

To generate pRTL2-GW-Luc, which was used to clone the different promoter fragments, the GW-Luc-Nos insert was amplified from pMDC140-Luc+-HA (Farre and Kay, 2007) using primers pRTL2-GW-F 5'- ctatgaccatgattacgccaatcaacaagtttgtacaaaaaagc-3' and Nos-pRTL2-R 5'-cgacggccagtgccaagctagtaacatagatgacacc-3'. Gibson Assembly (NEB) was used to clone the insert into the pRTL2-NYFP vector after digestion with HindIII. Promoter fragments of -287/-1 bp and -337/-1 bp for *PRR9* and *CCA1*, respectively, were amplified from Col-0 genomic DNA using the primers shown in Table S1. Promoter fragments were cloned into pENTR/D-TOPO (Invitrogen) and transferred to pRTL2-GW-Luc-Nos. Fragments with the G-boxes mutated for both *CCA1* and *PRR9* promoters were made by changing the G-box sequence from CACGTG to ACATGT or TGTACA using primers shown in Table S1. The fragments were cloned using the mega-primer strategy. The ACT2 promoter (-473/-1) was used as the promoter negative control, the pRTL2-35S-NYFP construct was used as the effector negative control, and the *Renilla reniformis* luciferase (Helfer et al., 2011) expressing vector pRTL2-35S-Renilla as the transformation control.

Protoplast transient transformation assays

Arabidopsis thaliana Col-0 or *prr5prr7prr9* (Liu et al., 2013) seeds were sown on soil (Sure-Mix) and placed at 4°C for 3-4 days. They were grown for 3-4 weeks at about 20°C under 16 h light (110 μmol $m^{-2}s^{-1}$ white light)/8h dark cycles. Leaves 5-7 were removed from 25-45

seedlings and cut into thin strips. The leaf strips were placed in 10 mL digestion buffer (400 mM mannitol, 20 mM potassium chloride, 20 mM MES pH 5.7, 15 mg mL^{-1} cellulase, 4 mg mL^{-1} macerozyme, 10 mM calcium chloride, 0.1% nuclease-free bovine serum albumin) and incubated in the dark for 3 hours. After lightly shaking the leaf strips to release the protoplasts, 10 mL of W5 buffer (2 mM MES pH 5.7, 125 mM calcium chloride, 154 mM sodium chloride, 5 mM potassium chloride) were added and protoplasts were filtered through a 75 μM nylon mesh. The protoplasts were centrifuged at 100 g and 4°C for 2 min. The protoplast pellet was resuspended in 5 mL chilled W5 buffer and centrifuged again at 100 g and 4°C for 2 min. The pellet was resuspended in 5 mL chilled W5 buffer and allowed to settle for 30 minutes on ice. The protoplasts were resuspended in MMG buffer (400 mM mannitol, 15 mM magnesium chloride, 4 mM MES pH 5.7) to 2.5 million protoplasts mL^{-1}. Ten micrograms of DNA was added to 250,000 protoplasts. The DNA mixture consisted of 5 μg effector, 4 μg target pRTL2-promoter-Luc, and 1 μg pRTL2-35S-Renilla. To transfect the protoplasts, 110 μL PEG solution (200 mM mannitol, 100 mM calcium chloride, and 40% PEG 4000) was added and samples were incubated at room temperature for 30 min. To stop the transfection, 440 μL of W5 buffer was added. Samples were centrifuged at 100 g and 22°C for 2 min. Protoplasts were washed twice with 1 mL W5 buffer and centrifuged again and spread in a thin layer on a plate treated with 5% BSA in MMG buffer. Protoplasts were left under 15 μmol m^{-2} s^{-1} light for ~16 hours. Transfected protoplasts were centrifuged at 200 g and 22°C for 20 min and assayed using the Promega Dual Luciferase kit (Promega). The protoplast pellet was resuspended in 50 μL extraction buffer (1x passive lysis buffer, 1x protease inhibitor, 5 mM benzamidine, 1 mM PMSF) and incubated on ice for 15 min. Samples were centrifuged for 10 min. at 18,000 g and 4°C. The supernatant was centrifuged for 5 min. at 18,000 g and 4°C. To measure the firefly luciferase activity, 25 μL of

Lar II was added to 5 μL of the protein extract and the luminescence was measured for 0.05 sec. To measure renilla luciferase activity, 25 μL of Stop and Glow was added and the luminescence was again measured for 0.05 sec using a Berthold LB960XS3 luminometer.

In planta luciferase expression of *PRR9* promoter fragments

The promoter fragments in pENTR/D-TOPO (Invitrogen) described above were transferred to the gateway compatible pFlash vector (Gendron et al., 2012) and used to transform *Arabidopsis thaliana* Col-0 (Clough and Bent, 1998). Transgenic seedlings were selected on MS medium containing 0.8% agar and gentamycin (100 μg ml^{-1}). For imaging, 12 day old T2 plants grown on gentamycin under 12 h white light/12 h dark were transferred to MS medium containing 0.8% agar and 2% sucrose and treated with 5 mM luciferin (Gold Biotechnology) in 0.01% Silwett. The next day, plants were transferred to 150 μmol m^{-2} s^{-1} light (25 % blue light LED, 75 % red light LED) and imaged using an Andor iKon-M DU-934N-BV camera every 2 h for 20 min. Two to four seedlings per line were analyzed. Phase and relative amplitude error were quantified using BRASS. The *PRR9::LUC* construct -1108/+225 has been described previously (Para et al., 2007).

Accession numbers

Sequence data from this article can be found in the NCBI GEO data libraries under accession numbers GSE35952 for the TOC1 ChIP-seq, GSE36361 for the PRR5 ChIP-seq, GSE49282 for the PRR7 ChIP-seq, and GSE71397 for both the PRR9 ChIP-seq and the processed data from this study.

Author contributions

T.L., M.L., S-H.S., and E.F. conceived the experiments. T.L., L.N., and M.L. performed the experiments. T.L., E.F., and M.L. analyzed the data. T.L., L.N. and E.F. wrote the manuscript.

SUPPLEMENTARY INFORMATION

Table S3.1. Primers used to generate promoter fragments.

Dataset S3.1. PRR binding sites and associated genes.

Dataset S3.2. Expression of putative PRR target genes identified by ChIP-seq.

Dataset S3.3. Enriched gene ontology terms in putative PRR target genes.

ACKNOWLEDGEMENTS

We thank the Shiu lab members for helpful discussions, especially Sahra Uygun. We are grateful to Jeff Landgraf and the rest of the Research Technology Sequencing Facility at MSU for handling the library preparation and sequencing. This work was funded by the National Science Foundation IOS-1054243 to E.F. and MCB-1119778 and IOS-1126998 to S-H.S. T.L. was also supported by graduate fellowships from Michigan State University.

APPENDIX

FIGURES

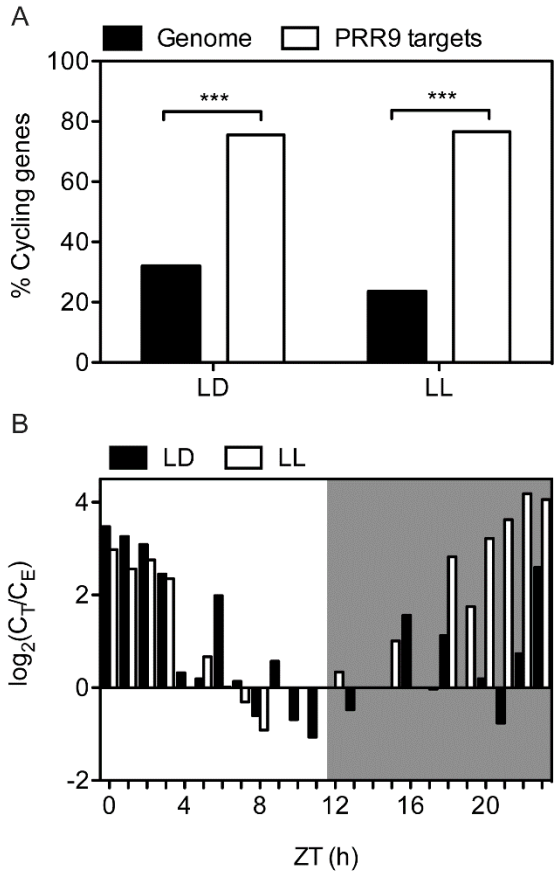

Figure 3.1. Cycling gene expression patterns of PRR9 putative target genes determined by ChIP-seq. (A) Percentage of PRR9 putative target genes that cycle in light/dark (LD) (Blasing et al., 2005) and constant light conditions (LL) (Edwards et al., 2006) compared to genome-wide cyclic gene expression patterns. Cycling gene expression is defined as having an mbpma (model-based, pattern-matching algorithm) > 0.8. Fisher's exact test: ***, *p-value* < 0.0001. (B) Phase of PRR9 putative target gene expression under LD (black bars) and LL (white bars). Shaded area indicates dark or subjective dark period in LD or LL, respectively. PHASER analysis: mbpma > 0.8 (Michael et al., 2008). C_T, count of targets; C_E, count of expected; ZT, Zeitgeber; h, hours.

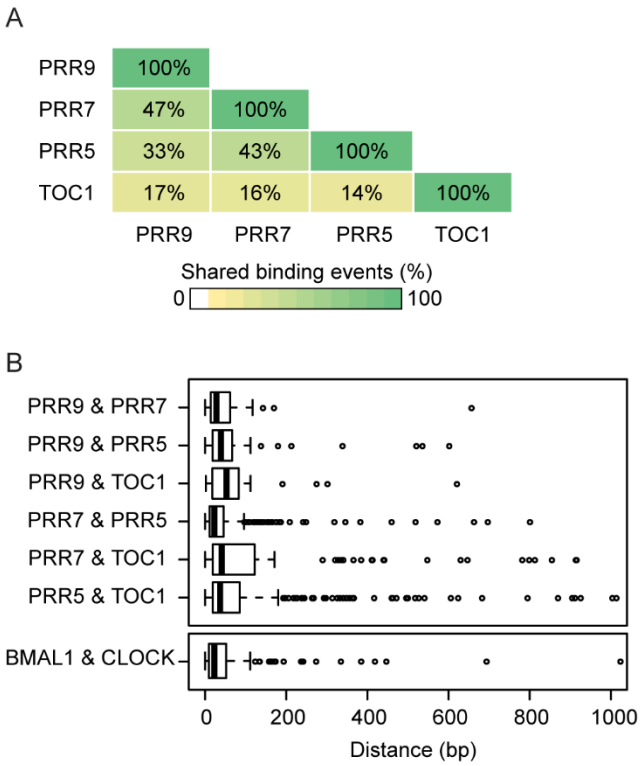

Figure 3.2. PRRs associate to the same chromatin regions. (A) Mean percentage of shared binding events from reciprocal pairwise comparisons of the top 150 binding regions in each PRR dataset determined by IntervalStats (Chikina and Troyanskaya, 2012) (p-value < 0.05). (B) Tukey boxplots of the distance between PRR binding summits with shared putative target genes. For graphical clarity, data points > 1000 bp were omitted, which included one PRR5 & TOC1 data point and 102 *Mus musculus* BMAL1 & CLOCK data points (Hatanaka et al., 2010; Yoshitane et al., 2014).

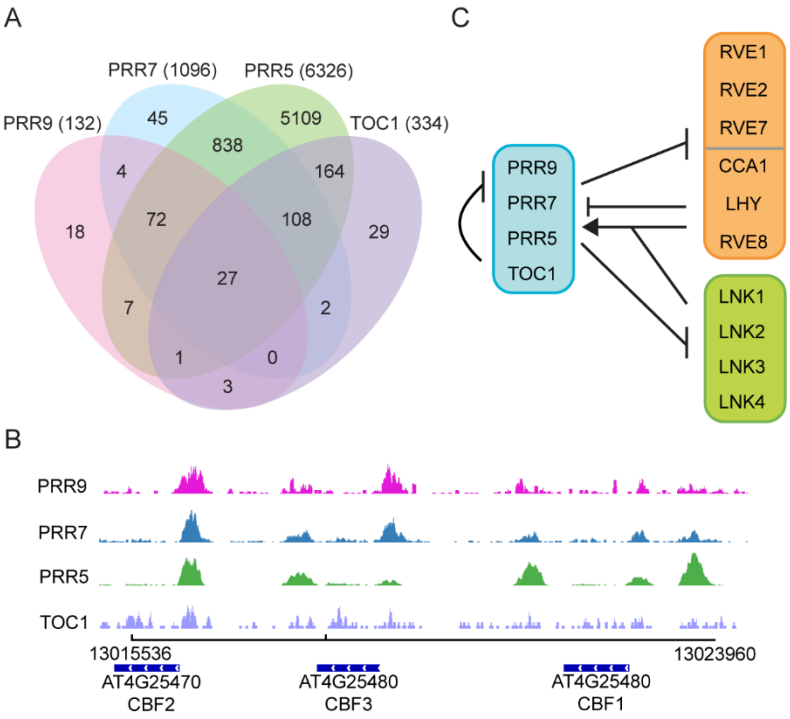

Figure 3.3. Shared putative target genes among PRR9, PRR7, PRR5, and TOC1. (A) Venn diagram of overlapping and distinct PRR target genes determined by ChIP-seq. The total number of target genes for each PRR is shown in parentheses. Putative target genes were defined by associating each binding region to the closest transcriptional start site. PRR9 is in pink, PRR7 in blue, PRR5 in green, and TOC1 in purple. (B) Binding profile of the PRRs at the CBF regulon. ChIP-seq reads (IP) were visualized using the Integrative Genomics Viewer (Robinson et al., 2011). (C) Model of transcriptional regulation between the PRRs (blue), CCA1/LHY/RVEs (orange), and LNKs (green). Arrows and tacks represent transcriptional activation and repression, respectively.

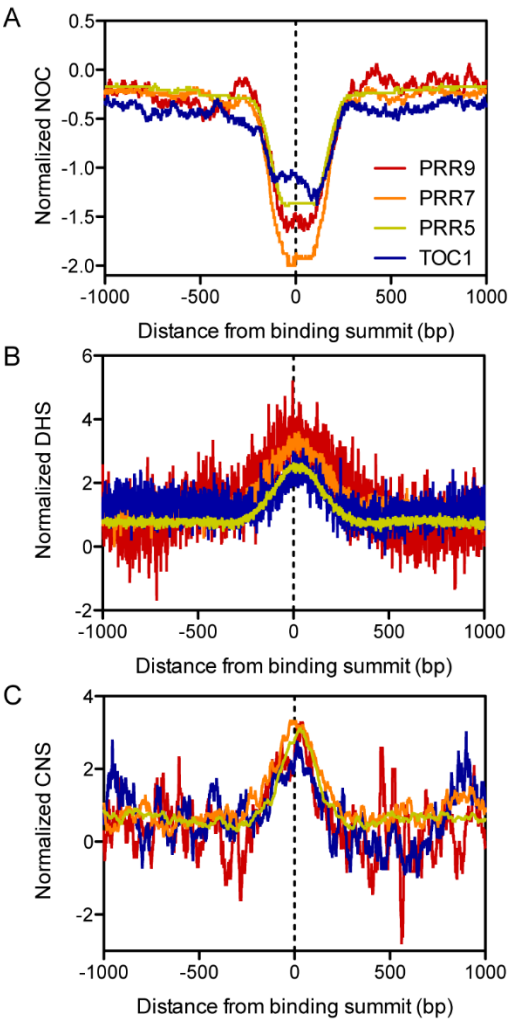

Figure 3.4. Chromatin profile of PRR binding regions. (A) Nucleosome occupancy (NOC), (B) DNase I hypersensitive sites (DHSs), and (C) presence of conserved noncoding sequences (CNS) around PRR binding summits. Binding summits were centered at zero on the x-axis. Normalized values represent the $\log_2$ ratio between the median (NOC) or average (DHS, CNS) score per base from -1 kbp upstream to +1 kbp downstream of the binding summit, to those with the same coordinates at randomly selected genes. All binding summits were used for NOC and DHS analyses, whereas binding summits located in noncoding regions were used for the CNS analysis. NOC data is from (Liu et al., 2015), DHS data from (Sullivan et al., 2014), and CNS data from (Haudry et al., 2013).

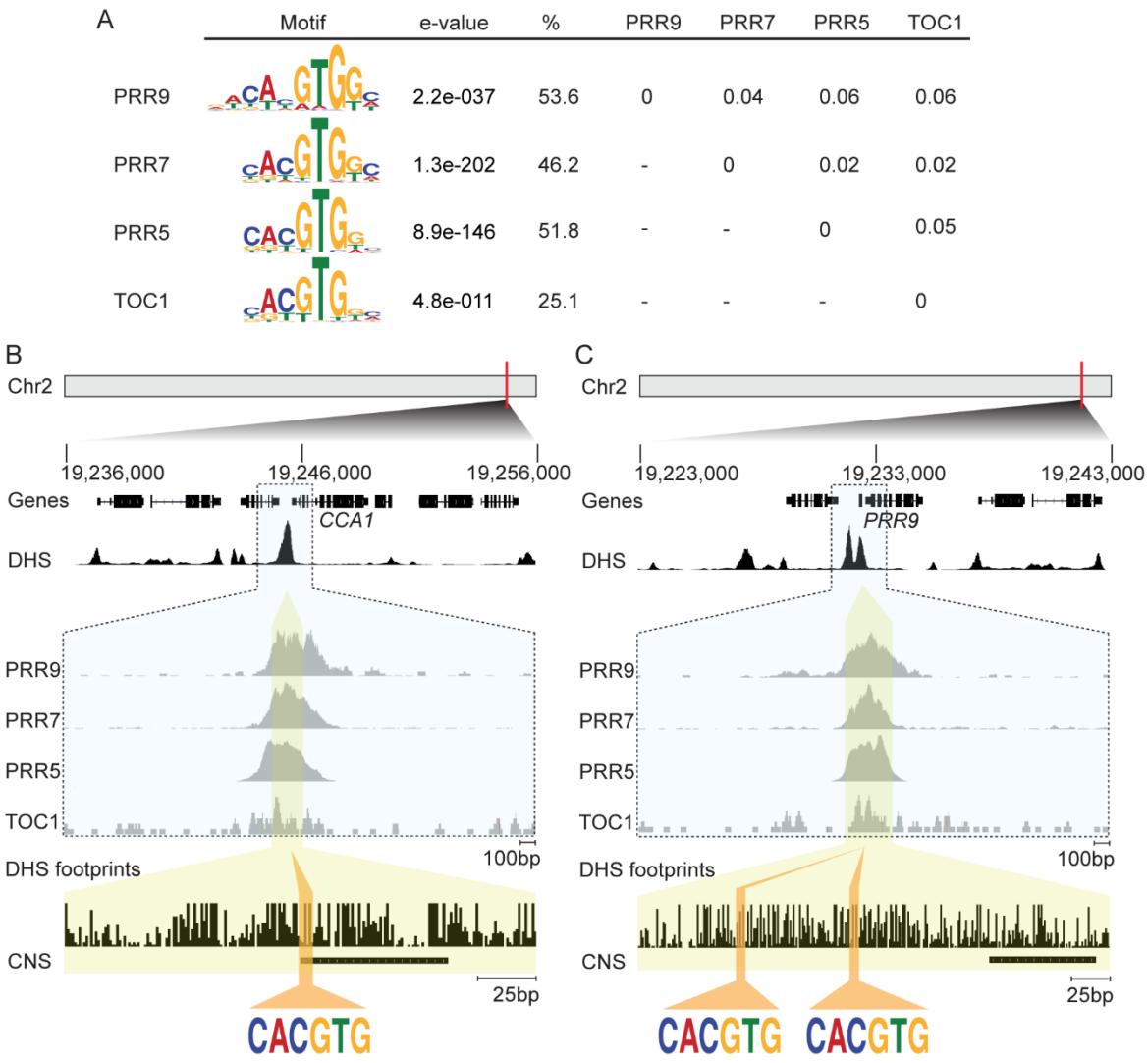

Figure 3.5. PRR binding regions are enriched with G-box containing motifs. (A) Enriched motifs in PRR binding regions located upstream of transcriptional start sites. Motifs identified *de novo* using MEME (Machanick and Bailey, 2011) with corresponding e-values, the percentage of upstream binding regions containing at least one motif, and distance matrix between PRR motifs (values represent 1 – Pearson Correlation Coefficient). Chromatin profiles of all four PRRs binding at the (B) *CCA1* and (C) *PRR9* promoters. ChIP-seq reads (IP) were visualized for each of the PRRs (blue background) and magnification of the DHS footprints within the PRR binding

Figure 3.5. (cont'd)

regions (yellow background) show G-box elements (orange). Chr2, Chromosome 2; DHS, DNase I hypersensitive site; CNS, conserved noncoding sequence.

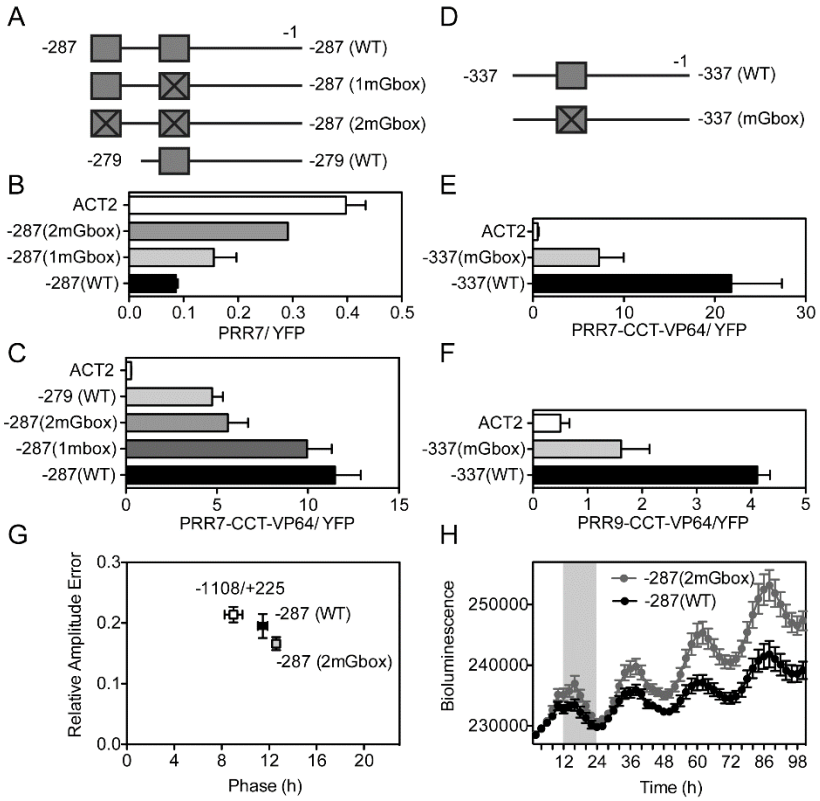

Figure 3.6. G-box motifs are necessary for transcriptional regulation by PRRs. (A) Graphic representation of *PRR9* promoter fragments. Boxes indicate G-box motifs; crossed boxes indicate mutated G-box motifs; numbers indicate the position with respect to the transcriptional start site. WT, wild type; 1mGbox, one mutated G-box; 2mGbox, two mutated G-boxes. Expression of *PRR9::LUC* constructs using (B) *35S::PRR7* as the effector in *prr579* protoplasts or (C) *35S::PRR7-CCT-VP16* as the effector in wild type protoplasts. (D) Graphic representation of *CCA1* promoter fragments. Labeling as in A; mGbox, mutated G-box. Relative expression of different *CCA1::LUC* constructs after the addition of (E) *35S::PRR7-CCT-VP16* or (F) *35S::PRR9-CCT-VP16* in wild type protoplasts. In B, C, E, and F, the luciferase expression was

Figure 3.6. (cont'd)

normalized to the *35S::REN* transformation control and to the *35S::YFP* vector control. Values are the average ± SEM of 2-4 independent experiments. (G) Rhythms of seedlings expressing *PRR9::LUC* fragments. Relative Amplitude Error is a measure of rhythmic strength that varies between 0 (perfect fitted rhythm) and 1 (no significant rhythm) and was determined under constant light. Phase was determined during the light/dark cycle. (H) Bioluminescence (counts/seedling/20 minutes) of *PRR9::LUC* expressing seedlings. The shaded area indicates dark period. For G and H, values are the average ± SEM of five -287(WT), ten -287(2mGbox) independently transformed lines, 2-4 T2 seedlings were analyzed per line. Eight homozygous seedlings were analyzed for the -1108/+225 line. Similar results were observed in three additional experiments.

SUPPLEMENTAL FIGURES

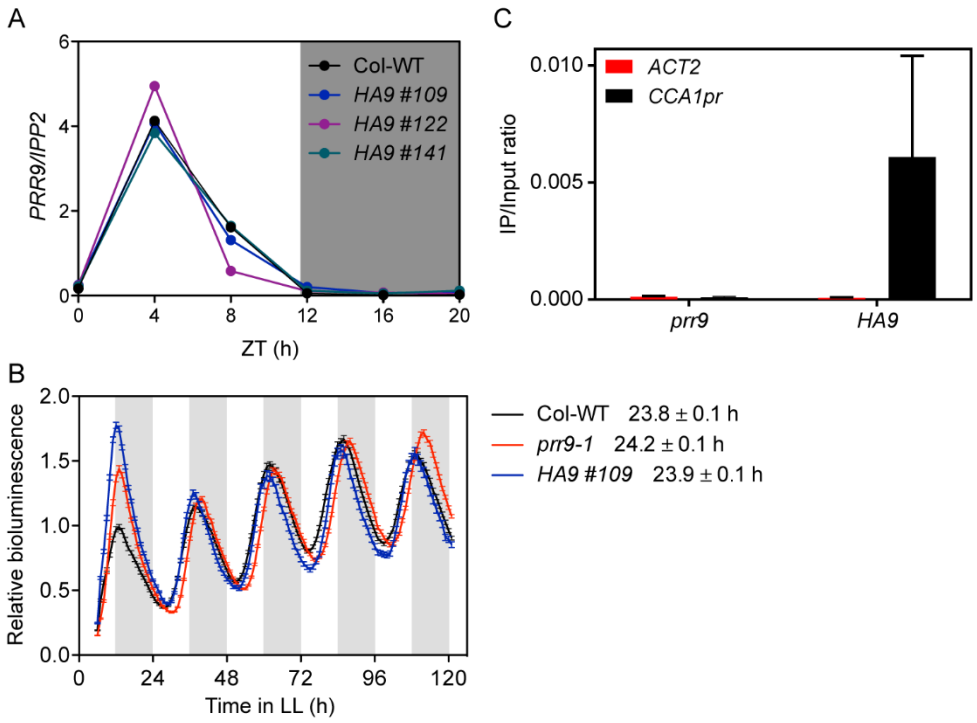

Figure S3.1. Characterization of prr9-1 PRR9::HA-PRR9 CCR2::LUC and quality testing of HA9 ChIPs. (A) Analysis of *PRR9* expression by RT-qPCR of wild type (Col-WT) and transgenic (HA9) two-week-old seedlings grown under 12 h light/12 h dark cycles. The *IPP2* gene (AT3G02780) does not display diurnal or circadian oscillations and was used as the control. The dark shaded area indicates the dark period. ZT, Zeitgeber; h, hours; *HA9, prr9-1 PRR9::HA-PRR9 CCR2::LUC*. (B) Bioluminescence rhythms of the *CCR2::LUC* reporter gene under constant light (normalized to the average luminescence of all time points for each respective genotype) (bars represent ± SEM, n ≥ 27). Seedlings were grown under 12 h light/12 h dark cycles for 7 days before transferring to constant light. Period length (average ± SEM, n ≥ 27) was estimated using the fast Fourier transform-nonlinear least-squares analysis (FTT-NLLS) (Millar et al., 1995). The light shaded areas indicate the subjective dark period. LL, constant light. (C) ChIP-qPCRs of *HA9* and *prr9* immunoprecipitated and input DNA confirm the

Figure S3.1. (cont'd)

enrichment of PRR9 binding at the *CCA1* promoter. Primers in the *ACT2* (AT3G18780) intron were used as the negative control. Values are the average ± SEM of three biological replicates.

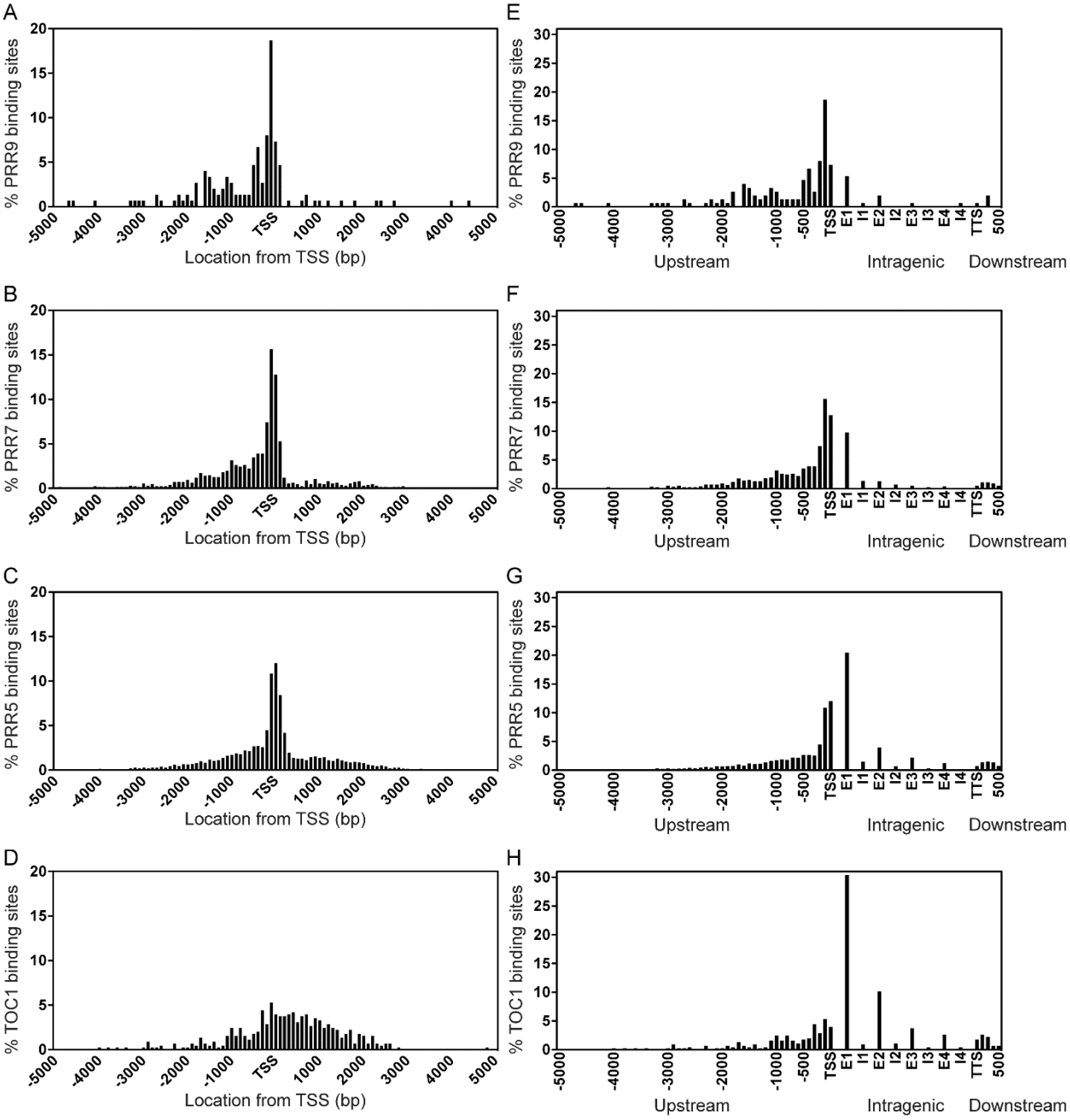

Figure S3.2. Relative positions of PRR binding summits determined by ChIP-seq. (A-D) Binding summit locations relative to transcriptional start sites or (E-H) gene features. A and E,

Figure S3.2. (cont'd)

PRR9; B and F, PRR7; C and G, PRR5; D and H, TOC1. In A-D, negative and positive numbers indicate upstream and downstream positions relative to transcriptional start site (TSS), respectively. In E-H, negative and positive numbers indicate positions upstream of TSS and downstream of transcriptional termination site (TTS), respectively. E, exon; I, intron.

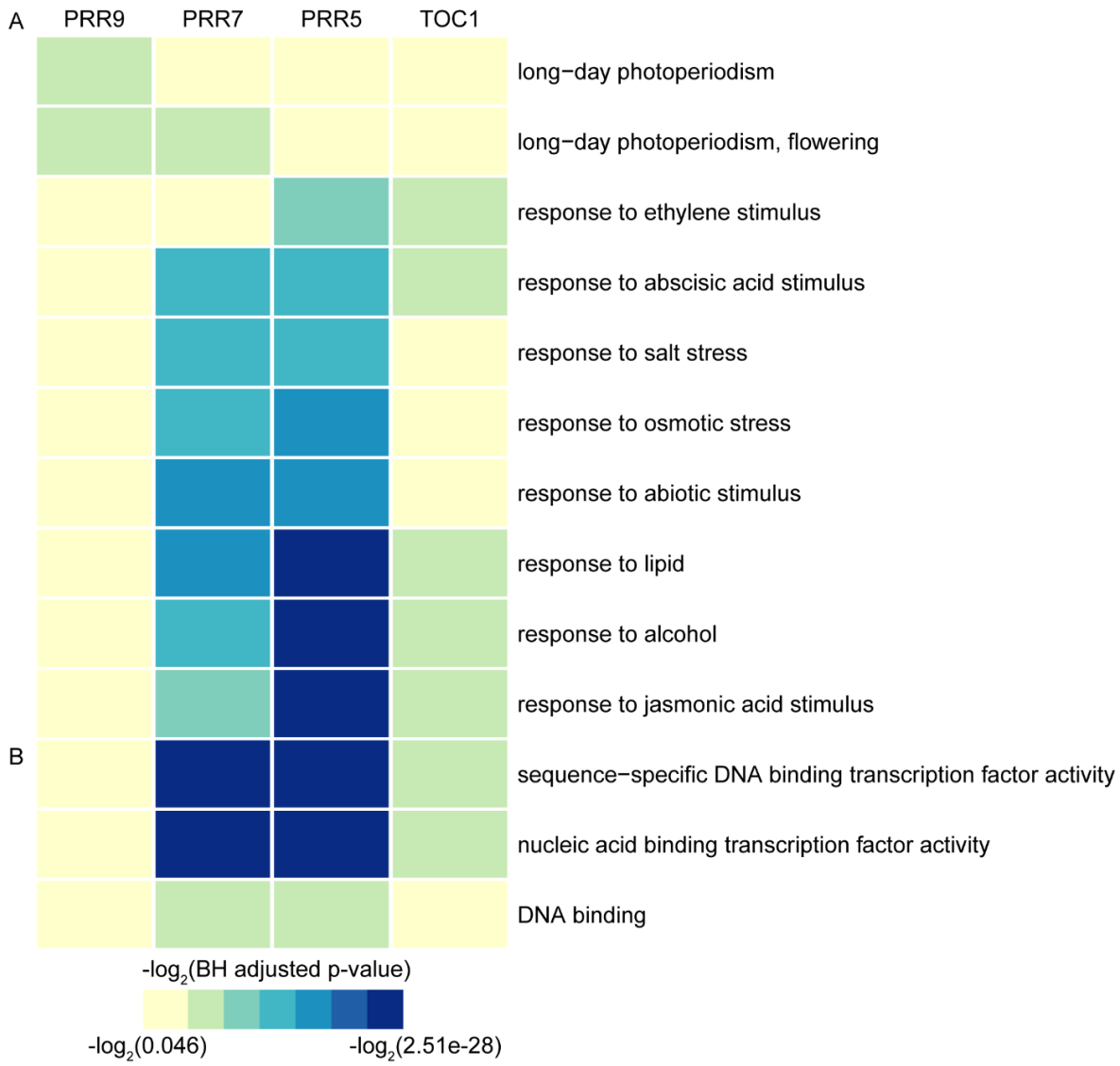

Figure S3.3. Comparison of overrepresented gene ontology terms among common PRR putative target genes identified by ChIP-seq. Enriched gene ontology terms for (A) biological process and (B) molecular function shared among the four PRRs. Gene ontology enrichment tests were conducted using ChIPpeakAnno (Zhu et al., 2010) with Benjamini Hochberg adjusted *p-values* < 0.05.

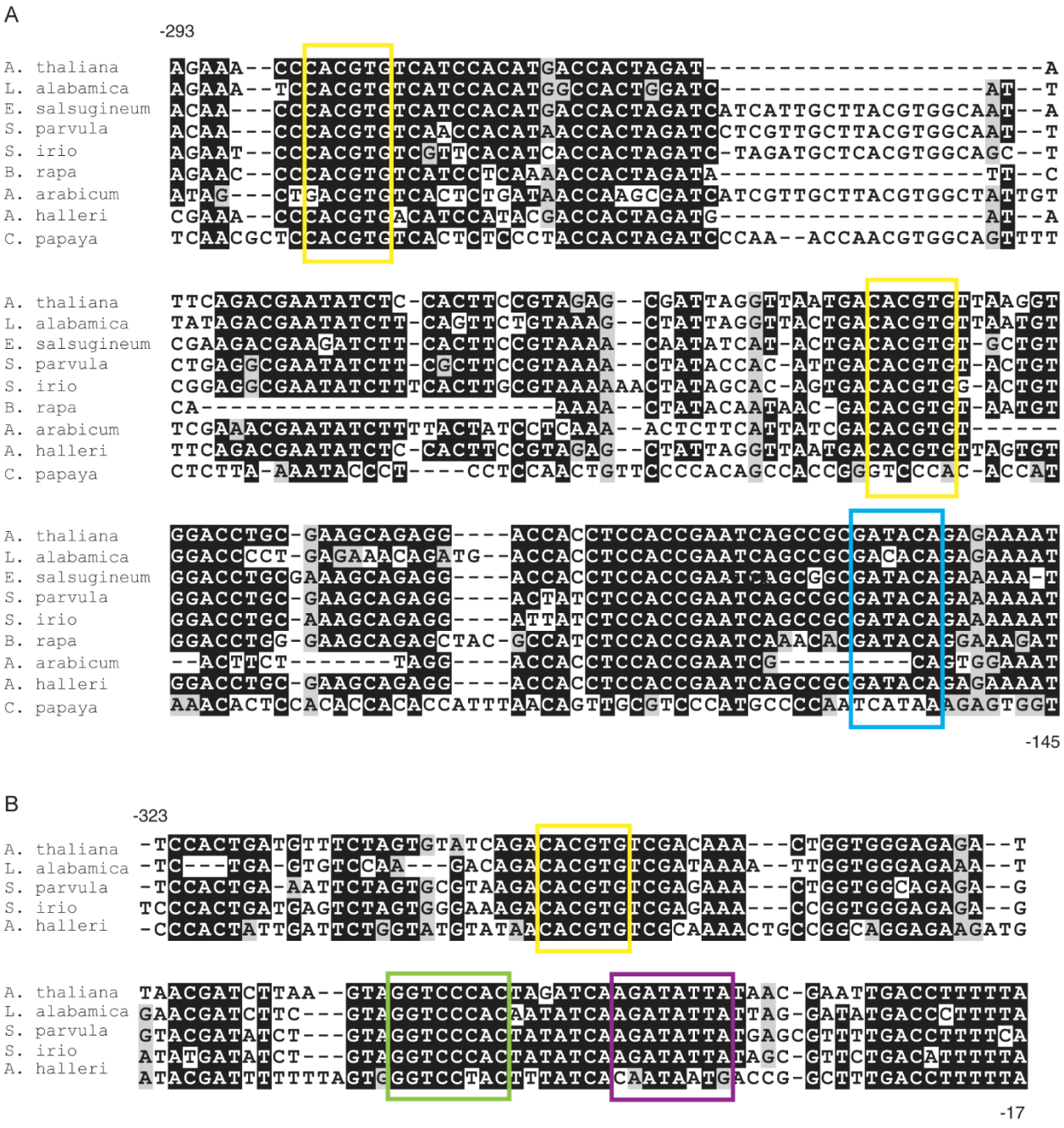

Figure S3.4. Conservation of the PRR9 and CCA1 promoters. Sequences were aligned using Muscle implemented in Mega5. Sequences have been previously described for *Brassicaceae* (Zdepski et al., 2008; Haudry et al., 2013). (A) Regions of the *PRR9* promoter from -293 to -145 with respect to the *Arabidopsis thaliana* transcriptional start site. (B) Regions of the *CCA1* promoter from -323 to -17 with respect to the *Arabidopsis thaliana* transcriptional start site. The

Figure S3.4. (cont'd)

yellow boxes indicate G-box motifs, the green box indicates a TCP-binding site (Pruneda-Paz et al., 2009), the purple box indicates an Evening-Element like motif, and the blue box indicates the LUX-binding site (Helfer et al., 2011). Species include *Arabidopsis thaliana*, *Leavenworthia alabamica*, *Eutrema salsugineum*, *Schrenkiella parvula*, *Sisymbrium irio*, *Brassica rapa*, *Aethionema arabicum*, Arabidopsis *halleri*, and *Carica papaya*.

SUPPLEMENTAL TABLE

Table S3.1. Primers used to generate promoter fragments.

Fragment	Forward primer	Intermediate primer to introduce G-box mutations	Reverse primer
PRR9pr-287/-1	CCACGTGTCATCCACATGACCAC		AACCACGAAAATATCTTCTCAGA
PRR9pr-279/-1	CACCTCATCCACATGACCACTAGATAT		AACCACGAAAATATCTTCTCAGA
PRR9pr-287/-1-1MutG	CCACGTGTCATCCACATGACCAC	CCACCTTAATGTACATCATTAACCTAATC	AACCACGAAAATATCTTCTCAGA
PRR9pr-287/-1-2MutG	CACATGTTCATCCACATGACCACTAGATATTC	CCACCTTAATGTACATCATTAACCTAATC	AACCACGAAAATATCTTCTCAGA
PRR9pr-279/-1-MutG	CACCTCATCCACATGACCACTAGATAT	CCACCTTAATGTACATCATTAACCTAATC	AACCACGAAAATATCTTCTCAGA
CCA1pr-337/-1	TTCGATTGTTGGTGAAGTAGTCG		ATCTTTAACCTCAAACTTTTTA
CCA1pr-337/-1-MutG	TTCGATTGTTGGTGAAGTAGTCG	CCAGTTTGTCGATGTACATCTGATACACTAG	ATCTTTAACCTCAAACTTTTTA
ACT2pr-473/-1	CACCGTTTTGACGAGTTCGGATGTAG		AAAAAAATAATTAAAATCGACAGACAC

Underlined bases indicate mutated sequences.

REFERENCES

REFERENCES

Alabadi D, Oyama T, Yanovsky MJ, Harmon FG, Mas P, Kay SA (2001) Reciprocal regulation between TOC1 and LHY/CCA1 within the Arabidopsis circadian clock. Science **293:** 880-883

Bailey TL, Machanick P (2012) Inferring direct DNA binding from ChIP-seq. Nucleic Acids Research **40**

Bell-Pedersen D, Cassone VM, Earnest DJ, Golden SS, Hardin PE, Thomas TL, Zoran MJ (2005) Circadian rhythms from multiple oscillators: Lessons from diverse organisms. Nature Reviews Genetics **6:** 544-556

Bell O, Tiwari VK, Thoma NH, Schubeler D (2011) Determinants and dynamics of genome accessibility. Nature Reviews Genetics **12:** 554-564

Berendzen KW, Bohmer M, Wallmeroth N, Peter S, Vesic M, Zhou Y, Tiesler FK, Schleifenbaum F, Harter K (2012) Screening for in planta protein-protein interactions combining bimolecular fluorescence complementation with flow cytometry. Plant Methods **8:** 25

Blasing OE, Gibon Y, Gunther M, Hohne M, Morcuende R, Osuna D, Thimm O, Usadel B, Scheible WR, Stitt M (2005) Sugars and circadian regulation make major contributions to the global regulation of diurnal gene expression in Arabidopsis. Plant Cell **17:** 3257-3281

Chikina MD, Troyanskaya OG (2012) An effective statistical evaluation of ChIPseq dataset similarity. Bioinformatics **28:** 607-613

Clough SJ, Bent AF (1998) Floral dip: a simplified method for Agrobacterium-mediated transformation of *Arabidopsis thaliana*. Plant Journal **16:** 735-743

Corellou F, Schwartz C, Motta JP, Djouani-Tahri E, Sanchez F, Bouget FY (2009) Clocks in the Green Lineage: Comparative Functional Analysis of the Circadian Architecture of the Picoeukaryote Ostreococcus. Plant Cell **21:** 3436-3449

Curtis MD, Grossniklaus U (2003) A gateway cloning vector set for high-throughput functional analysis of genes in planta. Plant Physiology **133:** 462-469

Dixon LE, Knox K, Kozma-Bognar L, Southern MM, Pokhilko A, Millar AJ (2011) Temporal Repression of Core Circadian Genes Is Mediated through EARLY FLOWERING 3 in Arabidopsis. Current Biology **21:** 120-125

Dodd AN, Salathia N, Hall A, Kevei E, Toth R, Nagy F, Hibberd JM, Millar AJ, Webb AAR (2005) Plant circadian clocks increase photosynthesis, growth, survival, and competitive advantage. Science **309:** 630-633

Edwards KD, Anderson PE, Hall A, Salathia NS, Locke JC, Lynn JR, Straume M, Smith JQ, Millar AJ (2006) FLOWERING LOCUS C mediates natural variation in the high-temperature response of the Arabidopsis circadian clock. Plant Cell **18:** 639-650

Endo M, Shimizu H, Nohales MA, Araki T, Kay SA (2014) Tissue-specific clocks in Arabidopsis show asymmetric coupling. Nature **515:** 419-422

Farinas B, Mas P (2011) Functional implication of the MYB transcription factor RVE8/LCL5 in the circadian control of histone acetylation. Plant Journal **66:** 318-329

Farre EM, Harmer SL, Harmon FG, Yanovsky MJ, Kay SA (2005) Overlapping and distinct roles of PRR7 and PRR9 in the Arabidopsis circadian clock. Current Biology **15:** 47-54

Farre EM, Kay SA (2007) PRR7 protein levels are regulated by light and the circadian clock in Arabidopsis. Plant Journal **52:** 548-560

Farre EM, Liu T (2013) The PRR family of transcriptional regulators reflects the complexity and evolution of plant circadian clocks. Current Opinion in Plant Biology **16:** 621-629

Filichkin SA, Breton G, Priest HD, Dharmawardhana P, Jaiswal P, Fox SE, Michael TP, Chory J, Kay SA, Mockler TC (2011) Global Profiling of Rice and Poplar Transcriptomes Highlights Key Conserved Circadian-Controlled Pathways and cis-Regulatory Modules. PLoS One **6**

Fornara F, Panigrahi KCS, Gissot L, Sauerbrunn N, Ruhl M, Jarillo JA, Coupland G (2009) Arabidopsis DOF Transcription Factors Act Redundantly to Reduce CONSTANS Expression and Are Essential for a Photoperiodic Flowering Response. Developmental Cell **17:** 75-86

Forsburg SL, Guarente L (1988) Mutational analysis of upstream activation sequence 2 of the CYC1 gene of Saccharomyces cerevisiae: a HAP2-HAP3-responsive site. Molecular and Cellular Biology **8:** 647-654

Franco-Zorrilla JM, Lopez-Vidriero I, Carrasco JL, Godoy M, Vera P, Solano R (2014) DNA-binding specificities of plant transcription factors and their potential to define target genes. Proceedings of the National Academy of Sciences of the United States of America **111:** 2367-2372

Fujiwara S, Wang L, Han L, Suh SS, Salome PA, McClung CR, Somers DE (2008) Post-translational regulation of the Arabidopsis circadian clock through selective proteolysis and phosphorylation of pseudo-response regulator proteins. The Journal of Biological Chemistry **283:** 23073-23083

Gendron JM, Pruneda-Paz JL, Doherty CJ, Gross AM, Kang SE, Kay SA (2012) Arabidopsis circadian clock protein, TOC1, is a DNA-binding transcription factor. Proceedings of the National Academy of Sciences of the United States of America **109:** 3167-3172

Gordon DB, Nekludova L, McCallum S, Fraenkel E (2005) TAMO: a flexible, object-oriented framework for analyzing transcriptional regulation using DNA-sequence motifs. Bioinformatics **21:** 3164-3165

Grant CE, Bailey TL, Noble WS (2011) FIMO: scanning for occurrences of a given motif. Bioinformatics **27:** 1017-1018

Gupta S, Stamatoyannopoulos JA, Bailey TL, Noble WS (2007) Quantifying similarity between motifs. Genome Biology **8**

Gutierrez RA, Ewing RM, Cherry JM, Green PJ (2002) Identification of unstable transcripts in Arabidopsis by cDNA microarray analysis: Rapid decay is associated with a group of touch- and specific clock-controlled genes. Proceedings of the National Academy of Sciences of the United States of America **99:** 11513-11518

Harari-Steinberg O, Ohad I, Chamovitz DA (2001) Dissection of the light signal transduction pathways regulating the two early light-induced protein genes in Arabidopsis. Plant Physiology **127:** 986-997

Hatanaka F, Matsubara C, Myung J, Yoritaka T, Kamimura N, Tsutsumi S, Kanai A, Suzuki Y, Sassone-Corsi P, Aburatani H, Sugano S, Takumi T (2010) Genome-Wide Profiling of the Core Clock Protein BMAL1 Targets Reveals a Strict Relationship with Metabolism. Molecular and Cellular Biology **30:** 5636-5648

Haudry A, Platts AE, Vello E, Hoen DR, Leclercq M, Williamson RJ, Forczek E, Joly-Lopez Z, Steffen JG, Hazzouri KM, Dewar K, Stinchcombe JR, Schoen DJ, Wang XW, Schmutz J, Town CD, Edger PP, Pires JC, Schumaker KS, Jarvis DE, Mandakova T, Lysak MA, van den Bergh E, Schranz ME, Harrison PM, Moses AM, Bureau TE, Wright SI, Blanchette M (2013) An atlas of over 90,000 conserved noncoding sequences provides insight into crucifer regulatory regions. Nature Genetics **45:** 891-898

Helfer A, Nusinow DA, Chow BY, Gehrke AR, Bulyk ML, Kay SA (2011) LUX ARRHYTHMO Encodes a Nighttime Repressor of Circadian Gene Expression in the Arabidopsis Core Clock. Current Biology **21:** 126-133

Herrero E, Kolmos E, Bujdoso N, Yuan Y, Wang MM, Berns MC, Uhlworm H, Coupland G, Saini R, Jaskolski M, Webb A, Goncalves J, Davis SJ (2012) EARLY FLOWERING4 Recruitment of EARLY FLOWERING3 in the Nucleus Sustains the Arabidopsis Circadian Clock. Plant Cell **24:** 428-443

Heyndrickx KS, Van de Velde J, Wang CM, Weigei D, Vandepoele K (2014) A Functional and Evolutionary Perspective on Transcription Factor Binding in *Arabidopsis thaliana*. Plant Cell **26:** 3894-3910

Hsu PY, Devisetty UK, Harmer SL (2013) Accurate timekeeping is controlled by a cycling activator in Arabidopsis. Elife **2**

Hsu PY, Harmer SL (2014) Wheels within wheels: the plant circadian system. Trends in Plant Science **19:** 240-249

Huang W, Pérez-García P, Pokhilko A, Millar AJ, Antoshechkin I, Riechmann JL, Mas P (2012) Mapping the Core of the Arabidopsis Circadian Clock Defines the Network Structure of the Oscillator. Science **336:** 75-79

Jiang JM (2015) The 'dark matter' in the plant genomes: non-coding and unannotated DNA sequences associated with open chromatin. Current Opinion in Plant Biology **24:** 17-23

Kidokoro S, Maruyama K, Nakashima K, Imura Y, Narusaka Y, Shinwari ZK, Osakabe Y, Fujita Y, Mizoi J, Shinozaki K, Yamaguchi-Shinozaki K (2009) The phytochrome-interacting factor PIF7 negatively regulates DREB1 expression under circadian control in Arabidopsis. Plant Physiology **151:** 2046-2057

Ko CH, Takahashi JS (2006) Molecular components of the mammalian circadian clock. Human Molecular Genetics **15:** R271-R277

Langmead B, Trapnell C, Pop M, Salzberg SL (2009) Ultrafast and memory-efficient alignment of short DNA sequences to the human genome. Genome Biology **10**

Li H, Handsaker B, Wysoker A, Fennell T, Ruan J, Homer N, Marth G, Abecasis G, Durbin R, Genome Project Data P (2009) The Sequence Alignment/Map format and SAMtools. Bioinformatics **25:** 2078-2079

Liu MJ, Seddon AE, Tsai ZT, Major IT, Floer M, Howe GA, Shiu SH (2015) Determinants of nucleosome positioning and their influence on plant gene expression. Genome Research **25:** 1182-1195

Liu T, Carlsson J, Takeuchi T, Newton L, Farre EM (2013) Direct regulation of abiotic responses by the Arabidopsis circadian clock component PRR7. Plant Journal **76:** 101-114

Machanick P, Bailey TL (2011) MEME-ChIP: motif analysis of large DNA datasets. Bioinformatics **27:** 1696-1697

Makino S, Matsushika A, Kojima M, Yamashino T, Mizuno T (2002) The APRR1/TOC1 quintet implicated in circadian rhythms of *Arabidopsis thaliana*: 1. Characterization with APRR1-overexpressing plants. Plant and Cell Physiology **43:** 58-69

Mathelier A, Zhao XB, Zhang AW, Parcy F, Worsley-Hunt R, Arenillas DJ, Buchman S, Chen CY, Chou A, Ienasescu H, Lim J, Shyr C, Tan G, Zhou M, Lenhard B, Sandelin A, Wasserman WW (2014) JASPAR 2014: an extensively expanded and updated open-access database of transcription factor binding profiles. Nucleic Acids Research **42:** D142-D147

Michael TP, Mockler TC, Breton G, McEntee C, Byer A, Trout JD, Hazen SP, Shen RK, Priest HD, Sullivan CM, Givan SA, Yanovsky M, Hong FX, Kay SA, Chory J (2008) Network discovery pipeline elucidates conserved time-of-day-specific cis-regulatory modules. PLoS Genetics **4**

Millar AJ, Carre IA, Strayer CA, Chua NH, Kay SA (1995) Circadian clock mutants in Arabidopsis identified by luciferase imaging. Science **267:** 1161-1163

Mizuno T, Nomoto Y, Oka H, Kitayama M, Takeuchi A, Tsubouchi M, Yamashino T (2014) Ambient temperature signal feeds into the circadian clock transcriptional circuitry through the EC night-time repressor in *Arabidopsis thaliana*. Plant and Cell Physiology **55:** 958-976

Mockler TC, Michael TP, Priest HD, Shen R, Sullivan CM, Givan SA, McEntee C, Kay SA, Chory J (2007) The Diurnal project: Diurnal and circadian expression profiling, model-based pattern matching, and promoter analysis. Cold Spring Harbor Symposia on Quantitative Biology **72:** 353-363

Nagel DH, Doherty CJ, Pruneda-Paz JL, Schmitz RJ, Ecker JR, Kay SA (2015) Genome-wide identification of CCA1 targets uncovers an expanded clock network in Arabidopsis. Proceedings of the National Academy of Sciences of the United States of America **112:** E4802-E4810

Nakamichi N, Kiba T, Henriques R, Mizuno T, Chua NH, Sakakibara H (2010) PSEUDO-RESPONSE REGULATORS 9, 7, and 5 Are Transcriptional Repressors in the Arabidopsis Circadian Clock. Plant Cell **22:** 594-605

Nakamichi N, Kiba T, Kamioka M, Suzuki T, Yamashino T, Higashiyama T, Sakakibara H, Mizuno T (2012) Transcriptional repressor PRR5 directly regulates clock-output pathways. Proceedings of the National Academy of Sciences of the United States of America **109:** 17123-17128

Nakamichi N, Kita M, Niinuma K, Ito S, Yamashino T, Mizoguchi T, Mizuno T (2007) Arabidopsis clock-associated pseudo-response regulators PRR9, PRR7 and PRR5 coordinately and positively regulate flowering time through the canonical CONSTANS-dependent photoperiodic pathway. Plant and Cell Physiology **48:** 822-832

Nakamichi N, Kusano M, Fukushima A, Kita M, Ito S, Yamashino T, Saito K, Sakakibara H, Mizuno T (2009) Transcript Profiling of an Arabidopsis PSEUDO RESPONSE REGULATOR Arrhythmic Triple Mutant Reveals a Role for the Circadian Clock in Cold Stress Response. Plant and Cell Physiology **50:** 447-462

Niwa Y, Yamashino T, Mizuno T (2009) The circadian clock regulates the photoperiodic response of hypocotyl elongation through a coincidence mechanism in *Arabidopsis thaliana*. Plant Cell Physiology **50:** 838-854

Olesen J, Hahn S, Guarente L (1987) Yeast HAP2 and HAP3 activators both bind to the CYC1 upstream activation site, UAS2, in interdependent manner. Cell **51:** 953-961

Panchy N, Wu GX, Newton L, Tsai CH, Chen J, Benning C, Farre EM, Shiu SH (2014) Prevalence, Evolution, and cis-Regulation of Diel Transcription in Chlamydomonas reinhardtii. G3-Genes Genomes Genetics **4:** 2461-2471

Para A, Farre EM, Imaizumi T, Pruneda-Paz JL, Harmon FG, Kay SA (2007) PRR3 is a vascular regulator of TOC1 stability in the Arabidopsis circadian clock. Plant Cell **19:** 3462-3473

Plautz JD, Straume M, Stanewsky R, Jamison CF, Brandes C, Dowse HB, Hall JC, Kay SA (1997) Quantitative Analysis of Drosophila period Gene Transcription in Living Animals. Journal of Biological Rhythms **12:** 204-217

Pruneda-Paz JL, Breton G, Para A, Kay SA (2009) A Functional Genomics Approach Reveals CHE as a Component of the Arabidopsis Circadian Clock. Science **323:** 1481-1485

Quinlan AR, Hall IM (2010) BEDTools: a flexible suite of utilities for comparing genomic features. Bioinformatics **26:** 841-842

Rawat R, Takahashi N, Hsu PY, Jones MA, Schwartz J, Salemi MR, Phinney BS, Harmer SL (2011) REVEILLE8 and PSEUDO-REPONSE REGULATOR5 form a negative feedback loop within the Arabidopsis circadian clock. PLoS Genetics **7**

Robinson JT, Thorvaldsdottir H, Winckler W, Guttman M, Lander ES, Getz G, Mesirov JP (2011) Integrative genomics viewer. Nature Biotechnology **29:** 24-26

Rugnone ML, Soverna AF, Sanchez SE, Schlaen RG, Hernando CE, Seymour DK, Mancini E, Chernomoretz A, Weigel D, Maac P, Yanovsky MJ (2013) LNK genes integrate light and clock signaling networks at the core of the Arabidopsis oscillator. Proceedings of the National Academy of Sciences of the United States of America **110:** 12120-12125

Sato E, Nakamichi N, Yamashino T, Mizuno T (2002) Aberrant expression of the Arabidopsis circadian-regulated APRR5 gene belonging to the APRR1/TOC1 quintet results in early

flowering and hypersensitiveness to light in early photomorphogenesis. Plant and Cell Physiology **43:** 1374-1385

Strayer C, Oyama T, Schultz TF, Raman R, Somers DE, Mas P, Panda S, Kreps JA, Kay SA (2000) Cloning of the Arabidopsis clock gene TOC1, an autoregulatory response regulator homolog. Science **289:** 768-771

Sullivan AM, Arsovski AA, Lempe J, Bubb KL, Weirauch MT, Sabo PJ, Sandstrom R, Thurman RE, Neph S, Reynolds AP, Stergachis AB, Vernot B, Johnson AK, Haugen E, Sullivan ST, Thompson A, Neri FV, Weaver M, Diegel M, Mnaimneh S, Yang A, Hughes TR, Nemhauser JL, Queitsch C, Stamatoyannopoulos JA (2014) Mapping and Dynamics of Regulatory DNA and Transcription Factor Networks in A-thaliana. Cell Reports **8:** 2015-2030

Takata N, Saito S, Saito CT, Nanjo T, Shinohara K, Uemura M (2009) Molecular phylogeny and expression of poplar circadian clock genes, LHY1 and LHY2. New Phytologist **181:** 808-819

Takata N, Saito S, Saito CT, Uemura M (2010) Phylogenetic footprint of the plant clock system in angiosperms: evolutionary processes of Pseudo-Response Regulators. Bmc Evolutionary Biology **10:** 14

Takeuchi T, Newton L, Burkhardt A, Mason S, Farre EM (2014) Light and the circadian clock mediate time-specific changes in sensitivity to UV-B stress under light/dark cycles. Journal of Experimental Botany **65:** 6003-6012

Wenkel S, Turck F, Singer K, Gissot L, Le Gourrierec J, Samach A, Coupland G (2006) CONSTANS and the CCAAT box binding complex share a functionally important domain and interact to regulate flowering of Arabidopsis. Plant Cell **18:** 2971-2984

Woelfle MA, Yan OY, Phanvijhitsiri K, Johnson CH (2004) The adaptive value of circadian clocks: An experimental assessment in cyanobacteria. Current Biology **14:** 1481-1486

Xie QG, Wang P, Liu X, Yuan L, Wang LB, Zhang CG, Li Y, Xing HY, Zhi LY, Yue ZL, Zhao CS, McClung CR, Xu XD (2014) LNK1 and LNK2 Are Transcriptional Coactivators in the Arabidopsis Circadian Oscillator. Plant Cell **26:** 2843-2857

Yerushalmi S, Green RM (2009) Evidence for the adaptive significance of circadian rhythms. Ecology Letters **12:** 970-981

Yerushalmi S, Yakir E, Green RM (2011) Circadian clocks and adaptation in Arabidopsis. Molecular Ecology **20:** 1155-1165

Yoshitane H, Ozaki H, Terajima H, Du NH, Suzuki Y, Fujimori T, Kosaka N, Shimba S, Sugano S, Takagi T, Iwasaki W, Fukada Y (2014) CLOCK-Controlled Polyphonic

Regulation of Circadian Rhythms through Canonical and Noncanonical E-Boxes. Molecular and Cellular Biology **34:** 1776-1787

Zdepski A, Wang W, Priest HD, Ali F, Alam M, Mockler TC, Michael TP (2008) Conserved Daily Transcriptional Programs in Carica papaya. Trop Plant Biol **1:** 236-245

Zhang Y, Liu T, Meyer CA, Eeckhoute J, Johnson DS, Bernstein BE, Nussbaum C, Myers RM, Brown M, Li W, Liu XS (2008) Model-based Analysis of ChIP-Seq (MACS). Genome Biology **9**

Zhu LJ, Gazin C, Lawson ND, Pages H, Lin SM, Lapointe DS, Green MR (2010) ChIPpeakAnno: a Bioconductor package to annotate ChIP-seq and ChIP-chip data. Bmc Bioinformatics **11**

Zou C, Sun K, Mackaluso JD, Seddon AE, Jin R, Thomashow MF, Shiu SH (2011) Cis-regulatory code of stress-responsive transcription in *Arabidopsis thaliana*. Proceedings of the National Academy of Sciences of the United States of America **108:** 14992-14997

CHAPTER 4

CONCLUSIONS AND FUTURE PERSPECTIVES

PSEUDO RESPONSE REGULATORs (PRRs) are conserved in the Kingdom Plantae and function as circadian clock components in a wide range of plant species. Arabidopsis PRRs also function as master regulators of diverse biological processes such as the photoperiodic control of flowering time and responses to abiotic stresses and light (Farre and Liu, 2013). PRR9 and PRR7 negatively regulate *CIRCADIAN CLOCK ASSOCIATED 1* (*CCA1*) and *LATE ELONGATED HYPOCOTYL* (*LHY*), whereas these two MYB transcription factors activate *PRR9* and *PRR7* in return (Farre et al., 2005; Farre and Kay, 2007; Nakamichi et al., 2010). My research focused on PRR9 and PRR7 to shed light on their essential roles in regulating circadian components as well as outputs of the clock. I used chromatin immunoprecipitation combined with high through-put sequencing to identify their global targets. These results have provided us with a better understanding of their expansive gene regulatory network.

Limitations of chromatin immunoprecipitation

Three major limitations exist in interpreting ChIP-seq data. The first limitation is that bound DNA may represent direct or indirect binding, such as in the case of proteins that interact in a complex to associate with DNA. To address the first limitation, I conducted a yeast-one-hybrid experiment and observed that PRR9 and PRR7 do not bind to DNA directly in a heterologous system (Figure 4.1). However, PRR9 and PRR7 may still be able to bind DNA directly *in planta* since the heterologous system might lack the required posttranslational changes necessary for proper PRR functioning (Farre and Kay, 2007; Fujiwara et al., 2008). The second limitation involves defining target genes, which is usually based on proximal location. I took two different approaches to define target genes in my ChIP-seq experiments. For the PRR7 ChIP-seq, I associated binding sites to genes located up to 1kbp away in either direction. Using this

approach, it is possible to have more than one candidate target, especially in the case of compact genomes. For my PRR9 ChIP-seq, I associated binding sites to the nearest transcriptional start site of a gene. The major assumption is that transcription factors are located near gene features, particularly the upstream region of transcriptional start sites. Moreover, targets of proteins bound to distant enhancer regions are not usually taken into account due to the difficulty of predicting such targets. Finally, the third limitation is that the presence or absence of a transcription factor does not necessarily equate to transcriptional regulation. For example, the failure to observe changes in target gene expression may be due to the presence of a transcription factor (TF) in a primed chromatin state in order to permit rapid responses dependent on other factors and/or under certain conditions (Guertin and Lis, 2010; John et al., 2011). There are also cases where expression changes are observed but the binding is not detected in ChIP studies, which may be due to the dynamics of TF binding. For instance, studies on bZIP1 by Para et al. (2014) revealed that transient binding events, ranging from 1-5 minutes upon nuclear localization, account for nearly 60% of its target regulation. The use of inducible TF nuclear translocation systems in conjunction with a translational inhibitor allows for the detection of expression changes resulting from direct regulation by the TF, as opposed to intermediate factors (Brockmann et al., 2001; Hsu et al., 2013). Therefore, I attempted to measure the expression of target genes associated with PRR7 binding using an inducible line. In particular, we generated PRR-glucocorticoid receptor (GR) translational fusion lines in the *prr7-3 CCA1::LUC* mutant background (*prr7-3 35S::HA-PRR7-GR CCA1::LUC*). Dexamethasone (DEX) treatment would enable PRR7-GR to move from the cytosol to the nucleus and regulate gene expression. I was unable to identify a satisfactory inducible line using this construct due to leakiness or inactivity. This effect may be

caused by the use of a strong constitutive promoter. An alternative approach would be to construct inducible lines with the native promoter.

Targets of PRR9 and PRR7

Mis-expression of any *PRR* core clock component results in alterations to the clock and downstream processes, such as altered periods and flowering times compared to wild-type plants. These changes are exacerbated in higher-order mutants, as seen in the arrhythmic and extremely late flowering triple mutant *prr5prr7prr9* (*prr579*) (Nakamichi et al., 2009). In order to identify the genome-wide targets of PRR9 and PRR7, I conducted ChIP-seq and found that PRR9 and PRR7 represses gene expression by binding to regions close to transcriptional start sites. Approximately 57-64% of PRR7 targets and more than 75% of PRR9 targets cycle under cycling light/dark (LD) and constant light (LL) conditions. Both PRR9 and PRR7 regulate circadian clock genes such as *CCA1*, *LHY*, *REVEILLE 8* (*RVE8*), *NIGHT LIGHT-INDUCIBLE 1* (*LNK1*), *LNK2*, and *PRR9*. In addition, PRR9 and PRR7 targets are significantly enriched in transcription factors according to gene ontology enrichment analyses, and many of these targets can explain the *prr579* triple mutant phenotypes. For example, higher order *prr* mutants flower late and we found that PRR7 negatively regulates repressors in the flowering pathway including *CYCLING DOF FACTOR 5* (*CDF5*). In addition, both PRR9 and PRR7 repress *CDF2* (Nakamichi et al., 2009; Song et al., 2010). The *prr579* triple mutant also exhibits elongated hypocotyls and correspondingly, PRR7 negatively regulates *PHYTOCHROME INTERACTING FACTOR 4* (*PIF4*) and *PIF5,* two basic helix-loop-helix (bHLH) transcription factors that promote hypocotyl elongation (Nakamichi et al., 2009; Leivar and Quail, 2011). Lastly, *prr579* is more cold- and drought-tolerant compared to wild-type plants, and I found that PRR9 and PRR7

associate with the promoters of *C-REPEAT/DRE BINDING FACTOR* genes, which encode for transcriptional activators in the cold response pathway (Gilmour et al., 1998; Nakamichi et al., 2009). Specifically, PRR7 associates with the promoter of *C-REPEAT/DRE BINDING FACTOR 1* (*CBF1*), and both PRR9 and PRR7 associate with the promoters of *CBF2* and *CBF3*.

G-box-containing motifs are enriched at PRR9 and PRR7 binding sites

TOC1 has been shown to bind DNA directly, but the identified DNA sequence bound in electrophoretic mobility shift assays is not enriched in our PRR9 and PRR7 ChIP-seq experiments, indicating that PRR9 and PRR7 bind to different DNA elements (Gendron et al., 2012). I observed an enrichment of G-boxes and G-box-related motifs such as ABREs (abscisic acid responsive elements) at PRR9 and PRR7 binding sites. Accordingly, putative PRR7 targets are enriched in abiotic stress responsive genes. We showed that PRR7 affects the ABA sensitivity of ABA responsive genes and is involved in the regulation of stomata conductance. G-boxes are also over-represented in the promoter regions of light-regulated genes and many PRR9 and PRR7 targets are involved in light signaling, such as *LONG HYPOCOTYL 5* (*HY5*) and *HY5 HOMOLOG* (*HYH*). Linsey Newton from the Farré laboratory tested the significance of G-box elements in the *PRR9* and *CCA1* promoters through promoter bashing assays as well as testing a promoter construct containing G-box multimers with a minimal promoter. Her findings show that certain G-boxes are more important, but alone are insufficient for transcriptional regulation by PRR9 and PRR7.

HY5 and HYH may mediate PRR9 and PRR7 binding to DNA

HY5 and *HYH* encode basic leucine zipper (bZIP) transcription factors that mediate light responses and promote photomorphogenesis (Chattopadhyay et al., 1998; Holm et al., 2002). bZIP and bHLH transcription factors can directly bind to G-box motifs (Ellenberger, 1994; Jakoby et al., 2002; Toledo-Ortiz et al., 2003). A comparison of our PRR9 and PRR7 ChIP-seq to ChIP-seq/ChIP-chip data for HY5 (Figure 4.2), PIF1, and FAR-RED ELONGATED HYPOCOTYL 3 (FHY3) show a high number of overlapping targets, indicating that PRR7 targets may be co-regulated by different light signaling components (Lee et al., 2007; Oh et al., 2009; Ouyang et al., 2011). These findings along with the failure to observe direct binding of PRR9 and PRR7 to DNA in my yeast-one-hybrid assays led me to hypothesize that HY5 may aid or mediate PRR7 binding to DNA, and is required for PRR7 to repress shared targets with HY5, such as *PIF4* and *PIF5* (Leivar and Quail, 2011; Liu et al., 2013). Work done by Tomomi Takeuchi, a former member of the Farré laboratory, indicated that PRR7 and HY5 interact in tobacco (Figure 4.3), but these experiments require further confirmation. Dr. Farré generated *hy5* mutants crossed to PRR7 overexpressing lines that exhibit long hypocotyl phenotypes similar to *hy5*, revealing that HY5 is epistatic to PRR7 in regulating hypocotyl elongation (Figure 4.4). Using these lines, I was interested in investigating the shared targets of PRR7 and HY5 that contain a G-box motif in their promoters, such as *CCA1*, *PRR9*, *PIF4*, and *PIF5*. I conducted ChIP-qPCR and expression studies, revealing that PRR7 maintained binding and regulation of shared target genes in the *hy5 35S::HA-PRR7* line, contrary to my hypothesis (Figure 4.5, Figure 4.6). It is possible that the presence of the HY5 homolog HYH may be sufficient to compensate for the loss of HY5. To account for both HY5 and HYH, we acquired the *hy5hyh* double mutant and we are selecting F3 lines expressing *PRR7::HA-PRR7* or *35S::HA-PRR7* in the double

mutant background. Ongoing selection and future characterization of these lines will shed light on the role of PRR7 associating with HY5 and HYH.

Impact and future perspectives

ChIP-chip and ChIP-seq studies have been conducted on transcription factors numbering from 52 TFs in *Drosophila melanogaster*, 93 TFs in *Caenorhabditis elegans*, and 165 TFs in humans (Boyle et al., 2014). ChIP-chip and ChIP-seq data in plants, on the other hand, still have plenty of room for expansion with a total of around 27 TFs (Heyndrickx et al., 2014). Predictive models for cis-regulatory modules are limited by existing data, and additional ChIP-seq data would lead to better predictions of co-regulators as well as other possible targets not detected by ChIP-seq (Neph et al., 2012). My contribution of the PRR7 ChIP-seq data was included in the Heyndrickx et al. (2014) study in plants, and my recent PRR9 ChIP-seq data will provide additional information for similar large-scale analyses in the future.

The current direction of ChIP-seq studies is to closely follow the dynamics of transcription factor regulation at a spatiotemporal resolution. In *C. elegans*, Araya et al. (2014) investigated 92 transcription factors at different developmental stages, resulting in a total of 241 ChIP-seq experiments. They examined the relationship between TF binding and transcriptional regulation by incorporating cell-type and tissue-specific expression data into their analyses (Araya et al., 2014). In mice, Rey et al. (2011) performed a ChIP-seq time course by collecting samples every 4 hours for 24 hours to follow the oscillation patterns of TF binding. Recently in Arabidopsis, ChIP-seq studies using an inducible system in protoplasts enabled Para et al. (2014) to examine dynamic TF binding in as quickly as 1 minute upon TF nuclear localization. Finally, in an expression study by Endo et al. (2014), separation of mesophyll from vasculature tissue revealed

an inverse relationship in phase of expression between cycling mesophyll-rich (morning expressed) vs. vasculature-rich (evening expressed) genes. They also found that the vasculature clock is hierarchically above the mesophyll clock in Arabidopsis, similar to how the suprachiasmatic nucleus is hierarchically above other clocks (e.g. liver) in mammals (Endo et al., 2014). Altogether, taking into account the spatiotemporal activity of circadian clock components is warranted to provide a dynamic and multidimensional view in regards to circadian rhythms, developmental stage, and tissue specificity, to name a few.

Clock components are master regulators of many agriculturally important traits such as drought and cold tolerance, pest resistance, and plant metabolism and nutrition (Dong et al., 2011; Farre and Weise, 2012; Goodspeed et al., 2012). In a study conducted by Dr. Norman Borlaug, segregating wheat was grown in northwestern Mexico, after which harvested grains were subsequently grown in central Mexico. The goal was to achieve two growing seasons in one year to speed up the breeding process (Borlaug, 2007). Known as "shuttle breeding," this also resulted in the unintended selection of photoperiod insensitive wheat cultivars that can survive in a broad range of environments (Borlaug, 2007). Photoperiod insensitivity in wheat was traced back to mutations in *Photoperiod-1* (*Ppd-1*) in the A, B, and D genomes, which interestingly shows highest similarity to Arabidopsis *PRR7* (Shaw et al., 2012). Mutations to *Ppd-1* did not affect the expression of clock genes such as *TOC1* and *PRR73*, suggesting that genetic redundancy masked the loss of *Ppd-1*, or that *Ppd-1* may play a photoperiod specific role and possibly resulted from a subfunctionalization of the circadian PRRs (Shaw et al., 2012). These insights reveal the value of studying the specific roles of each clock component, especially in the context of regulating diverse biological processes, which may provide avenues into applied research for further crop improvement.

Knowledge gained from fundamental research has given rise to the growing field of synthetic biology. Synthetic biology derives knowledge from basic research to construct new or re-design existing biological components or systems for useful applications. Engineered gene circuits are oftentimes fragile as evidenced when the organisms are exposed to fluctuating environmental conditions. The inclusion of circadian clock components can buffer against perturbations, such as temperature by conferring temperature compensation. Hussain et al. (2014) created a synthetic *Escherichia coli* using design principles of circadian clocks to incorporate the concept of temperature compensation and thereby increase the robustness of its gene circuits. It is possible that circadian clock components may also be utilized for temporal optimization of various processes and allocating resources at appropriate times to increase efficiency and production. Clock circuits can be as simple as those observed in *O. tauri* or cyanobacteria, but as we continue to gain more knowledge, we can create more complex systems such as those afforded by the Arabidopsis core clock components and master regulators PRR9 and PRR7.

APPENDIX

FIGURES

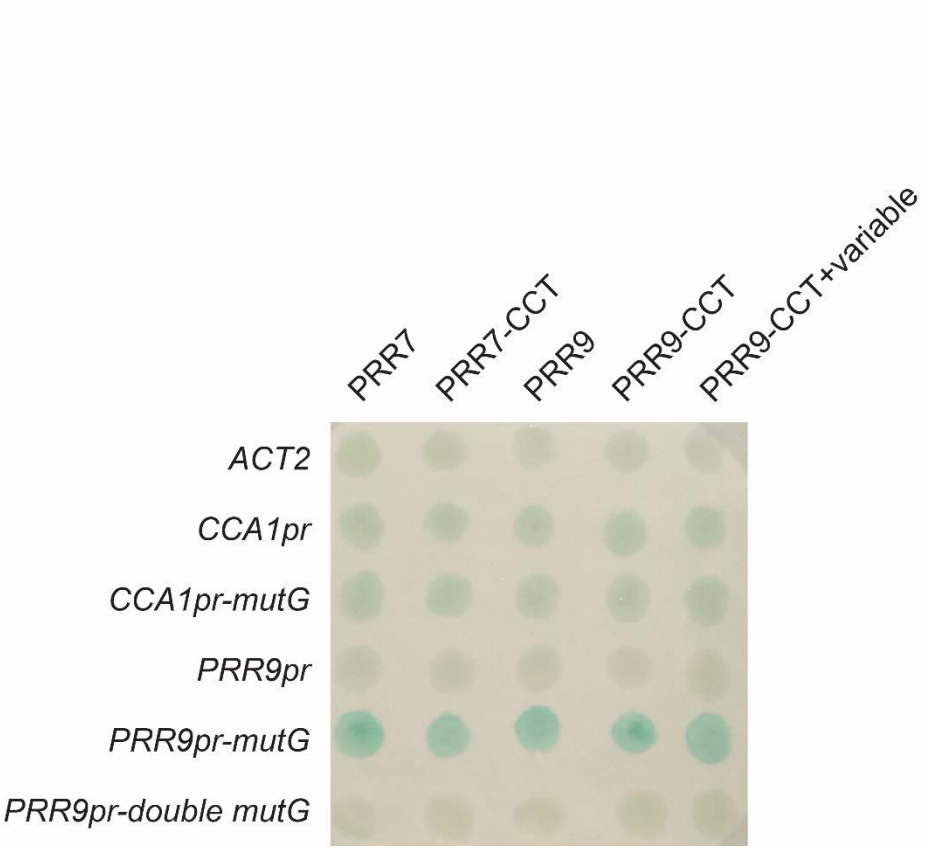

Figure 4.1. PRR7 and PRR9 do not directly bind to DNA in a heterologous system. Yeast one-hybrid β-Gal assay with rows specifying the DNA bait and columns specifying the transcription factor prey. The DNA bait was cloned into the PMW#3 destination vector and the transcription factor prey was cloned into the pACT2 vector. *ACT2* (AT3G18780) intron was used as a negative control. CCT, CONSTANS, CONSTANS-LIKE, TOC1 domain; variable, variable region located between the PR and CCT domains; *pr*, promoter; *mutG*, mutated G-box (*PRR9* mutated G-box is located at -280 bp to -286 bp upstream of TSS; *CCA1* mutated G-box is located at -268 bp to -274 bp upstream of TSS); *double mutG*, both *PRR9* G-boxes are mutated at locations -208 bp to -214 bp and -280 bp to -286 bp upstream of TSS.

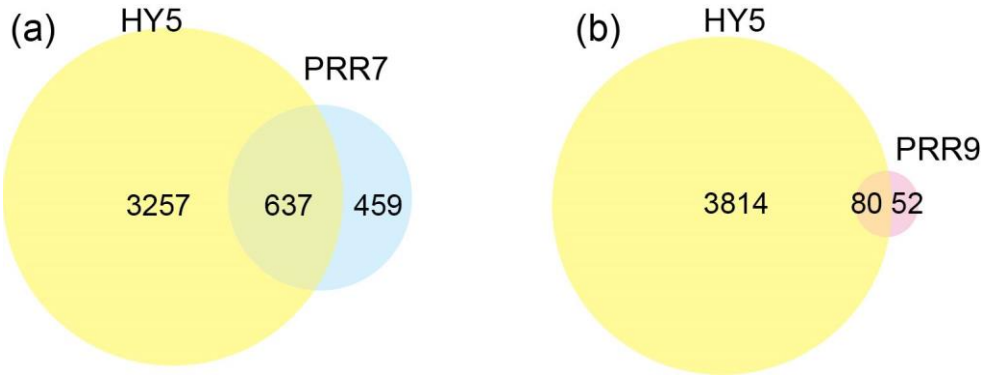

Figure 4.2. HY5 shares target genes with PRR7 and PRR9. Venn diagrams showing the overlap of HY5 target genes (Lee et al., 2007) with (a) PRR7 targets (data from Liu et al., 2013 as analyzed in Chapter 3) or (b) PRR9 targets (data from Chapter 3).

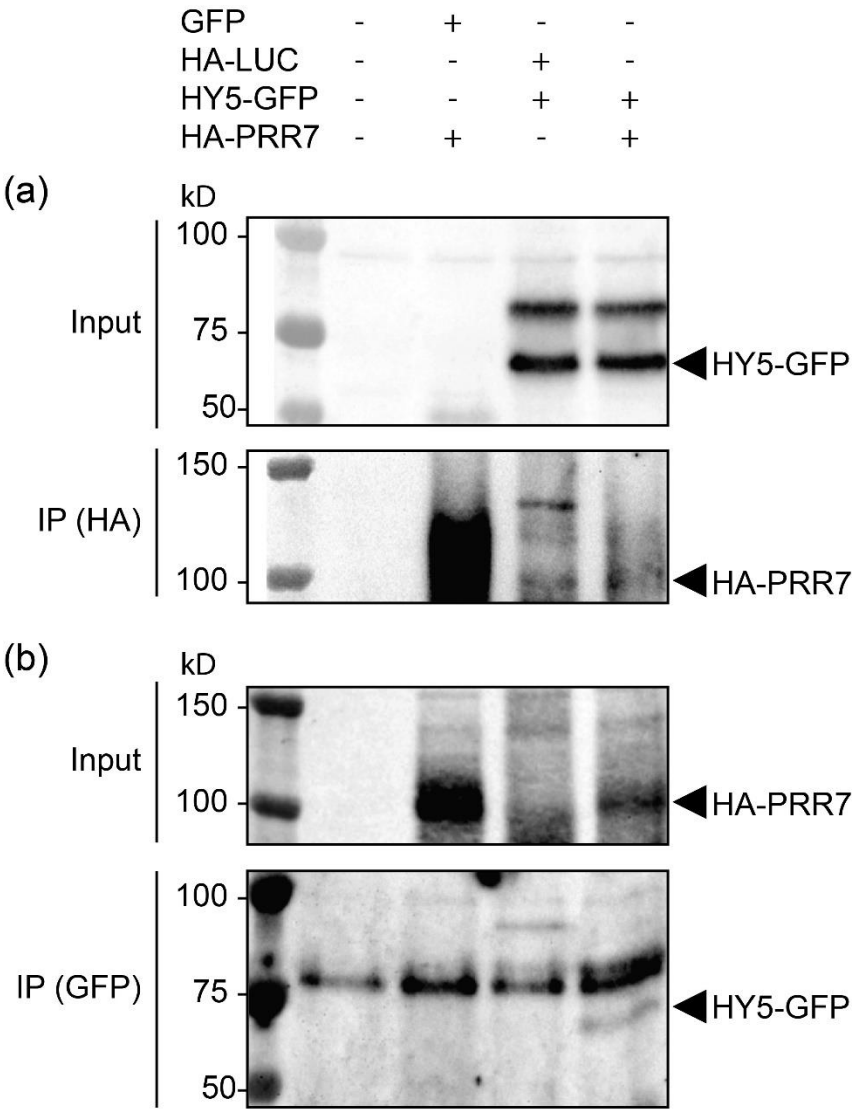

Figure 4.3. Testing the interaction of PRR7 and HY5 by transient expression and immunoprecipitation in *Nicotiana benthamiana*. Tobacco plants were co-infiltrated with *Agrobacterium tumefaciens* containing *35S::HY5-GFP* and *35S::HA-PRR7*. Extracted proteins were immunoprecipitated using anti-HA antibody. The input and IP were detected using (a) anti-GFP and anti-HA or (b) anti-HA and anti-GFP, respectively. IP, immunoprecipitation. Experiment done by Tomomi Takeuchi.

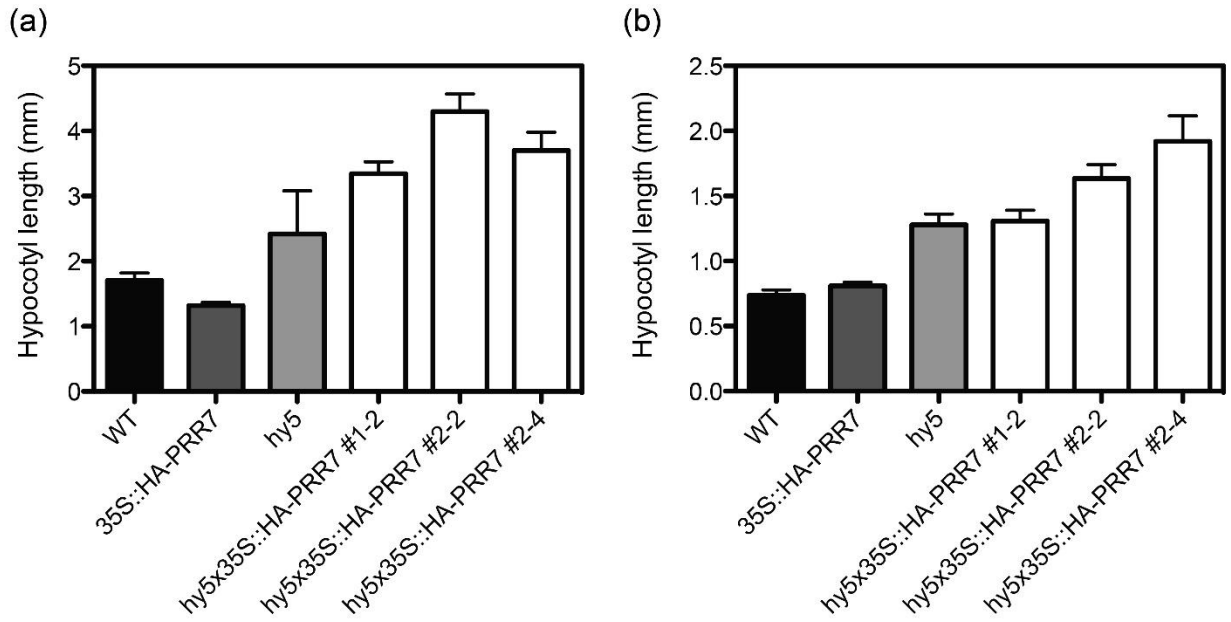

Figure 4.4. *hy5x35S::HA-PRR7* lines exhibit a long hypocotyl phenotype. Hypocotyl measurements of 5-day old seedlings grown in (a) cycling 12 h light/ 12 h dark or (b) constant light. Light intensity was set at 70µmol m^{-2} s^{-1} and temperatures were set to 22°C. Bars represent standard error with n ≥ 10 for all lines except for the *hy5* knockout line in LL (n=5). LD, light/dark; LL, constant light; WT, wild-type.

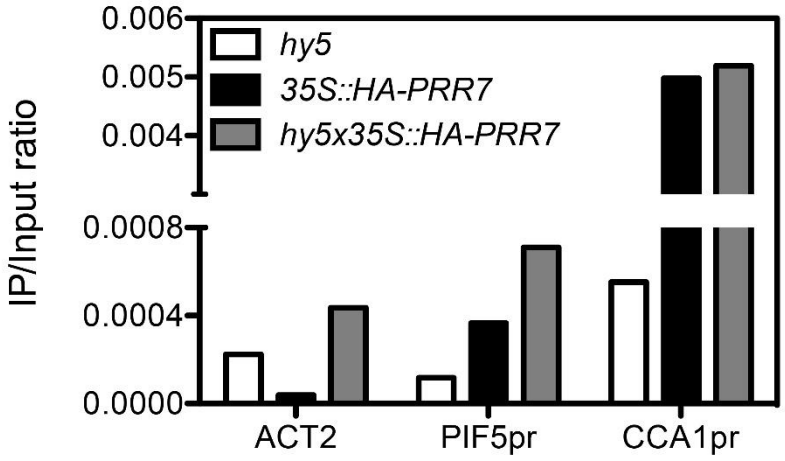

Figure 4.5. PRR7 binds to the *PIF5* and *CCA1* promoters in *hy5x35S::HA-PRR7* line. Plants were grown in cycling 12 h light/12 h dark for 2 weeks before harvesting at ZT11-12. ChIPqPCR of *hy5x35S::HA-PRR7* compared to *35S::HA-PRR7* (positive control) and *hy5* knockout mutant (negative control). The *ACT2* intron was used as a control. IP, immunoprecipitation.

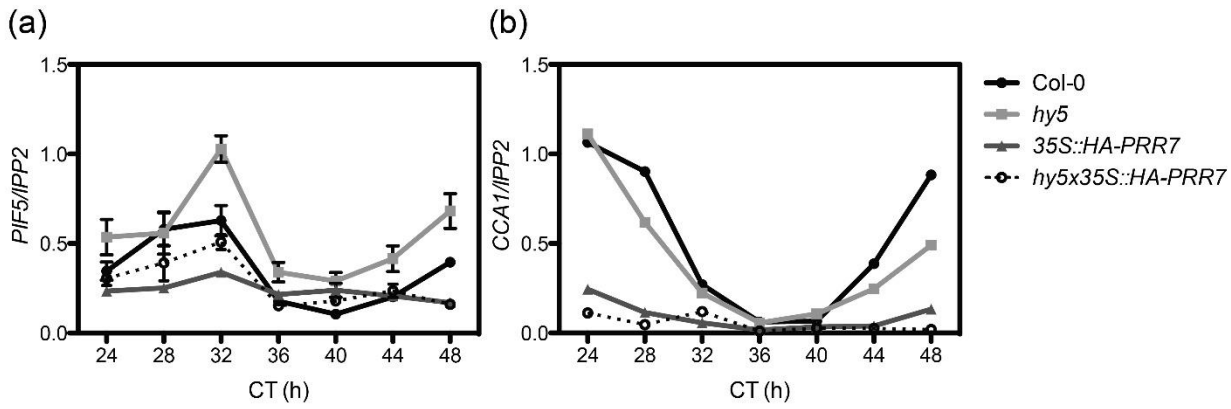

Figure 4.6. PRR7 represses *PIF5* and *CCA1* expression in the *hy5x35S::HA-PRR7* line. Expression analysis of HY5 and PRR7 target genes (a) *PIF5* and (b) *CCA1* in Col-0, *hy5*, PRR7 overexpressing line (*35S::HA-PRR7*) and *hy5x35S::HA-PRR7* line. Plants were grown in cycling 12 h light/12 h dark for 2 weeks, released to constant light, and samples were collected every 4 hours from CT24 to 48. Data are the average ± standard error of 3 biological replicates in both graphs. Expression levels were analyzed by RT-qPCR and normalized to *IPP2*.

REFERENCES

REFERENCES

Araya CL, Kawli T, Kundaje A, Jiang LX, Wu BJ, Vafeados D, Terrell R, Weissdepp P, Gevirtzman L, Mace D, Niu W, Boyle AP, Xie D, Ma LJ, Murray JI, Reinke V, Waterston RH, Snyder M (2014) Regulatory analysis of the C. elegans genome with spatiotemporal resolution. Nature **512:** 400-405

Borlaug NE (2007) Sixty-two years of fighting hunger: personal recollections. Euphytica **157:** 287-297

Boyle AP, Araya CL, Brdlik C, Cayting P, Cheng C, Cheng Y, Gardner K, Hillier LW, Janette J, Jiang LX, Kasper D, Kawli T, Kheradpour P, Kundaje A, Li JJ, Ma LJ, Niu W, Rehm EJ, Rozowsky J, Slattery M, Spokony R, Terrell R, Vafeados D, Wang DF, Weisdepp P, Wu YC, Xie D, Yan KK, Feingold EA, Good PJ, Pazin MJ, Huang HY, Bickel PJ, Brenner SE, Reinke V, Waterston RH, Gerstein M, White KP, Kellis M, Snyder M (2014) Comparative analysis of regulatory information and circuits across distant species. Nature **512:** 453-456

Brockmann B, Smith MW, Zaraisky AG, Harrison K, Okada K, Kamiya Y (2001) Subcellular localization and targeting of glucocorticoid receptor protein fusions expressed in transgenic Arabidopsis thaliana. Plant and Cell Physiology **42:** 942-951

Chattopadhyay S, Ang LH, Puente P, Deng XW, Wei N (1998) Arabidopsis bZIP protein HY5 directly interacts with light-responsive promoters in mediating light control of gene expression. Plant Cell **10:** 673-683

Dong MA, Farre EM, Thomashow MF (2011) CIRCADIAN CLOCK-ASSOCIATED 1 and LATE ELONGATED HYPOCOTYL regulate expression of the C-REPEAT BINDING FACTOR (CBF) pathway in Arabidopsis. Proceedings of the National Academy of Sciences of the United States of America **108:** 7241-7246

Ellenberger T (1994) Getting a grip on DNA recognition: structures of the basic region leucine zipper, and the basic region helix-loop-helix DNA-binding domains. Current Opinion in Structural Biology **4:** 12-21

Endo M, Shimizu H, Nohales MA, Araki T, Kay SA (2014) Tissue-specific clocks in Arabidopsis show asymmetric coupling. Nature **515:** 419-422

Farre EM, Harmer SL, Harmon FG, Yanovsky MJ, Kay SA (2005) Overlapping and distinct roles of PRR7 and PRR9 in the Arabidopsis circadian clock. Current Biology **15:** 47-54

Farre EM, Kay SA (2007) PRR7 protein levels are regulated by light and the circadian clock in Arabidopsis. Plant Journal **52:** 548-560

Farre EM, Liu T (2013) The PRR family of transcriptional regulators reflects the complexity and evolution of plant circadian clocks. Current Opinion in Plant Biology **16:** 621-629

Farre EM, Weise SE (2012) The interactions between the circadian clock and primary metabolism. Current Opinion in Plant Biology **15:** 293-300

Fujiwara S, Wang L, Han L, Suh SS, Salome PA, McClung CR, Somers DE (2008) Post-translational regulation of the Arabidopsis circadian clock through selective proteolysis and phosphorylation of pseudo-response regulator proteins. Journal of Biological Chemistry **283:** 23073-23083

Gendron JM, Pruneda-Paz JL, Doherty CJ, Gross AM, Kang SE, Kay SA (2012) Arabidopsis circadian clock protein, TOC1, is a DNA-binding transcription factor. Proceedings of the National Academy of Sciences of the United States of America **109:** 3167-3172

Gilmour SJ, Zarka DG, Stockinger EJ, Salazar MP, Houghton JM, Thomashow MF (1998) Low temperature regulation of the Arabidopsis CBF family of AP2 transcriptional activators as an early step in cold-induced COR gene expression. Plant Journal **16:** 433-442

Goodspeed D, Chehab EW, Min-Venditti A, Braam J, Covington MF (2012) Arabidopsis synchronizes jasmonate-mediated defense with insect circadian behavior. Proceedings of the National Academy of Sciences of the United States of America **109:** 4674-4677

Guertin MJ, Lis JT (2010) Chromatin Landscape Dictates HSF Binding to Target DNA Elements. PLoS Genetics **6**

Heyndrickx KS, Van de Velde J, Wang CM, Weigei D, Vandepoele K (2014) A Functional and Evolutionary Perspective on Transcription Factor Binding in Arabidopsis thaliana. Plant Cell **26:** 3894-3910

Holm M, Ma LG, Qu LJ, Deng XW (2002) Two interacting bZIP proteins are direct targets of COP1-mediated control of light-dependent gene expression in Arabidopsis. Genes & Development **16:** 1247-1259

Hsu PY, Devisetty UK, Harmer SL (2013) Accurate timekeeping is controlled by a cycling activator in Arabidopsis. Elife **2**

Hussain F, Gupta C, Hirning AJ, Ott W, Matthews KS, Josic K, Bennett MR (2014) Engineered temperature compensation in a synthetic genetic clock. Proceedings of the National Academy of Sciences of the United States of America **111:** 972-977

Jakoby M, Weisshaar B, Droge-Laser W, Vicente-Carbajosa J, Tiedemann J, Kroj T, Parcy F, b ZIPRG (2002) bZIP transcription factors in Arabidopsis. Trends in Plant Science **7:** 106-111

John S, Sabo PJ, Thurman RE, Sung MH, Biddie SC, Johnson TA, Hager GL, Stamatoyannopoulos JA (2011) Chromatin accessibility pre-determines glucocorticoid receptor binding patterns. Nature Genetics **43:** 264-U116

Lee J, He K, Stolc V, Lee H, Figueroa P, Gao Y, Tongprasit W, Zhao HY, Lee I, Deng X (2007) Analysis of transcription factor HY5 genomic binding sites revealed its hierarchical role in light regulation of development. Plant Cell **19:** 731-749

Leivar P, Quail PH (2011) PIFs: pivotal components in a cellular signaling hub. Trends in Plant Science **16:** 19-28

Liu T, Carlsson J, Takeuchi T, Newton L, Farre EM (2013) Direct regulation of abiotic responses by the Arabidopsis circadian clock component PRR7. Plant Journal **76:** 101-114

Nakamichi N, Kiba T, Henriques R, Mizuno T, Chua NH, Sakakibara H (2010) PSEUDO-RESPONSE REGULATORS 9, 7, and 5 Are Transcriptional Repressors in the Arabidopsis Circadian Clock. Plant Cell **22:** 594-605

Nakamichi N, Kusano M, Fukushima A, Kita M, Ito S, Yamashino T, Saito K, Sakakibara H, Mizuno T (2009) Transcript Profiling of an Arabidopsis PSEUDO RESPONSE REGULATOR Arrhythmic Triple Mutant Reveals a Role for the Circadian Clock in Cold Stress Response. Plant and Cell Physiology **50:** 447-462

Neph S, Vierstra J, Stergachis AB, Reynolds AP, Haugen E, Vernot B, Thurman RE, John S, Sandstrom R, Johnson AK, Maurano MT, Humbert R, Rynes E, Wang H, Vong S, Lee K, Bates D, Diegel M, Roach V, Dunn D, Neri J, Schafer A, Hansen RS, Kutyavin T, Giste E, Weaver M, Canfield T, Sabo P, Zhang MH, Balasundaram G, Byron R, MacCoss MJ, Akey JM, Bender MA, Groudine M, Kaul R, Stamatoyannopoulos JA (2012) An expansive human regulatory lexicon encoded in transcription factor footprints. Nature **489:** 83-90

Oh E, Kang H, Yamaguchi S, Park J, Lee D, Kamiya Y, Choi G (2009) Genome-Wide Analysis of Genes Targeted by PHYTOCHROME INTERACTING FACTOR 3-LIKE5 during Seed Germination in Arabidopsis. Plant Cell **21:** 403-419

Ouyang XH, Li JG, Li G, Li BS, Chen BB, Shen HS, Huang X, Mo XR, Wan XY, Lin RC, Li SG, Wang HY, Deng XW (2011) Genome-Wide Binding Site Analysis of FAR-RED ELONGATED HYPOCOTYL3 Reveals Its Novel Function in Arabidopsis Development. Plant Cell **23:** 2514-2535

Para A, Li Y, Marshall-Colon A, Varala K, Francoeur NJ, Moran TM, Edwards MB, Hackley C, Bargmann BOR, Birnbaum KD, McCombie WR, Krouk G, Coruzzi GM (2014) Hit-and-run transcriptional control by bZIP1 mediates rapid nutrient signaling in

Arabidopsis. Proceedings of the National Academy of Sciences of the United States of America **111:** 10371-10376

Rey G, Cesbron F, Rougemont J, Reinke H, Brunner M, Naef F (2011) Genome-Wide and Phase-Specific DNA-Binding Rhythms of BMAL1 Control Circadian Output Functions in Mouse Liver. PLoS Biology **9**

Shaw LM, Turner AS, Laurie DA (2012) The impact of photoperiod insensitive Ppd-1a mutations on the photoperiod pathway across the three genomes of hexaploid wheat (Triticum aestivum). Plant Journal **71:** 71-84

Song YH, Ito S, Imaizumi T (2010) Similarities in the circadian clock and photoperiodism in plants. Current Opinion in Plant Biology **13:** 594-603

Toledo-Ortiz G, Huq E, Quail PH (2003) The Arabidopsis basic/helix-loop-helix transcription factor family. Plant Cell **15:** 1749-1770